



## DEVELOPMENT OF A NOVEL CATALYTIC MEMBRANE REACTOR: APPLICATION IN WASTEWATER TREATMENT

Oscar Antonio Osegueda Chicas

Dipòsit Legal: T. 1015-2013

**ADVERTIMENT.** L'accés als continguts d'aquesta tesi doctoral i la seva utilització ha de respectar els drets de la persona autora. Pot ser utilitzada per a consulta o estudi personal, així com en activitats o materials d'investigació i docència en els termes establerts a l'art. 32 del Text Refós de la Llei de Propietat Intel·lectual (RDL 1/1996). Per altres utilitzacions es requereix l'autorització prèvia i expressa de la persona autora. En qualsevol cas, en la utilització dels seus continguts caldrà indicar de forma clara el nom i cognoms de la persona autora i el títol de la tesi doctoral. No s'autoritza la seva reproducció o altres formes d'explotació efectuades amb finalitats de lucre ni la seva comunicació pública des d'un lloc aliè al servei TDX. Tampoc s'autoritza la presentació del seu contingut en una finestra o marc aliè a TDX (framing). Aquesta reserva de drets afecta tant als continguts de la tesi com als seus resums i índexs.

**ADVERTENCIA.** El acceso a los contenidos de esta tesis doctoral y su utilización debe respetar los derechos de la persona autora. Puede ser utilizada para consulta o estudio personal, así como en actividades o materiales de investigación y docencia en los términos establecidos en el art. 32 del Texto Refundido de la Ley de Propiedad Intelectual (RDL 1/1996). Para otros usos se requiere la autorización previa y expresa de la persona autora. En cualquier caso, en la utilización de sus contenidos se deberá indicar de forma clara el nombre y apellidos de la persona autora y el título de la tesis doctoral. No se autoriza su reproducción u otras formas de explotación efectuadas con fines lucrativos ni su comunicación pública desde un sitio ajeno al servicio TDR. Tampoco se autoriza la presentación de su contenido en una ventana o marco ajeno a TDR (framing). Esta reserva de derechos afecta tanto al contenido de la tesis como a sus resúmenes e índices.

**WARNING.** Access to the contents of this doctoral thesis and its use must respect the rights of the author. It can be used for reference or private study, as well as research and learning activities or materials in the terms established by the 32nd article of the Spanish Consolidated Copyright Act (RDL 1/1996). Express and previous authorization of the author is required for any other uses. In any case, when using its content, full name of the author and title of the thesis must be clearly indicated. Reproduction or other forms of for profit use or public communication from outside TDX service is not allowed. Presentation of its content in a window or frame external to TDX (framing) is not authorized either. These rights affect both the content of the thesis and its abstracts and indexes.

UNIVERSITAT ROVIRA I VIRGILI  
DEVELOPMENT OF A NOVEL CATALYTIC MEMBRANE REACTOR: APPLICATION IN WASTEWATER  
TREATMENT  
Oscar Antonio Osegueda Chicas  
Depósito legal:

## **Doctoral Thesis**

# **Development of a novel catalytic membrane reactor: Application in wastewater treatment**

**Oscar Antonio Osegueda Chicas**



UNIVERSITAT ROVIRA I VIRGILI  
**Tarragona, 2013**



UNIVERSITAT ROVIRA I VIRGILI  
DEVELOPMENT OF A NOVEL CATALYTIC MEMBRANE REACTOR: APPLICATION IN WASTEWATER  
TREATMENT

Oscar Antonio Osegueda Chicas  
Depósito legal:

Oscar Antonio Osegueda Chicas

Development of a novel catalytic membrane reactor:  
Application in wastewater treatment

Doctoral thesis

Supervised by:

Prof. Dr. Francisco Medina

Dr. Anton Dafinov

Prof. Dr. Jesús Sueiras

Department of Chemical Engineering



UNIVERSITAT ROVIRA I VIRGILI

Tarragona, 2013





UNIVERSITAT  
ROVIRA I VIRGILI

ESCOLA TÈCNICA SUPERIOR D'ENGINYERIA QUÍMICA

DEPARTAMENT D'ENGINYERIA QUÍMICA

Avinguda Països Catalans, 26  
Campus Sescelades  
43007 Tarragona (Spain)  
Tels. 977 55 96 03/04  
Fax: 977 55 96 21  
e-mail: secdeq@urv.cat  
<http://www.etscq.urv.cat/DEQ>

Prof. Dr. Francisco Medina Cabello, Dr. Anton Dafinov and Prof. Dr. Jesús E.  
Sueiras Romero

**CERTIFY THAT:**

The present work, entitled "DEVELOPMENT OF A NOVEL CATALYTIC MEMBRANE REACTOR: APPLICATION IN WASTEWATER TREATMENT", presented by Oscar Antonio Osegueda Chicas for the award of the degree of doctor, has been carried out under our supervision at the chemical engineering department of this university, and it fulfills all the requirements to obtain the degree of Doctor in Chemical, Environmental and Process Engineering.

Tarragona, April 19<sup>th</sup> 2013

The supervisors of the doctoral thesis

Prof. Dr. Francisco Medina

Dr. Anton Dafinov

Prof. Dr. Jesús Sueiras

UNIVERSITAT ROVIRA I VIRGILI  
DEVELOPMENT OF A NOVEL CATALYTIC MEMBRANE REACTOR: APPLICATION IN WASTEWATER  
TREATMENT  
Oscar Antonio Osegueda Chicas  
Depósito legal:

## SUMMARY

There is an increasing concern about the quality and quantity of the freshwater and groundwater resources for life supporting and environmental needs. Mainly the increasing number of discharged pollutants that have toxic and/or recalcitrant character (e.g., newly emerging problem pollutants, heavy metals, pharmaceuticals etc.) requires stricter prescriptive limits for pollutant concentrations. Chemical oxidation processes are usually preferred among the others approaches due to their versatility and relatively fast destruction of contaminants. Advanced oxidation processes (AOP) are highly suitable when dealing with clean up of wastewaters and industrial effluents, which are often loaded with different types of recalcitrant pollutants. AOPs are based on generation of highly reactive oxygen species such as hydroxyl radicals ( $\bullet\text{OH}$ ) which can effectively attack a wide range of organic compounds. Even though this technique is considered as powerful regarding contaminant degradation, it faces several practical limitations in a large scale. Thus, the aim of this study was to propose and test a novel strategy in order to extend the applicability of AOP, whereby the integration of catalytic membrane reactors (CMRs) plays a key role.

Herein, various CMRs were prepared starting from commercial ultrafiltration and microfiltration ceramic hollow fibers. These hollow fibers are made of  $\alpha\text{-Al}_2\text{O}_3$  with an exceptional mechanical and chemical resistance. Metallic palladium Pd was loaded (deposited) onto the CMRs as a principal catalytic active phase in order to generate  $\text{H}_2\text{O}_2$  using gaseous  $\text{H}_2$  and  $\text{O}_2$ .

The hollow fibers were modified by two different procedures. The first protocol was carried out using an incipient wetness technique. Two types of membrane reactors were prepared: i) monometallic Pd membrane reactors

and ii) mixed double active phases membrane reactors, which are made of metallic Pd and transitional metal oxide. The second protocol is a novel procedure for preparing CMRs. This protocol is based on the sputtering technique, and it was developed to reduce the amount of palladium as well as to disperse it finely in the reaction zone. In fact the amount of Pd was reduced up to 200 times compared with the first protocol. As well, the noble metal was highly dispersed which leads to the formation of nanometer-sized particles.

The physicochemical properties of the prepared CMRs were studied with scanning electronic microscopy (SEM), environmental scanning electronic microscopy (ESEM), micro X-ray diffraction ( $\mu$ -XRD),  $N_2$ -physisorption,  $H_2$ -chemisorption, X-ray photoelectron spectroscopy (XPS).

The monometallic Pd membrane reactors were tested in the oxidation of phenol using in-situ generated  $H_2O_2$ . Several parameters have been thoroughly evaluated including: i) efficiency of hydrogen conversion to hydrogen peroxide, ii) efficiency in the use of  $H_2O_2$  for phenol oxidation, iii) reaction temperature, iv) intermediate products of the phenol oxidation, v) the phenol conversion, and vi) total organic carbon (TOC) conversion as well as the chemical oxygen demand (COD). The efficiency of hydrogen involved in the  $H_2O_2$  formation reaction was determined in all cases with respect to the formation rate and the maximum achievable  $H_2O_2$  concentration. The results clearly showed that the CMRs containing monometallic Pd have high catalytic activity towards  $H_2O_2$  generation, where the size of metallic Pd appears to play a key role. However, when the Pd-loaded CMRs were tested for the oxidation of phenol, no significant degradation of the organic substrate was monitored. In other words, a

second active phase has to be employed into the system in order to activate hydrogen peroxide and generate  $\bullet\text{OH}$ .

Mixed double-active phase membrane reactors were tested for the oxidation of phenol at neutral pH conditions. The bimetallic CMRs prepared by impregnation have shown to be very stable in the oxidation reaction, and up to 30 – 40% of the generated  $\text{H}_2\text{O}_2$  was involved in the oxidation of the phenol compound. Furthermore, it was observed that the transition metal oxide phases such as  $\text{CeO}_2$  and  $\text{Fe}_2\text{O}_3$  play an important role in the oxidation of phenol.

Despite the obtained results, it was detected that the catalytic membrane reactors undergo deactivation under certain reaction conditions. In the case of the CMRs prepared by impregnation method, it was demonstrated that the generated hydrogen peroxide oxidized the surface of the Pd. The sputtered Pd membrane reactors suffered a fast deactivation during the phenol oxidation reaction, and it has been proven that the  $\text{H}_2$  plays a major role in the loss of catalytic activity.

The role of the hydrogen in the membrane reactor deactivation was studied using Pd sputtered on corundum powder. Temperature programmed desorption (TPD) and high resolution transmission electron microscopy (HRTEM) analyses have shown that Pd nanoparticles absorb  $\text{H}_2$  until they are converted to palladium hydride with  $\beta$ -phase structure. And the beta Pd hydride seems not be able to activate the hydrogen.

Finally, Pd- $\text{CeO}_2$  and Pd- $\text{CeO}_2$ - $\text{Fe}_2\text{O}_3$  membrane reactors were tested in the catalytic reduction of nitrates and hydrodechlorination of 4-Cl-Phenol. The CMRs were operated in continuous mode using a proposed metal housing design. The preliminary results have shown the feasibility in the use of CMR operated in continuous mode to eliminate water contaminants.

In summary, it was shown that two different methods were developed to prepare and monometallic and bimetallic catalytic membrane reactors for the generation of hydrogen peroxide and oxidation of phenol in the aqueous phase at neutral pH conditions.

## **ACKNOWLEDGMENT**

En primer lugar, deseo expresar mi agradecimiento al Prof. Dr. Jesús Sueiras por la invitación que me realizó hace 4 años para iniciar mis estudios de doctorado en el grupo de catálisis heterogénea. Así mismo agradezco al Prof. Dr. Francesc Medina, jefe del grupo y director de este trabajo, por su invaluable papel en el desarrollo de esta tesis.

Deseo expresar mis verdaderos y sinceros agradecimientos al Dr. Anton Dafinov por orientarme en el mundo de la investigación, por brindarme su ayuda y sus consejos, pero sobre todo por su sincera amistad.

También debo agradecer al Dr. Francisco Chávez, quien me ha apoyado para que pueda desarrollar mis estudios. Extiendo estos agradecimientos a todos mis profesores, compañeros del departamento de ingeniería de procesos y ciencias ambientales y amigos en El Salvador, quienes han estado pendientes de mi trabajo y demás aspectos de mi vida.

Agradezco a la Fundación Carolina, Universitat Rovira i Virgili, Fundación Rovira i Virgili y la Universidad Centroamericana José Simeón Cañas por el apoyo económico que he recibido para realizar mis estudios de doctorado.

No puedo dejar de agradecer a todos mis compañeros de Catheter-Amic-Applicat por lo momentos vividos que sin duda no podré olvidar. Tampoco quiero dejar a un lado a los buenos amigos: Alex, Olivier, Luis, María, Dana, Dragos, Abel, Susana y Mayra con quienes he compartido tantos buenos momentos, he aprendido muchísimo y que han convertido de Tarragona en un hogar.

Gracias a mis hermanos y sobrinos que en la distancia siempre se han encontrado presentes.

Y finalmente deseo agradecer a Klari, quien me ha apoyado durante los momentos más duros, y con quien he compartido los más dulces de toda mi estancia.

**“It is the time you have spent for your rose that makes your rose so  
important.”**

## TABLES OF CONTENTS

SUMMARY .....	i
ACKNOWLEDGMENT .....	v
TABLES OF CONTENTS .....	vii
LIST OF FIGURES .....	xi
LIST OF TABLES .....	xv
Chapter 1. Introduction .....	1
Chapter 2. Introduction to membrane reactors .....	5
2.1 Membranes for membrane reactors .....	6
2.2 Inorganic membranes .....	7
2.2.1 Ceramic membranes .....	8
2.3 Function of ceramic membrane in membrane reactors .....	11
2.3.1 Membrane extractors .....	11
2.3.2 Membrane distributors .....	12
2.3.3 Membrane contactors .....	13
2.4 Catalytic membrane reactors .....	14
2.4.1 Palladium-based catalytic membrane reactors .....	16
2.4.2 Preparation of palladium-based membranes .....	17
2.4.3 Palladium-based membrane reactors in gas-liquid reactions .....	18
2.5 Selective oxidation of hydrogen to hydrogen peroxide .....	19
2.6 Pd-based membranes as a tool for destruction of contaminants in water .....	22
2.6.1 Chemical oxidation of organic contaminants .....	23
2.6.2 Catalytic reduction of water pollutants .....	25
Chapter 3. Aim and objectives .....	29
Chapter 4. Preparation and characterization of catalytic membrane reactors .....	31

4.1	Preparation of catalytic membrane reactors.....	31
4.1.1	Ceramic hollow fibers – starting material .....	32
4.1.2	Preparation of monometallic palladium membrane by impregnation method .....	33
4.1.3	Preparation of copper aluminate membrane with palladium active phase by impregnation method .....	34
4.1.4	Preparation of mixed double active phases, metallic palladium – metal oxide, membranes by impregnation method .....	35
4.1.5	Preparation of monometallic palladium membrane by sputtering technique .....	37
4.1.6	Preparation of mixed double active phases, sputtered palladium – metal oxide, membranes .....	40
4.1.7	Preparation of corundum powder with sputtered palladium .....	41
4.2	Characterization of catalytic membrane reactors.....	42
Chapter 5.	Experimental setup.....	51
5.1	Direct synthesis of H <sub>2</sub> O <sub>2</sub> in a semi batch mode .....	51
5.1.1	Synthesis of H <sub>2</sub> O <sub>2</sub> by means of H <sub>2</sub> /O <sub>2</sub> mixture dosage .....	51
5.1.2	Synthesis of H <sub>2</sub> O <sub>2</sub> by means of H <sub>2</sub> and synthetic air dosing .....	52
5.1.3	Reaction conditions, sampling and measurement of H <sub>2</sub> O <sub>2</sub> .....	53
5.2	Oxidation of organic compounds with in situ generated hydrogen peroxide.....	54
5.2.1	Sampling and measurement of phenol .....	55
5.3	Design of metal housing (module reactor) for continuous operation	56
5.4	Catalytic reduction of water contaminants.....	57
5.4.1	Selective reduction of nitrates .....	58
5.4.2	Hydrodechlorination of chlorinated aromatic compounds.....	59
Chapter 6.	Results and discussion .....	61

6.1	Ceramic hollow fibers.....	61
6.2	Monometallic Pd membrane reactors .....	66
6.3	Palladium bimetallic membrane reactors.....	79
6.4	Corundum powder with sputtered palladium.....	84
6.5	Catalytic activity of CMRs in batch system.....	85
6.5.1	Hydrogen peroxide generation .....	85
6.5.2	Phenol oxidation with catalytic membrane reactors prepared by impregnation .....	98
6.5.3	Phenol oxidation with catalytic membrane reactors prepared by sputtering method.....	105
6.5.4	Effect of hydrogen on sputtered palladium nanoparticles.....	111
6.6	Catalytic activity of CMRs in continuous system.....	114
6.6.1	Selective reduction of nitrates .....	114
6.6.2	Hydrodechlorination of chlorinated aromatic compounds.....	117
Chapter 7.	Conclusions.....	121
REFERENCES	.....	127



## LIST OF FIGURES

Figure 2-1 Scheme of a membrane reactor .....	5
Figure 2-2 Representation of a tubular ceramic membrane .....	9
Figure 2-3 Hollow fiber membrane and an industrial cartridge.....	11
Figure 2-4 Scheme of a membrane extractor .....	12
Figure 2-5 Illustration of a membrane reactor with a membrane distributor .....	12
Figure 2-6 Interfacial membrane contactor.....	13
Figure 2-7 Flow through membrane contactor .....	14
Figure 2-8 Catalytic membrane reactor with catalyst particles supported on membrane wall.....	15
Figure 2-9 Pd-H diagram phases.....	17
Figure 2-10 Catalytic membrane in a gas-liquid reaction.....	19
Figure 2-11 Anthraquinone process for industrial hydrogen peroxide production .....	20
Figure 2-12 Schematic of hydrogen peroxide synthesis with supported palladium.....	21
Figure 2-13 Scheme of different reactions using multifunctional Pd-based membranes .....	23
Figure 4-1 Single ceramic hollow fiber membrane .....	32
Figure 4-2 Assembly to prepare catalytic membrane reactors by sputtering .....	39
Figure 4-3 Pieces of the catalytic membrane reactor located in the XRD equipment.....	45
Figure 5-1 Scheme of experimental set up used in direct synthesis of hydrogen peroxide using a mixture of O <sub>2</sub> /H <sub>2</sub> .....	52

Figure 5-2 Experimental set up used in direct synthesis of hydrogen peroxide.....	53
Figure 5-3 Experimental setup for phenol degradation by in situ generated hydrogen peroxide.....	55
Figure 5-4 Image of the stainless steel reactor housing .....	56
Figure 5-5 Experimental setup for selective nitrate reduction.....	58
Figure 5-6 Experimental setup for hydrodechlorination of 4-Cl-Phenol.....	59
Figure 6-1 ESEM image obtained from the cross section of the 4 nm filtration pore size hollow fiber.....	62
Figure 6-2 Image of the cross section of 1400 nm hollow fiber.....	63
Figure 6-3 ESEM image of bulk of 1400 nm hollow fiber.....	64
Figure 6-4 $\mu$ -XRD analysis carried out over the 4 nm hollow fiber.....	65
Figure 6-5 $\mu$ -XRD analysis performed over the 20 nm hollow fiber.....	66
Figure 6-6 ESEM image of the external surface of the monometallic palladium membrane reactor (CMR1).....	67
Figure 6-7 Close ESEM image of the internal surface of the CMR3 .....	68
Figure 6-8 ESEM image from the external surface of the monometallic Pd membrane reactor (sCMR13).....	69
Figure 6-9 BSE image of the external surface of the CMR5 .....	70
Figure 6-10 Pd distribution on the monometallic Pd membrane reactor (sCMR13) .....	71
Figure 6-11 Electron mapping of different elements from the external surface of the sCMR13 .....	72
Figure 6-12 $\mu$ -XRD analysis performed over the a) internal and b) external surface of the CMR1 .....	75
Figure 6-13 $\mu$ -XRD analysis carried out over the external surface of the a) CMR2, b) CMR3, c) CMR4 and d) CMR5 .....	78

Figure 6-14 $\mu$ -XRD analysis carried out over the sCMR13 .....	79
Figure 6-15 ESEM images of the sCMR15 a) electronic image and b) Backscattering mode image .....	81
Figure 6-16 $\mu$ -XRD analysis carried out over bimetallic catalytic membrane reactor (CMR7).....	82
Figure 6-17 Diffractogram obtained from the bimetallic $\text{CeO}_2$ – sputtered Pd, sCMR15 .....	83
Figure 6-18 Diffractogram obtained from the CMR9.....	84
Figure 6-19 HRTEM image of Pd particles on corundum powder after sputtering and particle size distribution .....	85
Figure 6-20 Hydrogen peroxide generation in different palladium active phase CMRs prepared by impregnation.....	88
Figure 6-21 Effect of hydrogen on the in situ generated hydrogen peroxide concentration before and after hydrogen peroxide addition .....	90
Figure 6-22 Hydrogen peroxide generation with bimetallic CMR6 to CMR9 .....	93
Figure 6-23 Hydrogen peroxide generation in different CMR impregnated with two active phase, from CMR10 to CMR12 .....	94
Figure 6-24 Phenol oxidation with CMR1 .....	100
Figure 6-25 Phenol degradation with CMR6, CMR7, CMR8 and CMR9	102
Figure 6-26 Catalytic phenol oxidation with a Pd-Cerium oxide membrane reactor.....	104
Figure 6-27 Phenol degradation with sCMR14, sCMR15 and sCMR16...	106
Figure 6-28 Phenol oxidation using sCMR17 at 60 °C and consecutive runs .....	107
Figure 6-29 Phenol oxidation using sCMR17 at 80 °C .....	109

Figure 6-30 TPD-MS $m/z = 2$ signal obtained from Pd sputtered on corundum .....	112
Figure 6-31 TPD-MS $m/z = 2$ signal obtained from reactivated Pd-corundum .....	113
Figure 6-32 Hydrodechlorination of 4-Cl-phenol with CMR in continuous mode.....	118

## LIST OF TABLES

Table 2-1 IUPAC classification for porous ceramic membranes .....	10
Table 4-1 Prepared palladium based membrane by impregnation method..	34
Table 4-2 Prepared bi-functional catalytic membrane reactors .....	37
Table 4-3 Pd based and bi functional catalytic membranes prepared by sputtering.....	41
Table 6-1 Average of the Pd crystal sizes calculated for CMR1 to CMR5 .	76
Table 6-2 Catalytic results in hydrogen peroxide generation in monometallic Pd CMRs prepared by impregnation.....	87
Table 6-3 in-situ Pd 3d XPS data recorded over CMR1 after treatment under H <sub>2</sub> and H <sub>2</sub> O <sub>2</sub> .....	91
Table 6-4 Catalytic results in hydrogen peroxide generation with bimetallic Pd CMRs prepared by impregnation.....	95
Table 6-5 Summarized results obtained for the different catalytic membrane reactors in the hydrogen peroxide generation .....	97
Table 6-6 TPD program and the aim of each step .....	111
Table 6-7 Selective reduction of nitrates with CMRs under continuous operation regimen .....	116

UNIVERSITAT ROVIRA I VIRGILI  
DEVELOPMENT OF A NOVEL CATALYTIC MEMBRANE REACTOR: APPLICATION IN WASTEWATER  
TREATMENT  
Oscar Antonio Osegueda Chicas  
Depósito legal:

## **Chapter 1. Introduction**

Human well-being has been seriously affected by changes in water cycles. The availability of freshwater and its use are keys of human development and its future sustainability. In fact, there is an increasing concern about the quality and quantity of freshwater and groundwater resources for life supporting and environmental needs. The quality of water is impacted by numerous of human activities like agriculture, industry, mining, human waste disposition, population growth, urbanization and the climate change [1].

There are some alarming data about water pollution published by the United Nation Environmental Programme (UNEP) e.g. the indiscriminate use of pesticides around the world is estimated to be over 2 million metric ton; the industrial activities release around 300-400 tons of heavy metal, solvents, toxic sludge, and other wastes to water bodies; and every year almost 700 new chemicals are introduced into commerce in USA. The world health organization (WHO) states that 2.5 billion people live without improved sanitization, and 80% of developing countries are discharging untreated wastewater to receiving water bodies. All these factors are destroying the natural ecosystem and the natural cycle of water [2].

These social and environmental concerns have been stimulating and developing emerging technologies to treat industrial effluents. The advanced oxidation processes (AOPs) are attractive alternatives for destroying toxic organic contaminants. These chemical oxidation techniques operate at or near ambient temperature and pressure, and they are based on the generation of reactive hydroxyl radicals ( $\bullet\text{OH}$ ) that are able of mineralizing harmful organic contaminants [3-4]. One of the most known AOP is the catalytic

Fenton reaction. This commercial remediation technique uses hydrogen peroxide ( $\text{H}_2\text{O}_2$ ) and small amount of ferrous ions ( $\text{Fe}^{2+}$ ) which catalyze the generation of hydroxyl radicals. However, Fenton reaction possesses several drawbacks such as: it works under acid conditions (range of pH 2.5 to 3.5), not very high efficiency of the oxidant, and the catalyst recovery requires several steps that increase the operational costs. Therefore, different approaches have been developed to turn the homogeneous Fenton reaction to heterogeneous one, known as Fenton-like processes. Indeed the catalytic oxidation reaction with a solid catalyst and hydrogen peroxide, called catalytic wet hydrogen peroxide oxidation (CWHPO), is more attractive for wastewater remediation in terms of reuse and recovery of the catalyst compared to Fenton reaction.

Catalytic membrane reactors (CMRs) appear to be an attractive alternative to increase the efficiency of CWHPO. The CMRs possess considerable advantages over conventional heterogeneous catalysts, e.g. they work under a wide range of temperatures and pressures, they are pH resistant in the entire range, and the oxidant can be very efficiently dosed and uniformly delivered to the active catalyst sites. These features of the CMRs contribute in improving the contact between the contaminated water and the chemical oxidant and at the same time the catalyst deactivation can be avoided; if desired, complete mineralization of the organic pollutants can be achieved.

This work is focused on the application of the CMRs for direct oxidation of a model organic compound by the in-situ generated hydrogen peroxide. The inherent properties of the CMRs permit the direct synthesis of hydrogen peroxide starting from  $\text{H}_2$  and  $\text{O}_2$  using noble metal as an active phase. The catalytic membrane reactors have a well-defined three phase contact zone

for gas-liquid reactions. The gas and liquid phases are introduced from the opposite sides of the membrane into the reaction zone. The gas and the liquid reach the incorporated in the membrane catalytic active phase from the both sides and the reaction, i.e. hydrogen peroxide generation, takes place in the three phase contact point. The characteristics of the CMRs avoid the formation of an explosive mixture and the efficiency of the hydrogen consumption can be increased considerably. Because of the simplicity of the process it can be performed directly in the wastewaters effluents, where the in situ generated hydrogen peroxide will be directly involved in a subsequent reaction of e.g. organic matter oxidation.



## Chapter 2. Introduction to membrane reactors

According to the International union of pure and applied chemistry (IUPAC), a membrane reactor (MR) is a multifunctional reactor combining a membrane-based separation and a chemical reaction in one single unit [5-8]. In this way, the membrane not only plays the role of a separator, but also a reaction can take place in the same MR as it is represented in the Figure 2-1. Therefore, membrane reactor becomes an attractive alternative to traditional reactor (TR) owing to their characteristic to separate the final products from the reaction stream [9].

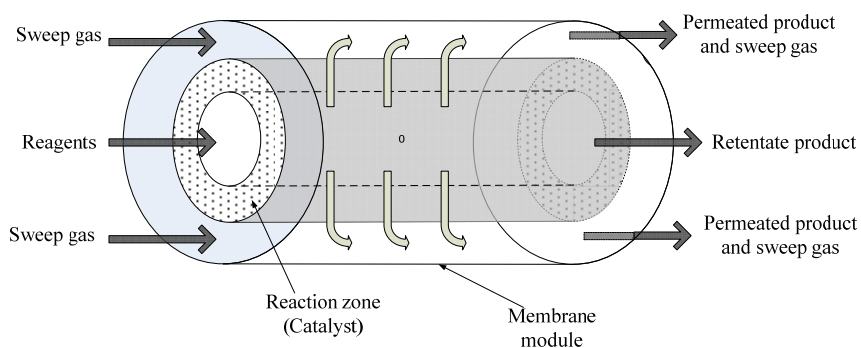


Figure 2-1 Scheme of a membrane reactor

From a reaction point of view, when a product is selectively removed (*shift effect*) the thermodynamic equilibrium can be overcome, thus the overall effects are higher: net reaction rate and residence time, conversion, selectivity, and yield [4,6,10].

All these effects observed in membrane reactors imply a reduction of the reactor volume. Furthermore, membrane reactor can be operated under mild conditions compared with the current conditions in industrial processes. In

fact, MRs are considered as a potential technology in many industrial fields including biotechnological applications, pharmaceutical sector, petrochemical, chemical plants, energetic sector and environmental applications, among others [5,10].

The application of MRs is gaining an increasing worldwide interest due to their operative advantages compared with TRs. In addition, MRs are in accordance to the logic of process intensification (PI) strategy. PI is an innovative alternative for sustainable growth, and it is a designed strategy to obtain benefits in manufacturing and processing. It is based on the reduction of the size of industrial equipments, capital costs, energy consumption, environmental impact, and increasing efficiency of the industrial plant and safety controls, and improving industrial automatization [11]. In order to satisfy the process intensification strategy, MRs have to be designed according to process parameters e.g. expected productivity, operational temperature and pressure, and taking in to account certain characteristics of the membrane like separation selectivity, mechanical and chemical resistances, investment costs, lifetime, among others.

Some aspects of the different types of membranes are presented below especially remarking their properties that can be directly implicated to their potential use as base for catalytic membrane reactors.

## **2.1 Membranes for membrane reactors**

Membrane science and technology is an important field in chemical, process and material engineering, which aims to discover new materials, provide special morphological and structural properties, obtain selective permeations, and other features.

The selection of the membrane to be used in membrane reactors depends on parameters such as: i) productivity, ii) separation selectivity, iii) membrane life time, iv) mechanical and chemical stability, v) operative conditions and vi) cost. The membrane with potentially to be employed in the preparation of MR can be classified according to their nature, geometry and separation regimen.

Membranes are classified according to their nature as i) biological or ii) synthetic membranes with respect to their functionality and structure. The biological membranes face several disadvantages such as restrictions in operation temperatures, limitation of biological functions to certain pH conditions, increasing operational costs due to the pre-cleaning processes, low selectivity, and susceptibility to microbial degradation [5-6].

Synthetic membrane can be subdivided in i) organic (polymeric) and ii) inorganic membranes. Polymeric membranes operate at mild temperatures up to 120 °C and are used for fine chemical manufacturing or in bioprocesses. There are wide brands of polymers used for synthesis of polymeric membranes e.g polyethersulfone (PES), polyvinylidenedifluoride (PVDF), etc [12]. Inorganic membranes are more interesting in process engineering as a result of their characteristics and advantages compared with other kind of membranes [6].

## **2.2 Inorganic membranes**

Inorganic membrane science and technology has been developed in the last four decades. Its beginning is dated in 1940, when the first inorganic membranes were used in the enrichment of uranium [13]. Inorganic membranes (IMs) are mainly used in liquid filtration; however, there is a trend to develop IMs for high quality gas separation for sustainable energy

production. There are several materials used in preparation of inorganic membranes. The most common IMs are: carbon [14-15], zeolite [16-18], ceramic membranes [19-29], and metallic [30-34].

Based on the material composition, inorganic membranes have strong advantages in chemical and engineering processes:

- High thermal stability compatible with temperature ranges of 300 – 800 °C, ceramic membranes up to 1000 °C.
- High chemical stability (possible operation under harsh environments).
- Inertness and biocompatibility (application in pharmaceutical and food industry).
- Mechanical strength at high operational pressures.
- Easy purification (cleaning) after fouling.
- Long lifetime.
- Easy incorporation of additional phases with catalytic activity in certain processes.

Actual disadvantages related to the high capital costs, or the fact that manufacturing process is still under development continuously vanish due to the technological achievements in the area.

### **2.2.1 Ceramic membranes**

Ceramic membranes (CMs) are considered as a permselective barrier or a fine sieve. The permeation factor in porous ceramic membrane is governed by the thickness, pore size and porosity of the membrane. CMs are known as composite membranes. In general, ceramic membranes can be formed by a support layer, and a thin skin layer where the filtration takes place (Figure

2-2). The support layer provides the mechanical strength to the membrane. However, some membranes can be designed as a single wall membrane, where the wall can be symmetric or asymmetric [19].

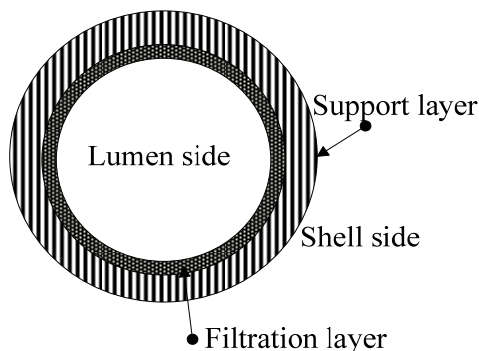


Figure 2-2 Representation of a tubular ceramic membrane

The most common materials used in the fabrication of ceramic membranes are alumina ( $\text{Al}_2\text{O}_3$ ), titania ( $\text{TiO}_2$ ), zirconia ( $\text{ZrO}_2$ ), silica ( $\text{SiO}_2$ ), or a combination of these metal oxides. Ceramic membranes can be divided into three types according to IUPAC guide as is presented in the Table 2-1. The porous membranes are classified according to the filtration pore size. Macroporous membranes provide high permeability, and they are used as a support in the synthesis of composite membranes, or as a distributor of reagents. Mesoporous membranes have high permeability and low selectivity. These membranes are used in the synthesis of composite membranes. Finally, microporous membranes have low pore size diameter with a potential use in molecular sieve separation [20].

Table 2-1 IUPAC classification for porous ceramic membranes

Porous membrane	Pore size diameter (nm)	Applications	Permeation mechanism
Macroporous	>50	Ultra and microfiltration	Poiseuille
Mesoporous	2-50	Ultra/nanofiltration, and gas separation	Knudsen
Microporous	<2	Gas separation	Sieve

Commercially, there are three available geometric configurations for ceramic membranes: flat, tubular and multichannel monolith. Among these configurations, tubular membranes (e.g. hollow fibers) have gained a considerable attention due to their versatility. The main advantage of hollow fiber membranes is high surface-to-volume ratios compared to other membrane systems (e.g. disc, plates and spiral wound). In order to increase the packing density, hollow fibers modules (see Figure 2-3) have densities around  $9000 \text{ m}^2 \text{ m}^{-3}$ , and they can be applied in industrial processes such as filtration of corrosive fluids, high temperature reactors, solid oxide fuel cells, and as a membrane contactor with catalytic activity. Hollow fibers are commonly prepared with  $\text{Al}_2\text{O}_3$  or perovskite materials [21-24].

All the mentioned characteristics of the ceramic membrane make them a potential material to be used as support in catalytic membrane reactors.



Figure 2-3 Hollow fiber membrane and an industrial cartridge, from 5

### 2.3 Function of ceramic membrane in membrane reactors

The membranes can have three different roles in membrane reactors: i) product removal (membrane extractors), ii) introduction and spreading of reactants to the reaction zone (membrane distributors) and iii) facilitate the contact between reactants and chemical catalyst (membrane contactors) [35]. Very important feature of the membranes is that they can be used as a support of catalyst active phases that combined with backward mentioned characteristics converts them to catalytic membrane reactors.

#### 2.3.1 Membrane extractors

In this configuration the membranes withdraw a reaction product from the reaction zone. Membrane reactors acting as extractors have higher conversions due to the shift effect in the thermodynamic equilibrium. A scheme of a membrane extractor is showed in the Figure 2-4.

In general, this configuration requires a selective membrane for one of the products. Membrane extractors are used in etherification, and dehydrogenation reactions where is required selective removal of water or hydrogen respectively [36].

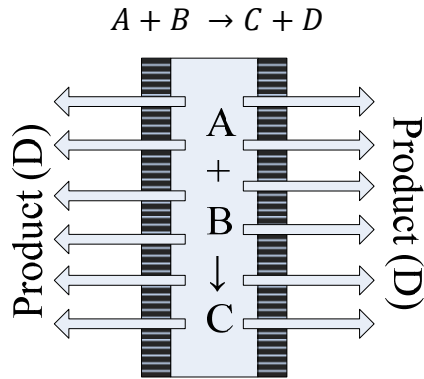


Figure 2-4 Scheme of a membrane extractor

### 2.3.2 Membrane distributors

In membrane distributors, the membrane doses one of the reagents in a controlled form to the reaction zone as is represented in the Figure 2-5. A controlled dosing of reagent (A) to the reaction zone allows enhancing the reaction selectivity. This configuration can be used in gas phase reaction e.g. to maintain the mixture below the explosion limits. Selective oxidation and hydrogenation reactions can be performed in membrane reactors with membrane distributors due to the exceptional performance of the membrane [37-40].

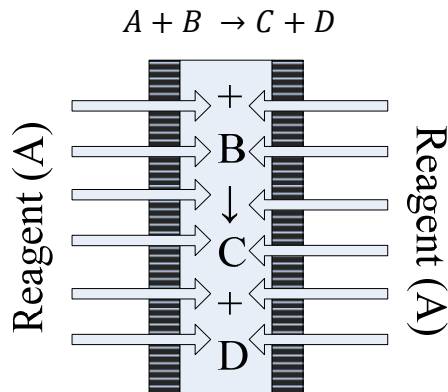


Figure 2-5 Illustration of a membrane reactor with a membrane distributor

### 2.3.3 Membrane contactors

The membrane contactors are used to facilitate the contact between the reagents and catalyst. In membrane contactors, the membrane can be intrinsically active as a catalyst or the catalyst can be supported onto the membrane matrix. There are two possible ways to bring the reagents to the catalytic sites. The first option is the interfacial membrane contactors mode, where the reactants are separately dosed from each side of the membrane (lumen/shell side), and they react over the catalytic site (see Figure 2-6). This configuration is mainly used in reactions with non-miscible reagents. And there is no restriction in the use of gaseous reactants because there is not risk of formation of explosive or flammable atmospheres [41-44].

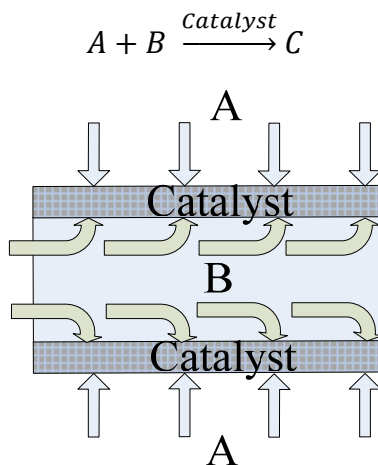


Figure 2-6 Interfacial membrane contactor

The second operation mode is the flow through membrane contactor (FTCMR). A mixture of reactants is forced to flow through the non-permeability selective catalytic porous membrane. The membrane provides a region where the reaction will take place; operational parameters can be

adjusted to improve residence time, and catalytic activity. A scheme of a flow through membrane contactor is depicted in the Figure 2-7.

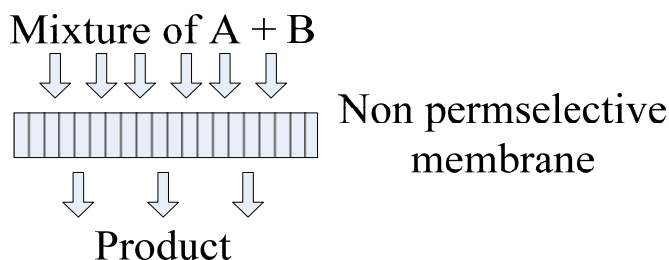


Figure 2-7 Flow through membrane contactor

This configuration provides a reaction place with short residence time with a high catalytic activity. As the catalyst is placed inside the membrane pores and the reactants flow through the pores, the resulting intensive contact between reagents and active phase (catalyst) induce higher activities [45-50].

The notion of membrane contactors is closely related with catalytic reaction, therefore in reaction engineering they are known as catalytic membrane reactors (CMRs).

## 2.4 Catalytic membrane reactors

The term catalytic membrane reactor (CMR) refers to a contactor membrane reactor used to carry out a catalyzed reaction, where the membrane can have separation properties. There are two types of membranes used in CMR: i) membranes intrinsically active for catalytic reactions, e.g. perovskites or ion/electron conducting ceramics, metallic dense membranes, zeolites, metal

oxide compounds, etc. and ii) inert membranes with an incorporated catalytic active phase as it is represented in Figure 2-8 [5].

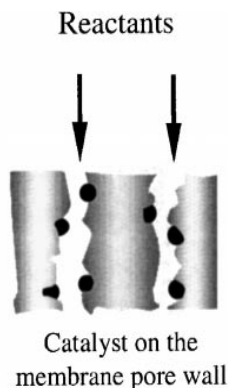


Figure 2-8 Catalytic membrane reactor with catalyst particles supported on membrane wall, from 36.

Several technical aspects have to be taken into account when dealing with the catalyst-on-membrane, the typical considerations about conventional heterogeneous catalysts: catalyst stability, size and shape of catalyst particles, catalyst loading, dimension and distribution of catalyst, catalyst stability under reaction conditions as well as the features related to the membrane (porosity, pore size, permeability etc.).

The catalyst can be introduced in the membrane by means formation of covalent binding, electrostatic interactions, weak interaction (Van de Waals or hydrogen bonds) or physically embedded in the matrix of casting membrane material [10, 23]. The CMRs can be operated in gas-gas applications [51-54], liquid-liquid applications [55-57] or gas-liquid reactions [58].

### 2.4.1 Palladium-based catalytic membrane reactors

Pd-based membranes are mainly applied in the field of gas separation and, particularly, in the issue of the hydrogen rich-stream purification. Hydrogen permeates through Pd-based membrane by means solution/diffusion mechanism, which evolves six important steps [34]:

1. Dissociation of molecular hydrogen at the gas/metal interface.
2. Adsorption of atomic hydrogen on membrane surface.
3. Dissolution of atomic hydrogen into palladium matrix.
4. Diffusion of atomic hydrogen through palladium matrix.
5. Recombination of atomic hydrogen to molecular hydrogen at the gas/metal interface.
6. Desorption of molecular hydrogen on membrane surface.

However, the commercialization of pure Pd-based membranes is limited by several factors:

- Susceptibility to embrittlement phenomenon when exposed to pure hydrogen at temperatures below 300 °C.
- Deactivation by carbon compounds at temperature above 450 °C.
- Irreversible poisoning by sulphur compounds.
- The high cost of Pd.

The reduction of operating costs can be achieved by the replacing of pure Pd by bimetallic palladium alloys such as Pd<sub>77</sub>Ag<sub>23</sub>, Pd<sub>58</sub>Cu<sub>42</sub> or Pd<sub>94</sub>Ru<sub>6</sub> (%wt.) Furthermore, this assembly reduces the lattice distortion in the membrane upon hydriding and dehydriding effects (*hydrogen embrittlement*) at temperature lower than 300 °C. This effect is observed in the Pd-H diagram

phase (Figure 2-9) by the formation of alpha and beta phases of palladium, and the consequent lattice expansion [5].

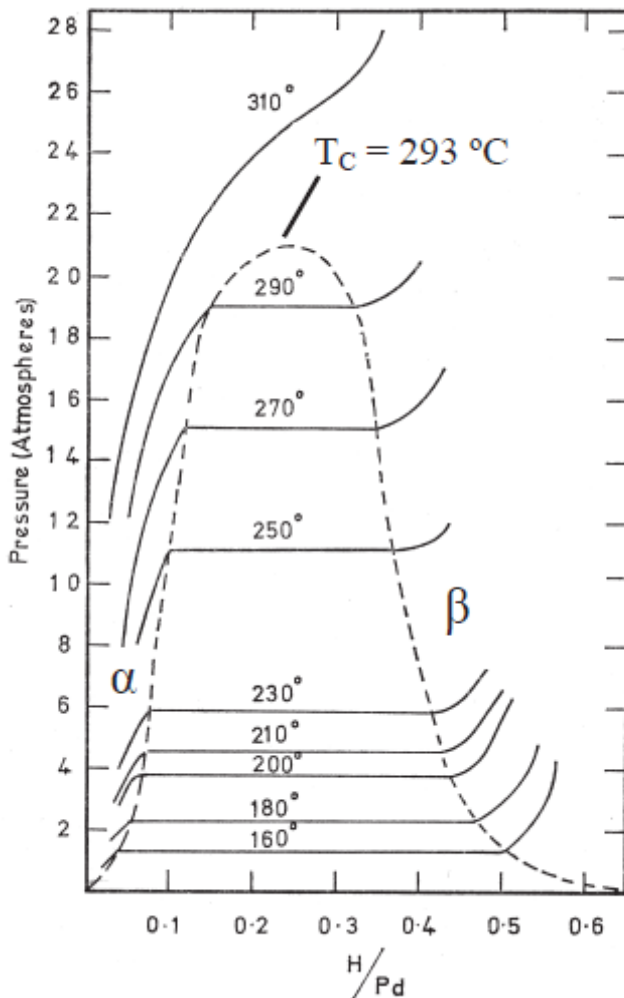


Figure 2-9 Pd-H diagram phases

#### 2.4.2 Preparation of palladium-based membranes

Nowadays, a great effort has been made in the reduction of the amount of Pd supported over porous membrane. Surface engineering has developed several techniques for metal coating e.g. physical vapor deposition (PVD),

chemical vapor deposition (CVD), ion implementation, sol-gel, electrodeposition, among others [8].

Physical vapor deposition consists in the evaporation of a solid material (palladium or a palladium-alloy) under a vacuum system by means of physical techniques such as thermal evaporation, sputtering, etc. This method allows a controllable layer formation. Spray pyrolysis, sputtering, and magnetron sputtering are some examples of physical deposition methods.

Chemical vapor deposition is based on a chemical reaction of a metal complex in gas phase at controlled temperature. The desired metal is deposited on the support by nucleation. PVD and CVD are commonly used techniques in the preparation of Pd-based membrane for hydrogenation/dehydrogenation membrane reactors [30-31].

### **2.4.3 Palladium-based membrane reactors in gas-liquid reactions**

Pd-based membrane reactors can be used in gas-liquid applications. In this design, the liquid and the gas are brought in close contact to the catalytic membrane, as it is represented in the Figure 2-10. The membrane works as an interface between liquid and gas phases where the reaction will take place [58].

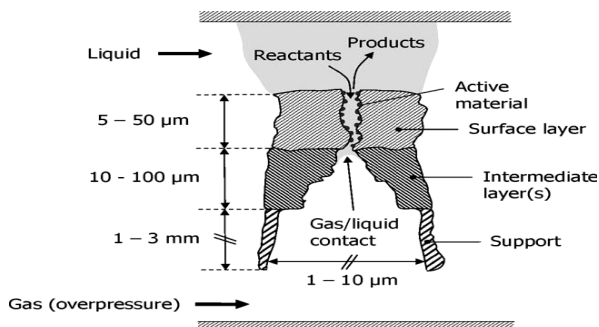


Figure 2-10 Catalytic membrane in a gas-liquid reaction, from 59

Membranes with built-in Pd catalyst for gas-liquid reactions have been mainly used in hydrogenation reactions such as: i) (hydrodechlorination) Chlorobenzene to benzene, ii) nitrates to nitrite and  $N_2$  and iii) hydrogenation of edible oils. Moreover, some application in oxidation reaction can be found in the literature [59].

## 2.5 Selective oxidation of hydrogen to hydrogen peroxide

Recently, Pd-based membranes emerged as a promising tool for the direct synthesis of hydrogen peroxide ( $H_2O_2$ ). Hydrogen peroxide is an important chemical commodity used in almost all areas of human activities e.g. in pulp and paper bleaching, electronic industry, textile industry, chemical synthesis, detergent, environmental applications, among others [60-62].  $H_2O_2$  is a strong oxidant, which can be used for destruction of various organic and inorganic contaminants in aqueous phase.  $H_2O_2$  is mainly produced by means of the industrial anthraquinone oxidation (AO) process (see Figure 2-11). The anthraquinone process consists of a number of sequential steps which involve hydrogenation/oxidation of anthraquinone, hydrogen peroxide extraction and purification, and treatment of working

solution. This procedure has been developed by *IG Farben Industries* (Germany) in 1940 and widely applied in many companies [61].

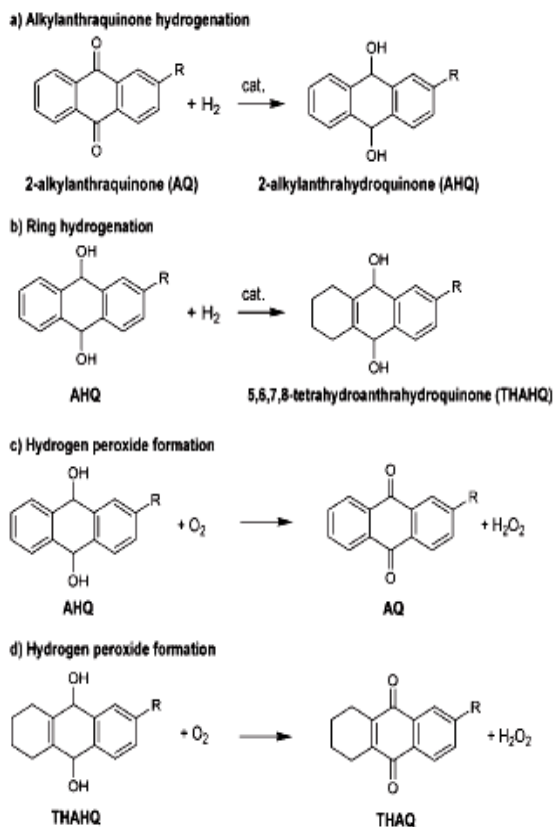


Figure 2-11 Anthraquinone process for industrial hydrogen peroxide production,  
from 61

However, due to the negative economical and environmental aspects of this process, there has been strong interest in replacing it with an alternative approach. In principle, hydrogen peroxide can be straightforward produced from its elements by a direct oxidation of hydrogen as it is represented in the following reaction [63-67]:



The scheme of  $H_2O_2$  formation via palladium-catalyzed  $H_2$  oxidation is depicted in Figure 2-12. Widely accepted catalyst for this reaction is the Pd. It can be supported on the surface of activated carbon, silica or zeolite. The basic mechanism consists of chemisorption and dissociation of molecular hydrogen to atomic hydrogen over reduced state of palladium surface. Then, molecular oxygen reaches and reacts with two atomic hydrogen forming hydrogen peroxide [68-76].

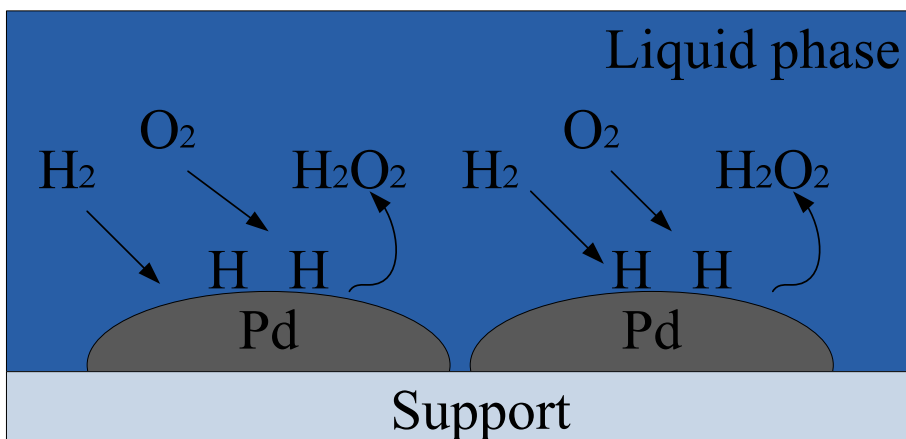


Figure 2-12 Schematic of hydrogen peroxide synthesis with supported palladium

The direct synthesis route can reduce investment and operation cost. However, one has to be aware that the direct synthesis of  $H_2O_2$  is a complex process including undesirable side reactions [77-81]:





Water formation,  $H_2O_2$  hydrogenation and  $H_2O_2$  decomposition reactions can be overcome by the selection of catalyst or an appropriate liquid phase, use of additives and promoters, and operating condition. The main issue of this approach is the high risk of explosive hydrogen/oxygen mixtures under a wide range of concentrations [78-82]. Hydrogen has a low explosive limit (LEL) of 4% and an upper explosive limit (UEL) of 75%, both values referenced by volume of air [61].

$H_2$  and  $O_2$  have to reach the palladium surface to react and produce hydrogen peroxide. As only the metal outer surface is involved in the reaction, it is believed that Pd deposited as nanoparticles will highly improve the process, due to the high surface/bulk ratio of the nanoparticles [83-86]. Furthermore, the direct synthesis of hydrogen peroxide can be performed using catalytic membrane reactors. CMRs provide the possibility to enhance the contact between hydrogen and oxygen, also there is a better distribution of reactant gases without risk of explosion; in a diverse number of publications it is combined the characteristic of Pd-based catalytic membrane reactors with the direct synthesis of hydrogen peroxide [87-94].

## **2.6 Pd-based membranes as a tool for destruction of contaminants in water**

Supported-Pd and Pd-based bimetallic catalysts are capable to activate  $H_2$  and catalyze reductive transformation of a number of water contaminants (in detailed described in Figure 2-13). More recently, Pd-based membranes have also been explored as a tool for chemical oxidation of organic pollutants with  $H_2O_2$  [5, 59]. Moreover, when the system is enriched with a

redox active metal or metal oxide that is capable to activate  $\text{H}_2\text{O}_2$ , highly reactive species like hydroxyl radicals ( $\cdot\text{OH}$ ) can be formed (2.6.1). A simplified scheme of reactions occurring in a system with ‘multifunctional’ Pd-based membrane is depicted below (Figure 2-13).

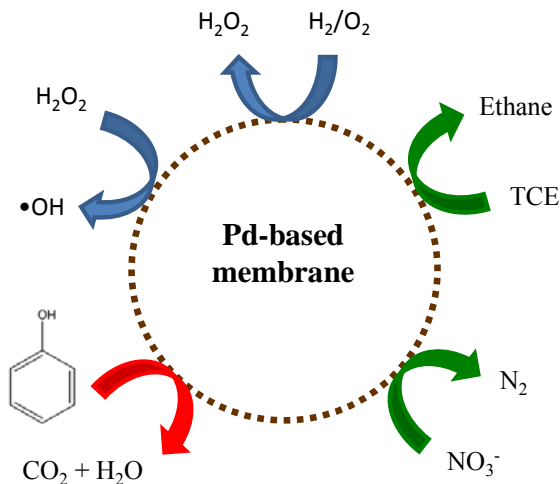


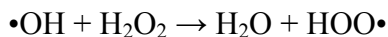
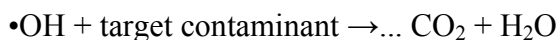
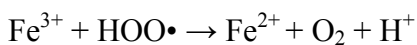
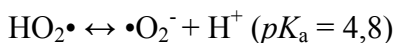
Figure 2-13 Scheme of different reactions using multifunctional Pd-based membranes

### 2.6.1 Chemical oxidation of organic contaminants

In case of contaminated groundwater, industrial effluents and wastewater with organic pollutants, chemical oxidation processes are the most universal tool for their treatment. Phenols are one of the most abundant pollutants in industrial wastewater. They are commonly employed in petrochemical, chemical, pesticide, paint, and textile industries. The toxicity of phenol is well known (lethal concentration 50%,  $\text{LC}_{50} = 3,9 \text{ mg L}^{-1}$ , and the increasing environmental consciousness has made more restrictive environmental legislation and stricter standards for industrial effluents. The

environmental protection agency (EPA) established a value of 0,05 mg L<sup>-1</sup> of phenol in wastewater for the pharmaceutical industry. Also, phenols compounds can react during the chlorination process of drinking water to produce chlorinated compounds; and those chlorinated compounds have higher toxicity and they can influence the taste of drinking water at even low concentration (0,002 mg L<sup>-1</sup>) [95-98].

AOPs are based on generation of reactive radicals, mainly the hydroxyl radical (•OH), which is able to oxidize a wide range of organic compounds. Ozone and hydrogen peroxide are the most often-used oxidants to generate •OH. Short-wave ultraviolet (UV) irradiation, catalysts or a combined application of O<sub>3</sub> and H<sub>2</sub>O<sub>2</sub> are used to initiate the reaction [99-100]. Catalytic activation of H<sub>2</sub>O<sub>2</sub> is achieved, e.g., by the Fenton mechanism presented in an abbreviated form [101]:



The classical Fenton reagent consisting of a homogeneous solution of iron ions and hydrogen peroxide, however, faces several operating problems. The use of metal salts as catalyst requires their subsequent removal from the treated water, mostly as iron oxide sludge, and it is necessary to work at acidic pH conditions (about pH 3) in order to achieve acceptable conversion

rates. These shortcomings can be prevented by replacement of dissolved iron ions by a solid catalyst (so-called heterogeneous Fenton-like catalyst). The reaction pathways are considered to proceed likewise in homogeneous Fenton reaction according to the Haber and Weiss mechanism [101-102].

In recent years, there have been made enormous efforts to develop catalysts suitable for practical application owing the following properties: i) a high reactivity towards removal of contaminant ii) efficient  $H_2O_2$  utilization, iii) stability over a broad range of working conditions (pH, temperature), and iv) environmental compatibility. Two approaches are followed when dealing with the heterogenization of Fenton system: i) catalysts supported on porous materials such as clays, silicates, polymers and carbon materials and ii) free catalyst particles, mostly consisting of metals or metal oxides [102].

A step forward is the in-situ generation of oxidizing agents by means of Pd-containing membranes [103-115]. The in-situ generation of hydrogen peroxide has been studied and coupled to different chemical processes. For example, Niwa et.al proposed a Pd-based membrane for benzene oxidation in a gas-gas system. The concept is based on the aromatic hydroxylation by in-situ generated  $H_2O_2$  [116-127]. In this system  $H_2$  and  $O_2$  are separately supplied to the catalytic zone, and the membrane reduces the risk of explosive atmosphere formation [41].

So far, Pd-based membranes have not been explored as an alternative for the heterogeneous Fenton reaction.

### **2.6.2 Catalytic reduction of water pollutants**

The Pd-based catalysts have been widely studied in diverse processes concerning water contaminants reduction: i) halogenated organics, ii) oxyanions, and iii) nitrosamines. There are particular emphasis for reduction

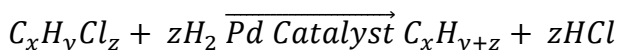
of nitrates ( $\text{NO}_3^-$ ), nitrites ( $\text{NO}_2^-$ ), bromates ( $\text{BrO}_3^-$ ), 1,2-dichloroethane, chlorinated benzenes, and polychlorinated biphenyls (PCBs) due to their toxic effect in living organisms. In general, Pd-based catalysts are more active for catalytic reduction compared with other metal supported catalyst e.g. platinum (Pt), iridium (Ir), rhodium (Rh), copper (Cu) or zinc (Zn). Moreover, supported bimetallic Pd-based catalysts are called to improve the catalytic activity and selectivity [128].

### Catalytic reduction of halogenated organic compounds

There is an environmental concern about chlorinated organic compounds (COCs). COCs are considered as toxic and carcinogenic substances, and unfortunately they can be found in industrial effluent, groundwater, surface water and soils. Chlorophenol and trichloroethylene (TCE) are the most common COCs used in several industrial applications: i) paint fabrication, ii) elaboration of degreasing agent, iii) herbicides, and iv) organic synthesis [129-130].

Chemical treatment by catalytic hydrodechlorination (HDC) is a promising approach for water decontamination. Palladium and Pd-based supported catalysts have shown high activity and selectivity toward hydrodechlorination in liquid phase. However, Pd catalysts are sensitive to deactivation in wastewater due to precipitations, dissolved organic matter, and poisoning compounds e.g. heavy metals and sulphur compounds [131-133]. Catalyst deactivation can be avoided by: i) optimization of the catalyst support, and ii) addition of doping elements to selectively bind the deactivation [133-140].

The HDC mechanism involves the adsorption of chlorinated compound and dissociative adsorption of H<sub>2</sub> followed by Cl removal and H addition steps leading less harmful products [141-145]. The overall HDC reaction is:



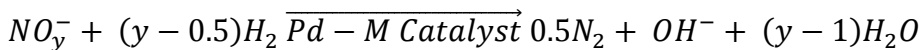
### Selective reduction of nitrates

Nitrates are considered as an important environmental problem. Ground and surface water have been contaminated by means of filtration of nitrates and nitrite produced by the industrialized agriculture and livestock manure. The nitrate and nitrite upper limits in drinking water have been set at 50 and 0,5 mg L<sup>-1</sup> respectively by the *drinking water directive (98/83/EEC)* in the European Union (EU) [146].

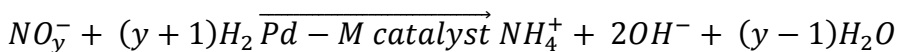
There are some established processes for water denitrification such as ion exchange, biological denitrification and membrane-based reverse osmosis. However, those techniques require post treatment steps of the effluents. Moreover, selective reduction of nitrates by Pd-based catalysts emerges as a promising denitrification process. Catalytic nitrate reduction has to face practical challenges: i) increase the catalytic activity by catalyst formulation, ii) enhance the selectivity toward desired product (N<sub>2</sub>) and iii) design an appropriate reactor system [128].

Pd-Cu based catalyst is the most active catalyst for nitrate reduction, however, different transition metals (Ni, Fe, Sn, Ag and In) have been used in catalyst formulation to improve the activity and selectivity [147].

The accepted nitrate reduction mechanism involves several steps and nitrogen oxyanions e.g. nitrite ( $\text{NO}_2^-$ ), NO and  $\text{N}_2\text{O}$  [148-149]. The overall reaction is:



However, an undesired reaction can take place to ammonia ( $\text{NH}_3$ ), which has a higher toxic effect compared with the nitrate:



### **Chapter 3. Aim and objectives**

The aim of this research project was to develop a novel approach for wastewater treatment using catalytic membrane reactors. The focus was to prepare membrane reactors with catalytic activity, and use them in three phase reactions as a contactor CMR.

In order to attain the aim of this work, several objectives were proposed to evaluate the progress in our main purpose:

Select adequate commercial ceramic membranes to be used as supports for the active phases in the preparation of catalytic membrane reactors.

Develop different methods to prepare catalytic membrane reactors to be used in the generation of hydrogen peroxide/oxidation of model compound reaction.

Choose different reduced metals and metal oxides as active phases for the generation of hydrogen peroxide reaction and heterogeneous Fenton reaction.

Characterize the catalytic membrane reactors with the classical heterogeneous catalysis characterization tools such as: i) scanning electron microscopy (SEM), ii) environmental scanning electron microscopy (ESEM), iii) Transmission electron microscopy (TEM and HRTEM), iv) physisorption, v) chemisorptions, and vi) temperature programmed desorption (TPD) to gather morphologic/structural and chemical information from the CMRs.

Design a properly experimental setup to screen, check and measure the generation of hydrogen peroxide using the CMRs.

Establish a suitable experimental setup to test CMRs in the oxidation of a model organic compound via in situ generated hydrogen peroxide.

Propose an appropriated module reactor to operate the CMRs in a continuous mode.

Test the CMRs in the catalytic reduction of water pollutants using the continuous module reactor.

Make appropriate calculation in order to scale up the developed process for treatment of real wastewater.

## **Chapter 4. Preparation and characterization of catalytic membrane reactors**

This chapter gives an overview of the experimental procedures developed in the preparation and characterization of catalytic membrane reactors. The membrane reactors were prepared and tested in different catalytic reactions e.g. oxidation of hydrogen to produce hydrogen peroxide, catalytic wet hydrogen peroxide oxidation, hydrodechlorination of chlorinated compounds and selective reduction of nitrates.

Morphology and structural properties of starting hollow fibers and membrane reactors were analyzed by electron microscopy techniques such as SEM, ESEM and TEM. These characterization techniques provide important information about membrane surface, texture and cross section. Also, typical characterization techniques in heterogeneous catalysis like nitrogen physisorption, micro X-ray diffraction analysis ( $\mu$ -XRD) among others were employed to determine physical and chemical properties from initial materials and resultant catalytic membranes, as well the amount of incorporated active phases over the bulk and outer membrane surface.

### **4.1 Preparation of catalytic membrane reactors**

This section describes the protocols followed in the preparation of the catalytic membrane reactors starting from commercial ceramic membranes. Different catalyst phases were chosen, loaded and tested in order to achieve the objectives of this thesis.

#### 4.1.1 Ceramic hollow fibers – starting material

The catalytic membrane reactors were prepared starting from commercial microfiltration and ultrafiltration ceramic membranes. The ceramic hollow fibers were purchased from Ceparation™. Each hollow fiber is made of alpha alumina ( $\alpha\text{-Al}_2\text{O}_3$ ) providing exceptional chemical resistances to different chemicals in a wide range of pH (1-14). Also, these fibers have high thermal stability so they can be operated up to 1000 °C. The chosen length of the used fibers was 130 mm with outer diameter 3 mm and internal diameter 2 mm. The Figure 4-1 shows an example of those hollow fibers used in this work.



Figure 4-1 Single ceramic hollow fiber membrane

Ceramic hollow fibers with different nominal filtration pore sizes (4, 20, 100, 200, 500, 800 and 1400 nm) were selected to prepare the CMRs.

The hollow fibers were modified by two different protocols. The first protocol was carried out by means the incipient wetness technique. This impregnation method was used to prepare two types of CMRs: i)

monometallic palladium membranes, and ii) mixed double active phase membranes, which are bi-functional catalytic membranes made from a mixture of metallic Pd with a transition metal oxide. In some cases instead of metal oxide in the membranes was generated copper aluminate with a chemical structure of copper spinel. These reactors have been prepared after acid hydrolyzation of the alumina, impregnation with  $\text{Cu}(\text{NO}_3)_2 \cdot 6\text{H}_2\text{O}$  followed by calcination at high temperature. Then, this membrane was impregnated with a palladium precursor solution, finally to obtain palladium copper spinel membrane reactors [150].

Novel procedure for the preparation of CMRs has been proposed and developed. This method aims to incorporate the palladium in the specific zone over the surface of the ceramic membrane where the studied reactions take place by means of sputtering technique. The main goal of this protocol was to reduce the amount of noble metal as well as to highly increase its dispersion. It has been applied in the preparation of the two types membrane reactors, the monometallic Pd ones as well as the double mixed membranes [151].

#### **4.1.2 Preparation of monometallic palladium membrane by impregnation method**

First of all, five different fiber membranes with nominal filtration pore sizes of 4, 20, 100, 500 and 1400 nm were selected to prepare monometallic palladium membrane. Initially each fiber was dried in an oven at 120 °C during three hours to remove any remaining humidity. Then, the dry fibers were impregnated with a concentrated catalyst precursor solution using incipient wetness technique. The concentrated solution was prepared using palladium (II) chloride ( $\text{PdCl}_2$ ) (Johnson Matthey) dissolved in Milli-Q

water acidified with hydrochloric acid (Fluka) to enhance the total dissolution of PdCl<sub>2</sub> salt. Thereafter, the impregnated membranes were calcined at 350 °C during 6 hours with a temperature rate of 10 °C min<sup>-1</sup>. Finally, a reduction step was carried out at 350 °C during 3 hours under flowing hydrogen (50 NmL min<sup>-1</sup>).

The amount of palladium loaded onto the catalytic membrane was calculated by the weight differences between the original fiber membrane and the modified membrane. The CMRs prepared with this protocol are summarized in the Table 4-1.

Table 4-1 Prepared palladium based membrane by impregnation method

Catalytic membrane reactor	Nominal filtration pore size (nm)	Active phase (wt %)
CMR1	4	1.1% Pd
CMR2	20	0.8% Pd
CMR2	100	0.9% Pd
CMR4	500	0.8% Pd
CMR5	1400	1.0% Pd

#### 4.1.3 Preparation of copper aluminate membrane with palladium active phase by impregnation method

The copper aluminate belongs to the family of spinel materials. The spinel materials are defined by the chemical formulation A<sup>2+</sup>B<sub>2</sub><sup>3+</sup>O<sub>4</sub><sup>2-</sup>.

The protocol followed by Alexandre et.al [152] was modified and used to prepare copper aluminate membranes. A hollow fiber with 200 nm of nominal filtration pore size was selected in the preparation of the spinel membrane. The fiber membrane was firstly washed in nitric acid 10% v/v

(Fisher chemical), and after that it was dried in an oven at 120 °C for 3 hours. Then, the dried fiber was impregnated with a concentrated solution of  $\text{Cu}(\text{NO}_3)_2 \cdot 6\text{H}_2\text{O}$  (Aldrich). Afterward, the membrane was placed in an oven, and it was calcined at 900 °C (temperature rate of 5 °C  $\text{min}^{-1}$ ) during 8 hours to obtain the copper spinel structure ( $\text{Cu}^{2+}\text{Al}_2^{3+}\text{O}_4^{2-}$ ). Once the thermal treatment has been finished, the modified membrane was washed with diluted nitric acid solution to remove the excess of CuO deposited in the surface of the membrane.

Finally, the spinel membrane was impregnated with a concentrated palladium precursor solution using incipient wetness technique. The metallic palladium phase was obtained following the protocol described in the section 4.1.2. The amount of incorporated Pd was calculated by the weight differences of the prepared copper spinel membrane and the final bi-functional membrane. The Table 4-2 shows the percentage of palladium loaded in the copper spinel membrane.

#### **4.1.4 Preparation of mixed double active phases, metallic palladium – metal oxide, membranes by impregnation method**

Ceramic membranes with different nominal filtration pore size (200, 500 and 800 nm) were selected in the preparation of mixed double active phases membrane reactors. Those membranes were selected in order to reduce any potential high trans-membrane pressure during the gas-liquid reactions.

As it was done in the preceding protocol, five fibers were dried in an oven during three hours at 120 °C. Then, the dried membranes were impregnated with a concentrated with one or mixture of catalysts precursor solutions such as  $\text{Ce}(\text{NO}_3)_3$  (Aldrich),  $\text{FeCl}_3$  (Sigma Aldrich),  $\text{Ti}(\text{Ter-butylate})_4$

(Sigma Aldrich),  $\text{AgNO}_3$  (Sigma Aldrich) and  $\text{HAuCl}_4 \cdot 3\text{H}_2\text{O}$  (Sigma Aldrich) by incipient wetness impregnation method.

Afterward, the impregnated membranes were calcined in an oven at  $400\text{ }^\circ\text{C}$  during four hours with a temperature rate of  $10\text{ }^\circ\text{C min}^{-1}$ . This thermal treatment allows decomposing the catalyst precursor into the respective metallic oxide ( $\text{CeO}_2$ ,  $\text{Fe}_2\text{O}_3$ ,  $\text{TiO}_2$ ,  $\text{Ag}_2\text{O}$ ,  $\text{Au}_2\text{O}_3$ ). The amount of metallic oxide incorporated onto the membrane was calculated by difference in the weight of the original membrane and the resultant modified membrane.

In addition, another membrane was impregnated with a concentrated solution of a  $\text{Ce}(\text{NO}_3)_3$ , followed by a second impregnation with a concentrated solution of  $\text{FeCl}_3$ . Afterward, a thermal treatment at  $400\text{ }^\circ\text{C}$  was carried out to attain a double metal oxide membrane.

Finally, the modified membranes were impregnated with a concentrated palladium (II) chloride (Johnson Matthey) solution. Afterward, the membranes were calcined at  $350\text{ }^\circ\text{C}$  during 6 hours with a temperature rate of  $10\text{ }^\circ\text{C}$ . Finally, a reduction step was carried out to activate the palladium, this procedure was done at  $350\text{ }^\circ\text{C}$  with flowing  $\text{H}_2$  ( $50\text{ mL min}^{-1}$ ) during 2 hours. The mixed double active phase membranes are summarized in the Table 4-2.

Table 4-2 Prepared bi-functional catalytic membrane reactors

Catalytic membrane reactor	Nominal filtration pore size (nm)	Active phase (wt. %)
CMR6	200	CuAl <sub>2</sub> O <sub>4</sub> – 1.2% Pd
CMR7	500	1.3% CeO <sub>2</sub> – 1.2% Pd
CMR8	800	2.7% Fe <sub>2</sub> O <sub>3</sub> – 1.1% Pd
CMR9	500	1.5% TiO <sub>2</sub> – 1.4% Pd
CMR10	200	0.8% Ag <sub>2</sub> O – 1.1% Pd
CMR11	200	1.0% Au <sub>2</sub> O <sub>3</sub> – 1.2% Pd
CMR12	200	1.3% CeO <sub>2</sub> – 1.5% Fe <sub>2</sub> O <sub>3</sub> – 1.2% Pd

As it is shown in the Table 4-2, there are not significant differences in the amount of noble metal loaded over CMR6 to CMR11. However, there is one exception in the TiO<sub>2</sub>-Pd membrane. The CMR9 has a slightly higher amount of palladium phase compared with the other CMRs listed in the Table 4-2.

#### 4.1.5 Preparation of monometallic palladium membrane by sputtering technique

At this point, the CMRs were prepared by an incipient wetness impregnation method. However, this procedure does not allow selective deposition of the active phases onto specific zone of the membranes. As the catalytic membrane reactor will be used as a three phase reactor for liquid-gas reactions, it is important that active phases are located in the outer surface where the reaction will take place; simply, the metal located out of this zone will not take place in the reaction. In order to save the amount of

noble metal introduced to the reactor at the same time it is decreased the economical cost of the CMR's, issue that is in major interest in a further scaling process from laboratory test to industrial plants. It was developed a modified sputtering procedure to incorporate metallic palladium phase onto the outer surface of the ceramic membranes.

Sputtering technique is classified as a physical vapor deposition (PVD) under vacuum. The sputtering procedure involves the removal of atoms from a solid target material. In order to remove those atoms, the target is bombarded with positive ions. The system consists in a vacuum chamber where the target and the membrane are placed. Basically, in sputtering process high energetic particles strike the target transferring its momentum and removing atoms from the target. Those atoms condensate over the membrane surface and produce a thin film in flat surfaces. In order to achieve a homogeneous coating, rotation is necessary for tubular shapes [8, 154-155].

The protocol was carried out as it is described here. Firstly, the hollow fiber was washed with a nitric acid solution (10 % v/v) (Fisher chemical) to hydrolyze the surface of the ceramic membrane, where the palladium atoms will be deposited. After the acid washing, the hollow fiber was dried in an oven at 120 °C for 1 hour. Then, the membrane was placed in a special assembly to be sputtered with palladium atoms. A scheme of the assembly is showed in the Figure 4-2. The assembly consists of small dc motor coupled by means of gears to the support where the membrane is fixed. The current is supplied from 2 x 1.5 V batteries. A membrane rotation velocity was adjusted to 90 rpm. The dimensions of the device takes into account the available free space of the sputtering chamber (K575X sputter coater, Qourom Technologies). The spinning of the membrane is started just before

the device is introduced into the sputtering chamber. During the sputtering process, the base where the membrane is placed is also rotating assuring homogeneous deposition of the Pd on the outer surface of the membrane. Adjacently to the membrane at the same height, it is placed a glass plate as reference material, which was used to determine the thickness (amount) of the Pd layer by means of X-ray reflectometry.

The assembly was located into the chamber of the sputter coater, which is equipped with a turbomolecular pump working at a background vacuum in the low  $10^{-5}$  Pa. Pd target with a 99.95% of purity (Hauer metallische werkstoffe) was used. Deposition was carried out using pure Argon as working gas. Palladium deposition was carried out at 30 mA for 60 seconds of exposition. This time has been chosen after different previous tests that showed that at this condition the time is not enough for uniform layer generation rather the Pd is highly dispersed onto the rough membrane surface. Finally, the membranes were calcined at 350 °C during 3 hours with a temperature rate of 10 °C min<sup>-1</sup>, followed by a reduction step at 350 °C in a H<sub>2</sub> flowing (50 NmL min<sup>-1</sup>) during 2 hours.

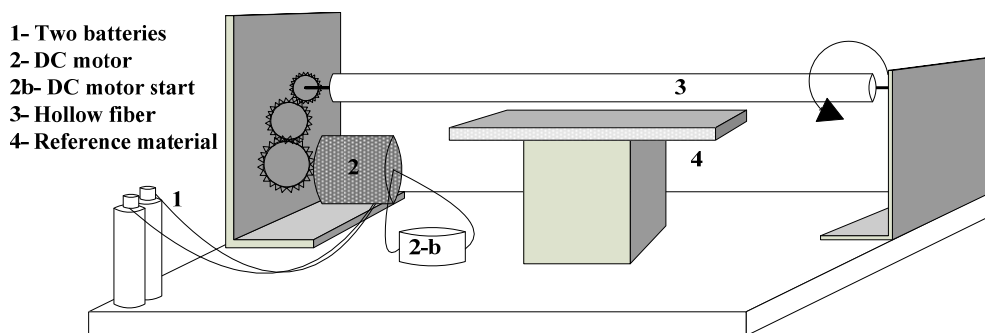


Figure 4-2 Assembly to prepare catalytic membrane reactors by sputtering

The thickness of the Pd layer deposited over the glass plate was measured by means of X-ray reflectometry using a Bruker-AXS D8-Discover diffractometer. The thickness of Pd layer was calculated from the X-ray diffractogram by means the fast Fourier transform (FFT) method.

The deposition rate of Pd was calculated from the thickness and exposition time and estimated to approximately  $14.7 \text{ nm min}^{-1}$ . The CMR prepared by means of this protocol is represented in the Table 4-3.

#### **4.1.6 Preparation of mixed double active phases, sputtered palladium – metal oxide, membranes**

In addition, mixed double active phases - sputtered palladium and metal oxide - membranes were prepared. Ceramic hollow fibers with nominal filtration pore size of 100 and 200 nm were selected to be used in this procedure.

Firstly, the ceramic fibers were dried in an oven at  $120 \text{ }^\circ\text{C}$  for two hours. Then, different metal oxides were supported onto membranes by means the protocol described in the section 4.1.3. Also, the protocol in the section 4.1.4 was carried out to prepare copper spinel membrane. Afterward, the modified membranes were ready to be placed in sputter coater chamber. The Pd deposition was carried out at the same sputter condition described in the previous section, however the exposition time was increased up to 90 seconds.

Table 4-3 Pd based and bi functional catalytic membranes prepared by sputtering

Catalytic membrane reactor	Nominal filtration pore size (nm)	Active phase (% w/w)
sCMR13	20	0,003% Pd
sCMR14	100	CuAl <sub>2</sub> O <sub>4</sub> – 0,005% Pd
sCMR15	100	3% CeO <sub>2</sub> – 0,005% Pd
sCMR16	100	2% Fe <sub>2</sub> O <sub>3</sub> – 0,005% Pd
sCMR17	200	1,3% CeO <sub>2</sub> – 1,5% Fe <sub>2</sub> O <sub>3</sub> – 0,005% Pd

As it is shown in Table 4-3, the amount of palladium incorporated onto the membrane was successfully reduced by sputtering technique. The sCMR13 has 260 times less amount of palladium compared with CMR2. In the same way, it can be compared the CMR12 and the sCMR17. Both membrane reactors have the same actives phases, however the amount of palladium loaded onto the sCMR15 is 240 times lower.

Here, it is important to emphasize that sputtering technique not only reduce the amount of Pd, but also, the palladium can be selectively deposited onto the external membrane surface, where the reaction takes place.

#### 4.1.7 Preparation of corundum powder with sputtered palladium

Commercial corundum powder (Norton) was sputtered with palladium. The alumina oxide was pretreated with the same procedure described in the section 4.1.5. The powder was distributed over a glass plate. Then, the plate was introduced into the sputtering chamber. The palladium has been sputtered at the same conditions as the membranes. Afterward, the powder

with sputtered palladium and the membranes were calcined and reduced in the same manner.

Also, corundum powder was impregnated with  $\text{Ce}(\text{NO}_3)_3$ , and a mixture of  $\text{Ce}(\text{NO}_3)_3$  -  $\text{FeCl}_3$  solution. The impregnated materials were calcined to obtain the respective supported metal oxide: i)  $\text{CeO}_2/\text{Al}_2\text{O}_3$  and ii)  $\text{CeO}_2\text{-Fe}_2\text{O}_3/\text{Al}_2\text{O}_3$ . Then, these materials were sputtered with palladium. Finally, thermal treatment was carried out. The amount of sputtered palladium was calculated to be about 0.05 wt%.

## 4.2 Characterization of catalytic membrane reactors

This section deals with the characterization techniques carried out over the hollow fibers and catalytic membrane reactors.

Classical characterization tools in heterogeneous catalysis were chosen to study our CMRs. Electronic microscopy,  $\text{N}_2$ -physisorption,  $\text{H}_2$ -chemisorption, among others were selected and adapted to analyze the membrane reactors. According to K. Li, characterization techniques for membranes can be divided depending on the nature of the targeted parameters: i) morphology and structure parameters and ii) permeation related parameter [7].

Here, morphologic and structural parameters were studied to better understand the activity of the catalytic membrane reactors in liquid – gas phase reactions. The bubble point was experimentally determined for each membrane. In present study this important parameter allowed us to control the hydrogen dosing without wasting it as gas.

Electronic microscopy techniques were used to examine the surface and cross section of the hollow fibers and CMRs [7].

The scanning electron microscopy (SEM) is a microscope that uses electrons to form an image. SEM gives qualitative information about membrane morphology, but it cannot be used at higher magnification values ( $>10^5$  times) due to its low resolution. For conventional SEM images, the samples require to be electrically conductive; however, in case of non conductive samples, they have to be coated with a gold or carbon layer to make them electrical conductive. In this work, 1 cm length samples from the hollow fibers and membrane reactors were observed with a scanning electron microscope. The samples were introduced into the microscope chamber to examine their morphology. A JEOL electronic microscope, model JSM-6400, coupled to X-ray spectrophotometer detector was used. A semi quantitative elemental analysis was obtained with the X-ray detector. The samples were not coated to preserve the real morphology of the starting fibers and membrane reactors.

The environmental scanning electron microscopy (ESEM) is a microscope with the same fundamentals as SEM, but it works under low background pressure. This characteristic makes possible to analyze the samples without carbon or gold coating, therefore there is not external influence over the real membrane structure. ESEM was coupled with X-ray spectrophotometer detector for microanalysis to determine different atomic specimens in the samples. The ESEM was also used in backscattering mode (BSD). The image in BSD mode provides a semi qualitative analysis of the chemical composition of the sample. In a gray scale, it can be distinguished the composition of a specific zone in the sample. ESEM analysis was carried out with a JEOL electronic microscope (model JSM-6400), coupled with an X-ray micro analyzer. 1 cm length samples of the hollow fibers and membrane reactors were placed into the microscope chamber. A semi

quantitative elemental microanalysis was carried out over the membrane reactor samples.

Also, transmission electron microscopy (TEM) technique was selected to analyze the membrane reactor. In TEM, the images are formed from the interaction of electrons transmitted through the specimens on the sample. TEM analysis requires to cut the samples in thin slides, therefore an alternative strategy was performed to analyze the membrane reactors avoiding the membrane reactor destruction. Therefore in order to study the sputtered palladium particles, TEM analysis was carried out over the corundum powder prepared in the section 4.1.7. A JEOL electronic microscope, model 1011, was used. As well the Pd sputtered corundum was analyzed by high resolution transmission electron microscopy (HRTEM). This technique is performed using an objective aperture which allows several diffracted beams to interfere with the axial transmitted beam to form the image. Under this mode, the images contrast reflects the relative phases of the various beams. Phase contrast imaging is the preferred imaging mode for resolving the atomic lattice of the sample. Images obtained with HRTEM can be directly related with atomic structure of the sample. The microstructural characterization by high resolution TEM was performed at an accelerating voltage of 200 kV in a JEOL 2010F instrument equipped with a field emission source. The point to point resolution was 0.19 nm. No induced damage of the samples was observed under prolonged electron beam exposure. The samples were dispersed in alcohol using an ultrasonic bath. A drop of supernatant was poured onto a holey carbon coated grid.

X-ray diffraction (XRD) is an important technique used in heterogeneous catalysis to identify crystal phases. In membrane science, XRD analysis is used to determine changes in the crystalline structure of membrane materials

[155]. A  $\mu$ -X ray diffraction analysis was performed over 1 cm length samples of the hollow fiber and the membrane reactors. The internal and outer surface was analyzed using a Bruker-AXS D8-Discover diffractometer equipped with parallel incident beam (Göbel mirror), vertical  $\theta$ - $\theta$  goniometer, XYZ motorized stage and with a GADDS (General Area Diffraction System). Samples were placed directly on the sample holder, and the area of interest was selected with the aid of a video-laser focusing system. The X-ray diffractometer was operated at 40 kV and 40 mA to generate  $\text{CuK}\alpha$  radiation. The GADDS detector was a HI-STAR (multiwire proportional counter of  $30 \times 30 \text{ cm}^2$  with a  $1024 \times 1024 \text{ pixel}^2$ ). The frames were collected (2D XRD pattern) covering  $25$ - $59^\circ$   $2\theta$  from at a distance of 15 cm from the sample to the detector. Each sample was analyzed across a straight line taken a frame each 0.5 mm as it can be observed in the Figure 4-3. The exposition time was 300 seconds per frame and it was chi-integrated to generate the conventional  $2\theta$  vs. intensity diffractogram. In the case of those membranes with sputtered palladium, the exposition time was increased up to 900 seconds to obtain an optimal signal from the low amount of palladium.

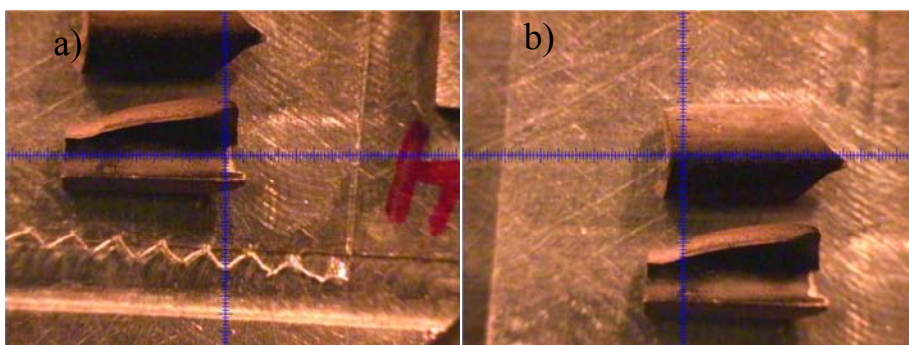


Figure 4-3 Pieces of the catalytic membrane reactor located in the XRD equipment

X-ray photoelectron spectroscopy (XPS) is a characterization technique that measures the surface elemental composition in a sample. The XPS analysis provides information from the surface and down up to 1 nm depth of the samples. The sample is irradiated with X-rays in order to excite its atoms, which emits electrons from different atomic levels. The electrons are collected, analyzed and classified according to their kinetic energy. The electrons contain information about their bonding energy, and it is specific for each element. The information is collected in form of binding energy spectrum [156]. The membrane reactors were sent to the Institute of energy technologies and centre for research in NanoEngineering in the Universitat Politècnica de Catalunya to be analyzed. The XPS analyses were carried out in a SPECS system equipped with a conventional dual Mg/Al X-ray source and a Phoibos 150 analyzer. Spectra were recorded at a pressure below  $10^{-7}$  Pa. Binding energies were referred to adventitious carbon at 284.8 eV. In-situ treatments were performed at atmospheric pressure in a catalytic chamber equipped with an infrared lamp. Temperature was monitored directly in the sample holder and maintained at 40 °C. For the reduction treatment, a hydrogen flow of  $20 \text{ mL min}^{-1}$  was passed over the sample for 20 min.

Gas adsorption is a common method to study porous materials as ceramic hollow fibers. It provides surface areas, pore volume and pore size distribution. Nitrogen ( $\text{N}_2$ ) and krypton (Kr) are used as adsorbent gases within the porous materials [155, 157]. This characterization technique is based in adsorption-isotherms, and relates the amount of gas versus relative pressures (pressure/saturation vapor pressure of adsorbent gas), and the data is analyzed assuming capillary condensation. The vapor pressure ( $P$ ) of the adsorbent liquid in the pore with radius ( $r_p$ ) is given by Kelvin's equation:

$$\ln \frac{P}{P_0} = - \frac{2\gamma V}{r_p RT} \cos \theta \quad \text{Kelvin's equation}$$

Where  $P_0$  is the saturation vapor pressure,  $\gamma$  is the surface tension of the adsorbent,  $V$  is the molar volume of the adsorbent liquid, and  $\theta$  is the contact angle. In the case of  $N_2$ ,  $\theta$  has a value equal to zero.

The surface area can be calculated by Brunauer, Emmett and Teller (BET) method. This equation relates the volume absorbed at a given partial pressure, and the volume absorbed at monolayer coverage.

$$\frac{P}{V(P_0-P)} = \frac{1}{V_m C} + \frac{(C-1)P}{V_m C P_0} \quad \text{BET equation}$$

Where  $V_m$  is the volume of absorbed gas in a monolayer coverage, and  $C$  is a constant. The equation has to be linearized by plotting  $P/V(P_0-P)$  against  $P/P_0$ , in which the slope is  $(C-1)/V_m C$ , and the intercept is  $1/V_m C$ . The sum of slope and intercept yield the inverse of  $V_m$ .

$$S_{BET, total} = \frac{V_m N s}{V} \quad \text{Total surface area (BET area)}$$

$$S_{BET} = \frac{S_{BET, total}}{a} \quad \text{Specific surface area (SSA)}$$

Where  $a$  is the mass of porous material and  $s$  is the cross section of monolayer coverage.

Specific surfaces areas (SSA) were calculated from  $N_2$  adsorption-desorption isotherms using BET method. 11 cm length samples from different hollow fibers and membrane reactors were analyzed. The samples

were firstly degassed at 120 °C at vacuum background during three hours. Then, the degassed samples were placed into standard glass reactors. The analysis was carried out using an automated surface area & pore size analyzer Quadrasorb SI, from Quantachrome Instrument. The isotherms were obtained at the temperature of liquid nitrogen (-196 °C).

Selective gas adsorption, referred to as chemisorptions, is used to measure the available catalytic active sites. The analysis relates the amount of adsorbed gas per unit of catalyst weight. It is important to know the stoichiometric factor between chemisorbed molecules of adsorbate and surface metal atoms. From the amount of gas adsorbed is calculated the amount of accessible active sites. The selection of adsorbate is based on the chemical interaction with the supported metal. Hydrogen (H<sub>2</sub>) and carbon monoxide (CO) are the most common adsorbate used for many supported metals such as palladium and platinum. The analysis is carried out in static vacuum system as in the physisorption analysis. During the analysis, the gas pressure above the sample is finely increased, and the amount of adsorbed gas is measured at equilibrium. As soon as the adsorbate is not more chemisorbed, it is assumed a completely coverage by a monolayer of gas onto the available catalytic sites [8]. Hydrogen chemisorption analysis was also carried out with an accelerated surface area and porosimetry system (ASAP 2010) from Micromeritics. 11 cm length of monometallic palladium membrane reactors were placed in a quartz reactor, and analyzed at 100 °C, but firstly, the samples were in situ pretreated with the following conditions: i) an evacuation step under flowing He at 100 °C during 30 min, ii) reduction step under flowing H<sub>2</sub> at 350 °C during 30 minutes, iii) a second evacuation step with flowing He at 350 °C during 30 min to withdraw the H<sub>2</sub> from the system, and finally iv) a cooling step until 100 °C with flowing

He during 60 min to ensure the analysis temperature in the whole system. A stoichiometric factor of 1:1 for Pd:H was used for calculations.



## **Chapter 5. Experimental setup**

### **5.1 Direct synthesis of H<sub>2</sub>O<sub>2</sub> in a semi batch mode**

According to our research objectives, the catalytic membrane reactors (CMR) were tested for the generation of hydrogen peroxide. However, the production of H<sub>2</sub>O<sub>2</sub> was not the main purpose in this research work, but it was used as in the oxidation reaction of a model compound.

All the monometallic and bimetallic CMRs were tested for the direct synthesis of hydrogen peroxide starting from hydrogen and synthetic air. The reaction was carried out in a semi batch system to follow the catalytic activity of those CMRs. Two different systems were tested to find their suitability in the generation of H<sub>2</sub>O<sub>2</sub> and its applicability in the subsequent oxidation of organic compounds.

#### **5.1.1 Synthesis of H<sub>2</sub>O<sub>2</sub> by means of H<sub>2</sub>/O<sub>2</sub> mixture dosage**

In the first design, it was proposed to dose hydrogen and synthetic air to the lumen side of the catalytic membrane reactor. Both gases were brought together to the active phase sites. The synthesis of H<sub>2</sub>O<sub>2</sub> was carried out in a semi batch mode as it is represented in the Figure 5-1.

Hydrogen and synthetic air were supplied to the catalytic membrane reactor at different O<sub>2</sub>/H<sub>2</sub> molar ratios (5, 3, 0.33 and 0.17) below or above to the explosion limit. The molar ratios were selected in order to determine the most favorable condition for the generation of H<sub>2</sub>O<sub>2</sub> with the CMRs.

The synthesis of hydrogen peroxide was carried out in a cylindrical glass vessel containing 100 mL of Milli-Q water. The CMR was completely submerged into the reactor, where one end of the CMR was tightly closed with a metallic cap. H<sub>2</sub> and synthetic air (as an oxygen supplier) were dosed

to the inner side of the membrane reactor. Two mass flow controllers were used in order to dose and keep constant the chosen  $O_2/H_2$  molar ratios. The gases were mixed in a three ways valve before to introduce them into the system.

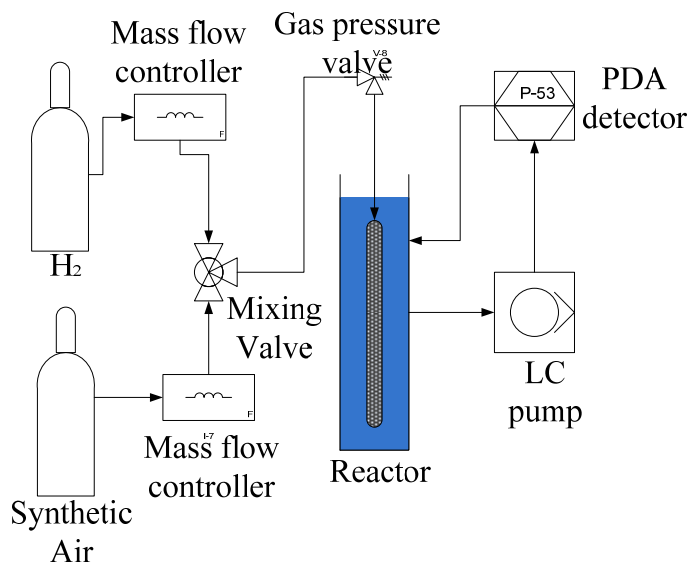


Figure 5-1 Scheme of experimental set up used in direct synthesis of hydrogen peroxide using a mixture of  $O_2/H_2$

### 5.1.2 Synthesis of $H_2O_2$ by means of $H_2$ and synthetic air dosing

A second configuration was proposed and tested in the synthesis of  $H_2O_2$ . In this configuration,  $H_2$  and synthetic air were separately dosed for the synthesis of hydrogen peroxide.

The experimental setup is showed in the Figure 5-2. In this system,  $H_2$  was supplied to the inner side of membrane reactor, whereas synthetic air was supplied to the liquid phase (Milli-Q water), where the catalytic reactor is submerged as in the previous section.

The hydrogen flows through the membrane wall, and it is activated onto the palladium surface. The synthetic air was dosed to the Milli-Q water controlled by means of needle valve. The synthetic air flow was kept high in order to dissolve the maximum amount of oxygen in the Milli-Q water. The activated  $H_2$  reacts with the dissolved  $O_2$  into the aqueous phase.

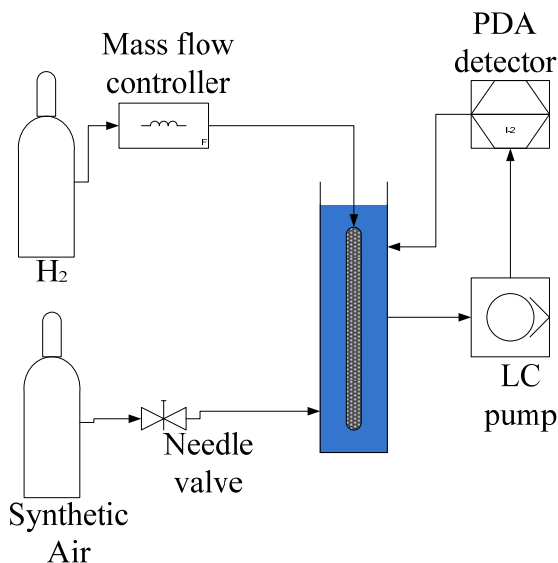


Figure 5-2 Experimental set up used in direct synthesis of hydrogen peroxide

The  $H_2$  flow was controlled with a flow mass controller, and it was supplied at  $6 \text{ NmL min}^{-1}$ . The transmembrane gas pressures were recorded.

### 5.1.3 Reaction conditions, sampling and measurement of $H_2O_2$

In both configurations, the reactions were carried out at room temperature ( $25 \text{ }^\circ\text{C}$ ), and the glass vessel was kept at atmospheric pressure. The reaction was monitored using a liquid chromatographic pump (Shimadzu, LC-20A)

coupled with a diode array detector (Shimadzu, SPD-M10Avp) in a close loop.

The aqueous solution containing the generated  $\text{H}_2\text{O}_2$  was directly passed through the flow cell of the detector. The absorbance of the solution was monitored and recorded at  $\lambda = 193$  nm. Then the hydrogen peroxide concentration was calculated using the  $\text{H}_2\text{O}_2$ -absorbance correlation. This method for quantification of  $\text{H}_2\text{O}_2$  was validated using a method indicated by the literature. The titration by iodometric method was used to validate the detection of the concentration of hydrogen peroxide in an aqueous solution.

## **5.2 Oxidation of organic compounds with in situ generated hydrogen peroxide**

The catalytic membrane reactors were tested in the oxidation of an organic model compound. The objective was to determine the applicability and efficiency of in situ generated  $\text{H}_2\text{O}_2$  for oxidation reaction. Phenol was selected and used as model compound.

Monometallic and bimetallic CMRs were tested for phenol oxidation in a semi batch system. The reaction was performed in a closed system as is represented in the Figure 5-3. Each CMR was immersed in a glass vessel containing 100 mL of phenol (Panreac) solution (100 ppm).

One end of the membrane reactor was tightly closed, whereas hydrogen was supplied to the lumen side of the CMR. A mass flow controller was used to dose the  $\text{H}_2$  at  $6 \text{ NmL min}^{-1}$ . The synthetic air was dosed to the phenol solution using a needle valve. The synthetic air flow was kept high in order to dissolve the maximum amount of  $\text{O}_2$  into the solution at atmospheric pressure.

The glass vessel with the CMR was introduced into a temperature programmable bath system to work at different temperatures.

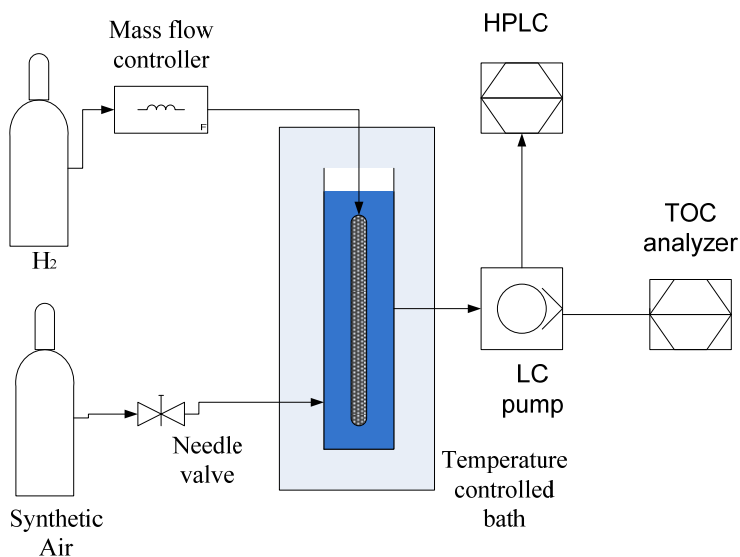


Figure 5-3 Experimental setup for phenol degradation by in situ generated hydrogen peroxide

### 5.2.1 Sampling and measurement of phenol

The phenol degradation was monitored by sampling at regular time intervals and analyzing by high performance liquid chromatography (HPLC, Shimadzu LC-2010). The HPLC system is equipped with a diode array detector (Shimadzu SPD-M10Avp).

A C-18 separation column (Omnisphere, Varian) was used to separate, identify and quantify the compounds coming from the reaction. Calibration curves for phenol (Panreac), hydroquinone (Sigma-Aldrich), catechol (Aldrich), and some carboxylic acids such as acrylic (Fluka), oxalic (Sigma-Aldrich) and maleic acid (Panreac) were prepared from standard solutions.

The solutions were prepared using the corresponding reagent. The mobile phase was prepared with Milli-Q water and acetonitrile (Panreac) (60:40) and adjusted at pH 3.8 with acetic acid (Fluka).

The mineralization degree was monitored with a TOC analyzer (TOC-5000A, Shimadzu).

### 5.3 Design of metal housing (module reactor) for continuous operation

Here, a metal housing design is proposed to be used as module reactor for continuous operation of the catalytic membrane reactors. The housing was built of stainless steel, and the Figure 5-4 shows an image of the housing.

The main body, where the membrane reactor is located, is 30 cm length with 0.9 cm of internal diameter. The metal housing is provided with two 3.175 mm axial feed connections, and two radial connections. One of the radial connections is used as a gas feed connection (3.175 mm), and a pressure gauge was connected to the second radial connection (6.5 mm) to monitor the gas pressure in the system.

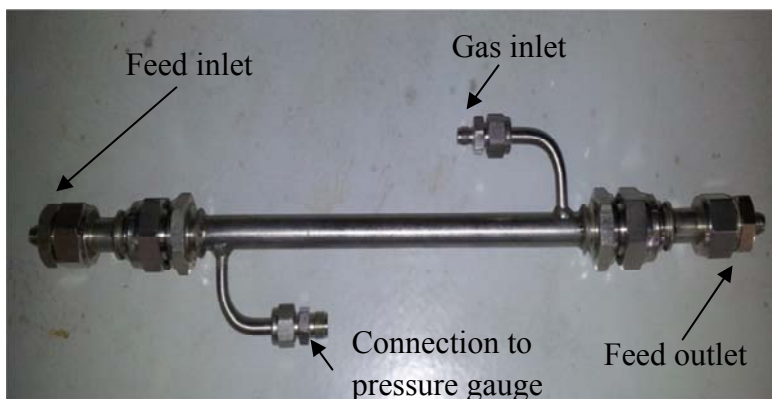


Figure 5-4 Image of the stainless steel reactor housing

To operate this configuration, 30 cm length membrane reactors were prepared by the impregnation method described in the section 4.1.4 above. The loadings of active phases were kept constant to observe the catalytic activity of the CMRs in this arrangement. In order to completely isolate the permeate and the feed sides of the CMR, special tips have been fabricated at each end of the membranes. Thereafter the both sides of the membrane are isolated by using o-ring joints pressured between the nuts and the reactor housing.

The ceramic seals were fabricated with commercial pottery (clay) material, and a metal mold was used to give a desire form to the ceramic seals. Firstly, each hollow fiber was centered and fixed in the middle of the mold, and then the mold was full filled with the pottery material. Then, the hollow fiber with the mold was introduced in an oven during night at 60 °C. After one night, the mold was removed.

Afterward, the membrane with the clay seal was dried in an oven at 120 °C during two hours, and then, the seals were cooked at 650 °C during 8 hours to transform the clay into ceramic. Finally, the seals were covered with a commercial inorganic glaze, followed by a calcinations step at 950 °C to obtain an adequately vitrified ceramic seals. The deposition of the active phase was carried out after the previous procedure, and the membrane reactor was fixed in the steel house by means of Viton O-rings.

#### **5.4 Catalytic reduction of water contaminants**

The catalytic membrane reactors and the metal housing design were tested in the catalytic reduction of water contaminants. The reactions were operated under a continuous mode to observe the effectiveness of the proposed system. Selective reduction of nitrates and hydrodechlorination of

chlorinated aromatic compounds reactions were selected to observe the catalytic activity under this operative mode.

#### 5.4.1 Selective reduction of nitrates

The 30 cm length CMR6 (Pd-CeO<sub>2</sub>) and CMR12 (Pd-CeO<sub>2</sub>-Fe<sub>2</sub>O<sub>3</sub>/Al<sub>2</sub>O<sub>3</sub>) were used in the selective reduction of nitrates. The Figure 5-5 shows the experimental setup used to carry out the reaction in a continuous mode.

Each catalytic membrane reactor was placed into the metallic housing. The feed solution was supplied by means a peristaltic pump at 15 mL min<sup>-1</sup> to the lumen side of the CMR.

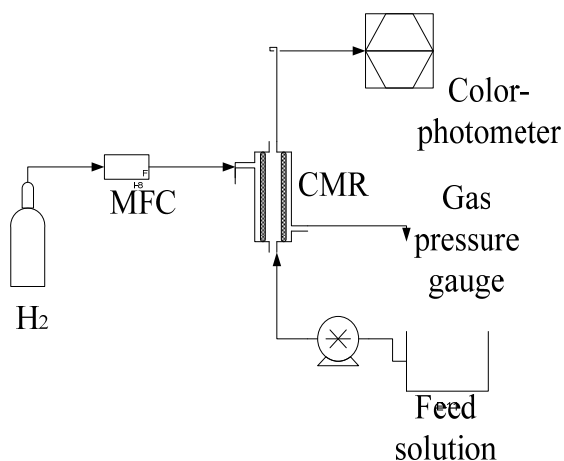


Figure 5-5 Experimental setup for selective nitrate reduction

A nitrate solution (100 ppm) was prepared using NaNO<sub>3</sub> (Sigma Aldrich) and Milli-Q water. Whereas, H<sub>2</sub> was dosed through the shell side by means of a mass flow controller. Different H<sub>2</sub> flows were used to perform this reaction (6 and 10 NmL min<sup>-1</sup>). The reaction was carried out at 25 °C.

The reaction was monitored with a colorimetric method using a color photometer (Lovibond photometer). The nitrate concentration was measured using standard Vario Nitrx reagent (detection range: 0.50 – 133 mg L<sup>-1</sup>), the nitrite concentration was measured with Vario Nitrite reagent (detection range: 0.03 – 1.6 mg L<sup>-1</sup>) and ammonia concentration was analyzed with Vario AM tube test reagent (detection range: 0.03 – 3.25 mg L<sup>-1</sup>).

#### 5.4.2 Hydrodechlorination of chlorinated aromatic compounds

The hydrodechlorination of chlorinated aromatic compounds was carried out in a closed system as is represented in the Figure 5-6. The reaction was performed with the 30 cm length CMR12 (Pd-CeO<sub>2</sub>-Fe<sub>2</sub>O<sub>3</sub>/Al<sub>2</sub>O<sub>3</sub>) in a continuous operation mode. 4-Cl-Phenol (Sigma Aldrich) was used as model compound, and formic acid (Panreac) was used as hydrogen donor.

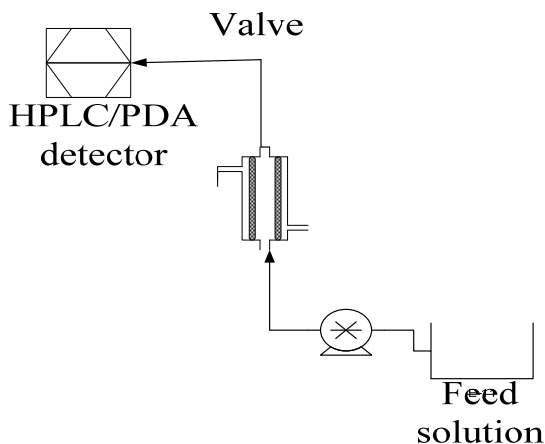


Figure 5-6 Experimental setup for hydrodechlorination of 4-Cl-Phenol

Each membrane reactor was placed in a glass housing. The feed solution was dosed at 10 mL min<sup>-1</sup> to the lumen side of the CMR with a peristaltic

pump (Masterflex L/S). The feed solution was a mixture of 4-Cl-phenol (100 ppm) and formic acid (2000 ppm).

The progress of the reaction was monitored by sampling at regular intervals and analyzing with a HPLC (HPLC, Shimadzu LC-2010) equipped with a diode array detector (Shimadzu SPD-M10Avp). Then, the samples were analyzed with the same protocol used in the phenol oxidation reaction.

## **Chapter 6. Results and discussion**

This chapter summarized the characterization and experimental results obtained from the use of the catalytic membrane reactors.

### **6.1 Ceramic hollow fibers**

The main objective of this work is the preparation of catalytic membrane reactors. The starting materials were commercial ceramic hollow fibers as catalyst support. The performance of the CMRs is intrinsically related with the structural and morphological characteristic of the membrane support, thus the hollow fibers were firstly studied by different techniques. The found characteristics are used for better understanding of the catalytic activities of the CMRs.

The Figure 6-1 shows an ESEM image of the cross section of the 4 nm filtration pore size ceramic membrane.

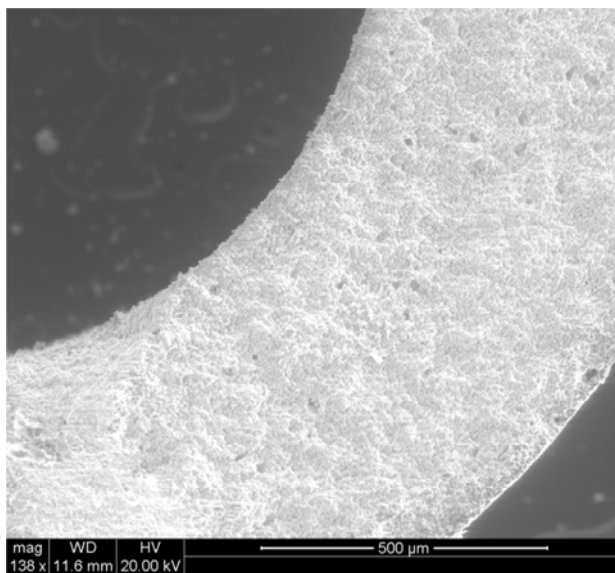


Figure 6-1 ESEM image obtained from the cross section of the 4 nm filtration pore size hollow fiber

The cross section reveals a symmetric structure as well as the absence of skin layer. The thickness is mainly formed by a dense sponge like structure, also finger like structures (small black dots) are observed. During the membrane fabrication process, the fingers like structures are formed at the sintering step, and offer an optimal place where the active phases can be deposited [158]. The sponge like structure provides mechanical resistance to the ceramic membranes.

Figure 6-2 shows an ESEM image obtained from the cross section of the 1400 nm hollow fiber. As in the 4 nm ceramic fiber, it was also observed a symmetric cross section with a sponge like structure. As it was previously observed, small finger like structures are present in the fiber. Whereas Figure 6-3 shows a magnified image from the bulk of the 1400 nm, and

offers a closed image of a high dense packing of particles, which form the core of the membrane.

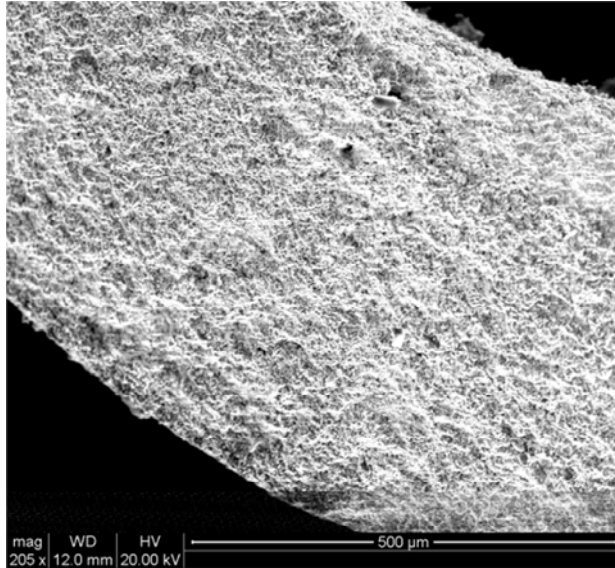


Figure 6-2 Image of the cross section of 1400 nm hollow fiber

The rest of the hollow fibers were observed by means ESEM microscopy technique, and as it was observed in the previous membranes, symmetric cross section with sponge like structure were detected in all cases.

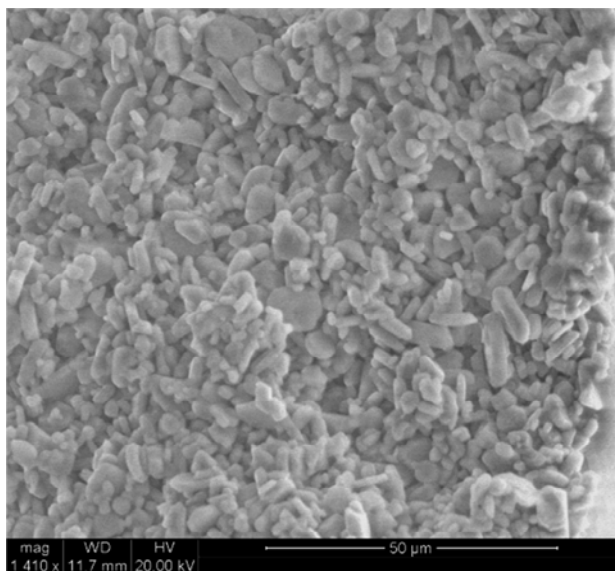


Figure 6-3 ESEM image of bulk of 1400 nm hollow fiber

The sponge like structure identified in the commercial hollow fibers represented an important feature for gas-liquid applications. Hollow fibers with uniform structure provide flow resistance through the entire thickness of the ceramic membrane [159-160].

The  $\mu$ -XRD analysis was conducted over the hollow fibers. The Figure 6-4 and Figure 6-5 show the XRD diffractograms from the 4 and 20 nm ceramic membranes, respectively. The analysis was carried out over the internal and external surfaces. The identification of the crystal structures were achieved by comparison of the XRD diffractogram with the ICDD data base (release 2007) using Diffrac<sup>plus</sup> Evaluation software (Brucker 2007). An unique crystal phase was detected corresponding to  $\alpha$ -Al<sub>2</sub>O<sub>3</sub>. The XRD results demonstrate that the used ceramic fibers have a homogeneous corundum composition along the inner and outer surface.

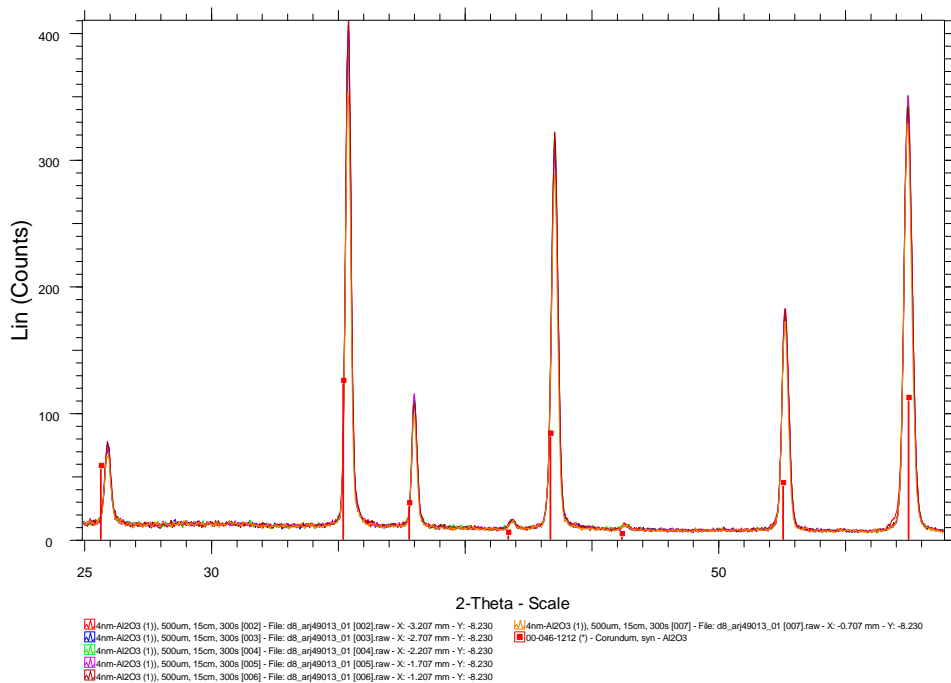


Figure 6-4 μ-XRD analysis carried out over the 4 nm hollow fiber

N<sub>2</sub> adsorption at -196 °C analysis was carried out over the parent fibers used in the preparation of the CRMs. The apparent specific surface area (aSSA) was calculated by application of the BET model to the N<sub>2</sub> adsorption – desorption isotherms, and it was 3 m<sup>2</sup> g<sup>-1</sup> for all the hollow fibers. This aSSA is typical for the corundum that is the fabrication material of the used membranes. It is nonporous, and the main pore network is generated by the interparticles voids.

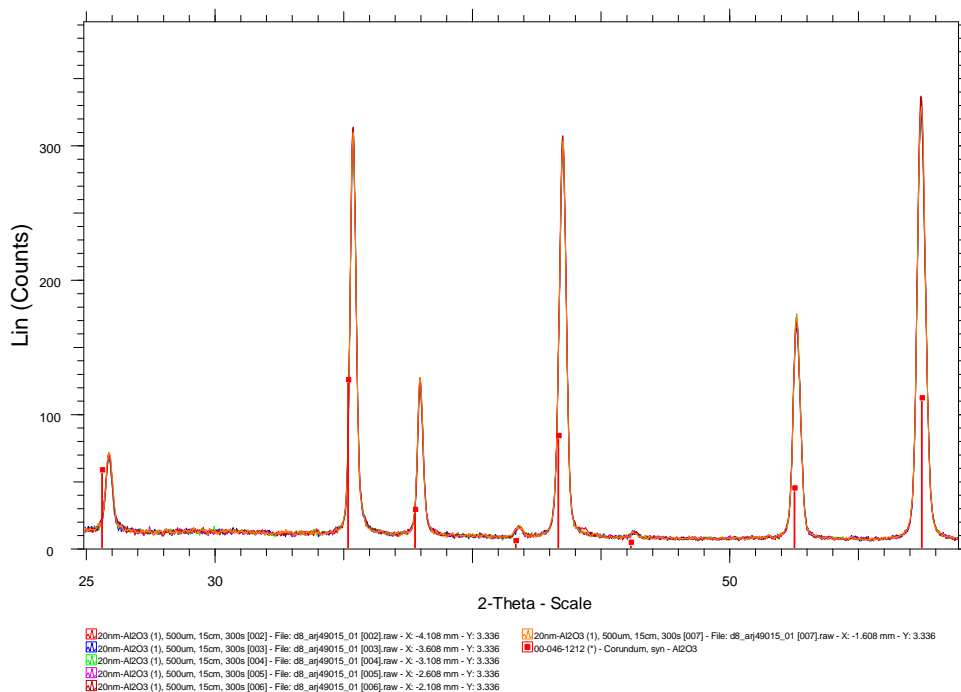


Figure 6-5  $\mu$ -XRD analysis performed over the 20 nm hollow fiber

## 6.2 Monometallic Pd membrane reactors

Monometallic Pd membrane reactors were prepared by two different protocols: i) impregnation and ii) developed novel sputtering protocol. By the sputtering method the amount of Pd is highly reduced, e.g. in the case of the sCMR13 the amount of Pd loaded onto the membrane reactor was reduced up to 260 times compared with the CMR prepared by impregnation. Moreover, the sputtering protocol allowed the selective deposition of the noble metal over the external surface of the ceramic fiber, where the reaction takes place.

The monometallic Pd membrane reactors were analyzed by ESEM, and the analysis has shown that the morphology of the ceramic membranes do not seem to be modified after palladium deposition.

Figure 6-6 shows a close image from the outer surface of the CMR1. There is no evidence of morphological changes in the  $\alpha$ -Al<sub>2</sub>O<sub>3</sub> particles in the surface, and the filtration pore were not closed by the incorporation of the noble metal.

The internal surface of the CMR3 is shown in the Figure 6-7, and as well the CMR1, there are not proofs of alteration of the corundum particles of the hollow fiber. Also, the rest of CMRs prepared by impregnation do not reflect appreciable changes in the morphological structure, which is important to keep the integrity of the membrane.

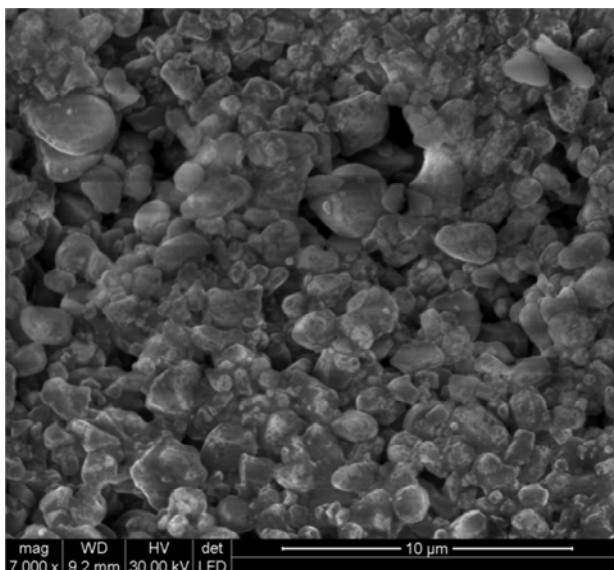


Figure 6-6 ESEM image of the external surface of the monometallic palladium membrane reactor (CMR1)

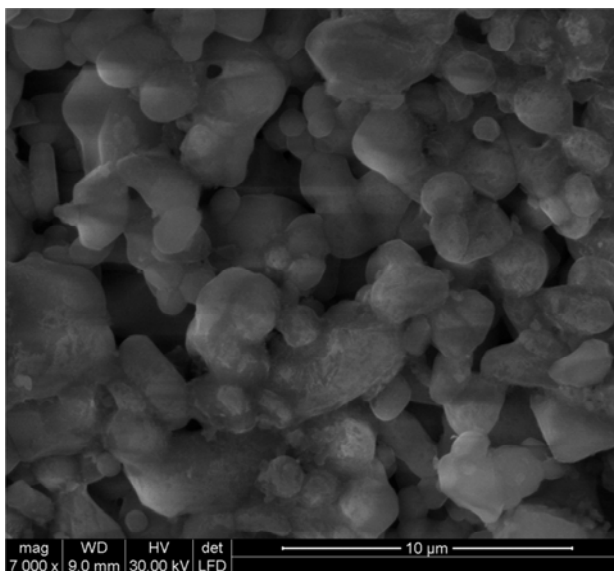


Figure 6-7 Close ESEM image of the internal surface of the CMR3

The membrane reactor prepared by sputtering procedure is shown in the Figure 6-8. The morphology of the external surface is the same as for the starting membrane. In fact, the filtration pores are present and there is no evidence of Pd clusters growing over the ceramic membrane surface.

Also, the CMRs were examined by ESEM in backscattering mode (ESEM-BSE). The Figure 6-9 shows the external surface of the CMR5. The impregnation method leads to the formation of Pd cluster over the alumina particles. The noble metal is found to be homogeneously distributed over the entire surface. The rest of monometallic Pd membrane reactors, prepared by the same method, have presented similar distribution of Pd over the external and internal surfaces. Therefore, the porosity of the membrane does not present steric limitations to the ions from the precursor solution.

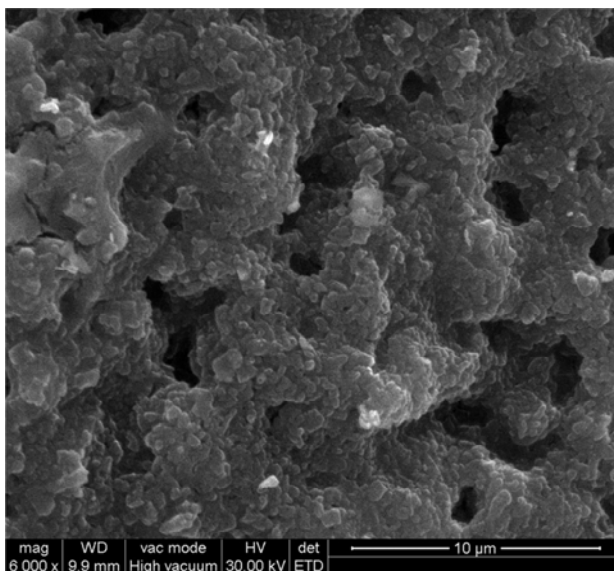


Figure 6-8 ESEM image from the external surface of the monometallic Pd membrane reactor (sCMR13)

The distribution of the incorporated Pd was determined by a micro chemical analysis (ESEM-EDX). The analysis was carried out over the cross section of the monometallic CMRs. A homogeneous distribution of Pd in the membrane wall has been found in the membrane reactors prepared by impregnation.

The distribution of the Pd on the membrane reactor is very important due to its influence on the catalytic activity of the CMR. According to Reif et al [45], concerning the concept of a catalytic membrane reactor operated as membrane contactor-diffuser, the palladium has to be deposited only on the top of the membrane so meaning that the Pd in the membrane bulk does not participate in the reaction. Indeed, the catalyst location corresponds to a zone where the reaction takes place. As a matter of fact, when a CMR is used as three phase reactor, the gas-liquid interface has to be kept in the

zone where the active phase is located. The amount of noble metal dispersed out of the catalytic zone will not participate in the reaction [161].

In our case, the impregnation method allowed us to incorporate the active phases to the membrane. However, the selective deposition of the Pd is limited and no special efforts in this direction have been done using this method. Thus, the wetness impregnation method is very easily applicable but increases the amount of Pd used in the preparation of the CMRs, and consequently increases the cost of the membrane reactors.

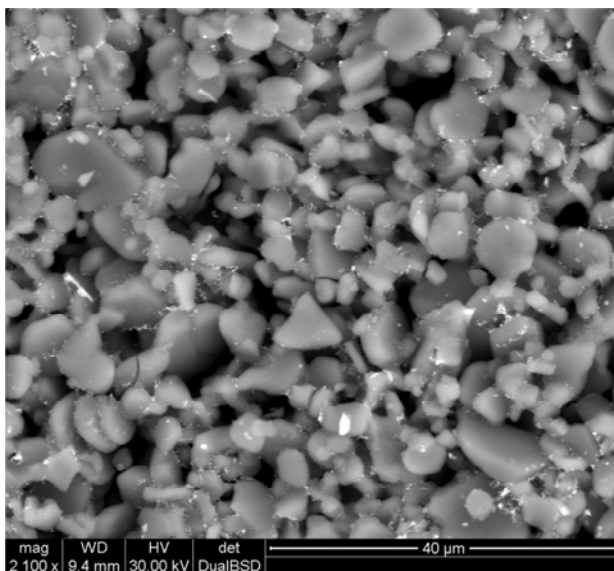


Figure 6-9 BSE image of the external surface of the CMR5

The main goal of the developed method for CMR preparation by sputtering is to avoid the over dosage of Pd.

A representative example of the CMRs prepared by sputtering is the sCMR13. The sputtered Pd monometallic membrane reactor presents a different distribution of the noble metal on the ceramic membrane. As it is

shown in the Figure 6-10, the Pd is selectively located over the top layer of the outer surface. The EDX analysis shows that Pd was selectively deposited over the external surface. The distances shown in the figure have been measured starting from the external surface to the bulk of the ceramic membrane. The Pd is located in the upper layer, 10  $\mu\text{m}$  from the top of the external surface, and afterward it was not detected any signal of the noble metal in the bulk of the fiber. The exposure time in the sputtering chamber as well as the roughness of the membrane surface are factors that prevent the formation of continuous Pd layer over the hollow fiber.

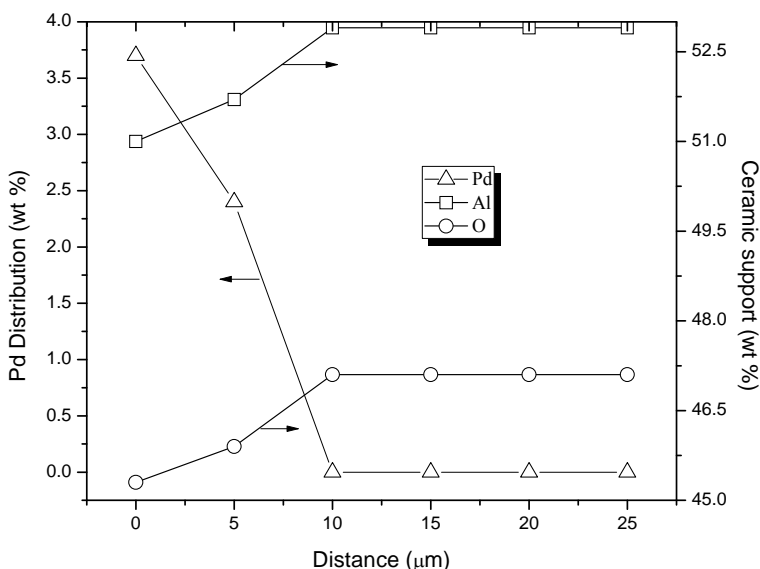


Figure 6-10 Pd distribution on the monometallic Pd membrane reactor (sCMR13)

Also, an element mapping of the external surface of the sCMR13 using the backscatter detector was performed. The Pd dispersion over a selected area is shown in the Figure 6-11. From the image we can conclude that the noble metal is homogeneous and finely dispersed over the entire surface of the

membrane reactor. The high dispersion of Pd over the membrane surface can improve the catalytic activity of the CMR. This feature is an important step to increase the efficiency of the noble metal.

As it was expected, the novel procedure to incorporate Pd by means sputtering protocol presents a high efficiency for the selective deposition of the active metal on the external surface of the hollow fiber. Likewise, this method reduces the amount of Pd used in the preparation of the catalytic membrane reactor.

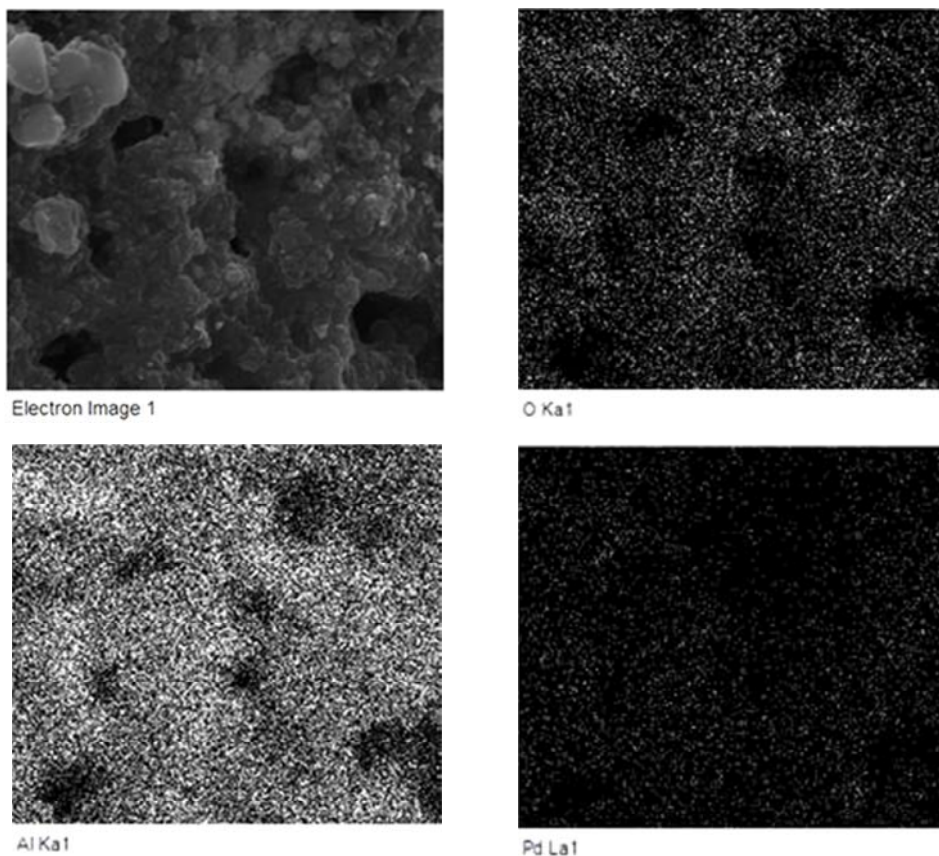


Figure 6-11 Electron mapping of different elements from the external surface of the sCMR13

We consider that the main advantages that are achieved in the preparation of the sCMRs by sputtering method lie on the reduction of the amount of noble metal (around 200 times in the present study) compared with the CMR prepared via impregnation. Additionally, it is expected the formation of very small grains of palladium over the membrane surface; hence, this extremely dispersed palladium will highly increase the catalytic activity of membrane reactors.

Other techniques applied in order to study the morphology, the different phase compositions, crystal sizes, homogeneity of the phase distributions along the membrane reactors were XRD as well as micro XRD. The monometallic Pd CMRs were analyzed by XRD to obtain information about the size of the Pd crystals as well as to determine the Pd distribution along the inner and outer surface of the membrane. The analyses were done over a straight line over the internal/external surface. Different points were analyzed and the diffractograms from each point were collected and studied to determine the distribution of the active phase over the surface. The

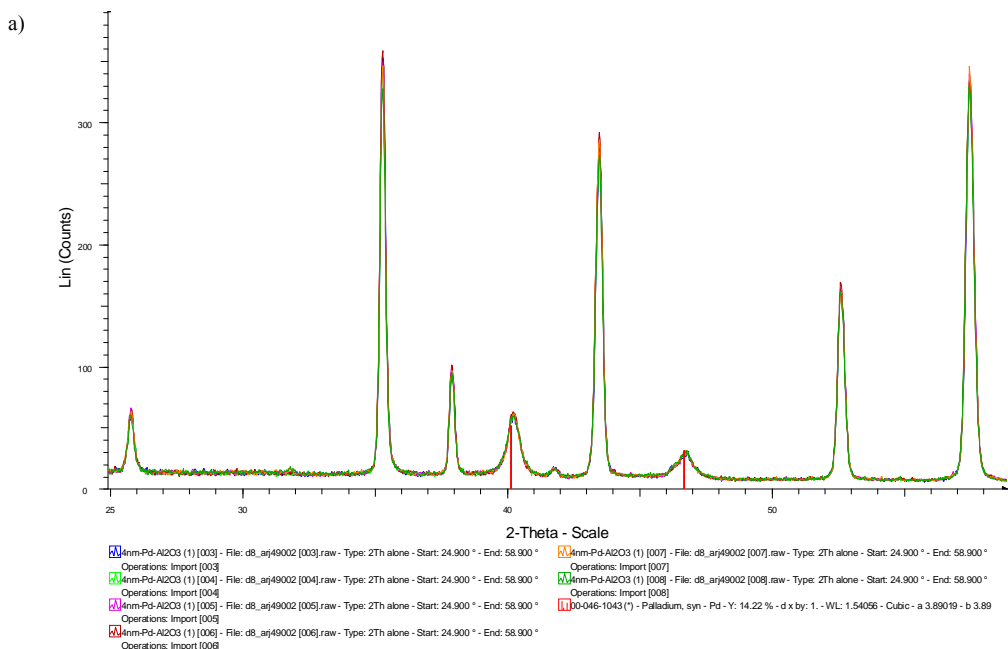
Figure 6-12 shows the diffractogram of the internal and external surface of the CMR1.

The micro XRD analysis showed a homogeneous distribution of Pd over the inner/outer membrane surfaces. The Pd signals correspond to a face centered cubic (fcc) system with a strong line of detection in the plane (111) at  $2\theta = 40.25$ . The signal has been indexed as black palladium (ICDD data file: 46-1043). The rest of CMR prepared by impregnation were also analyzed by  $\mu$ -XRD, and likewise the CMR1, homogeneous distribution of palladium was also found. The diffractogram of external surface of the CMR2 to CMR5 are shown in the Figure 6-13. The diffractograms were used to obtain some parameters to calculate the size of the Pd crystals loaded on the catalytic membrane reactors.

The palladium crystal size was calculated using the Scherrer equation:

$$\tau = \frac{\lambda k}{\beta \cos \theta} \times \frac{180}{\pi}$$

Where  $\tau$  is the size of the crystal in nm,  $\lambda$  is the X-ray wavelength,  $k$  is a dimensionless shape factor,  $\beta$  is the net broadening of the peak calculated as  $\beta^2 = \beta_{\text{obs}}^2 - \beta_{\text{ins}}^2$ , and  $\theta$  is the Bragg angle.



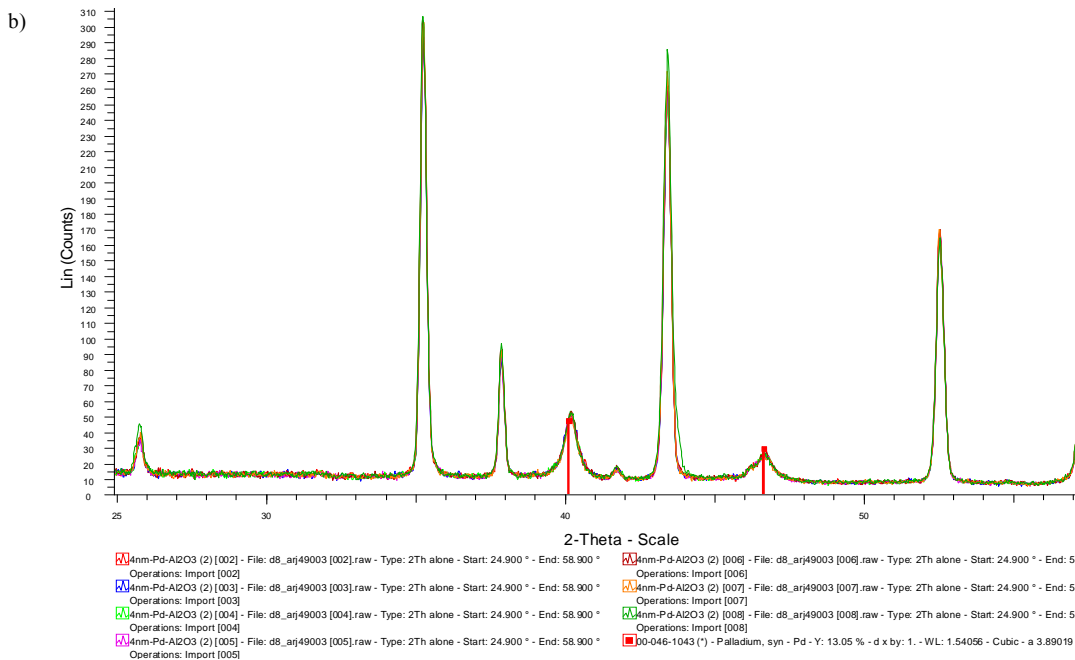


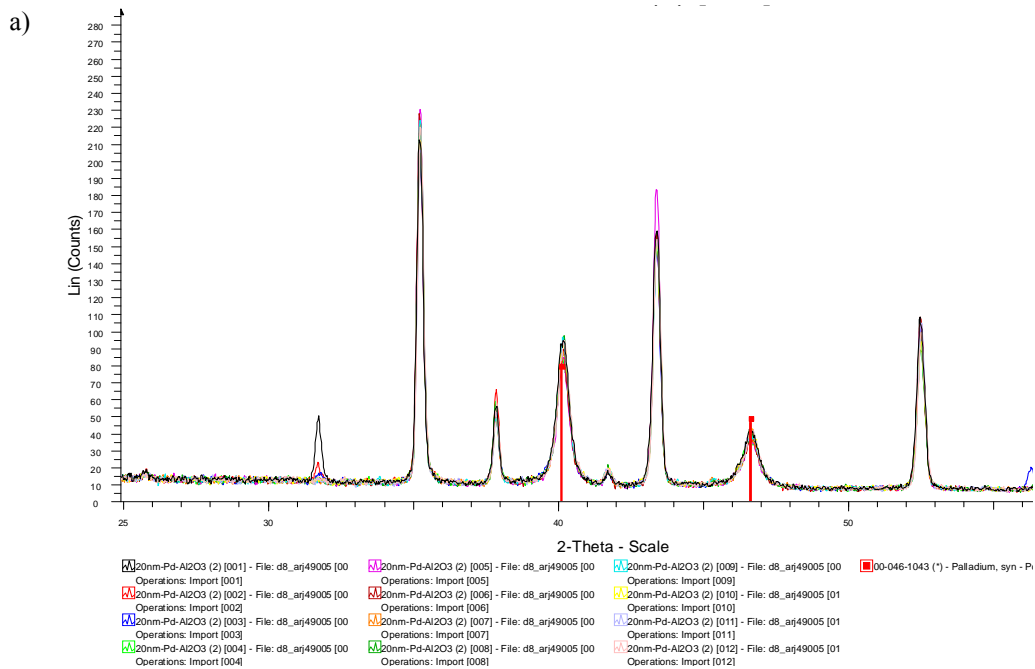
Figure 6-12  $\mu$ -XRD analysis performed over the a) internal and b) external surface of the CMR1

In the Table 6-1 summarized the sizes of Pd crystals calculated by Scherrer equation. And as it was expected, the sizes of the Pd crystal vary depending of the starting filtration pore size of the hollow fiber. The lower value of Pd crystal was found in the CMR1.

Table 6-1 Average of the Pd crystal sizes calculated for CMR1 to CMR5

CMR	Pd crystal size (nm)
CMR1	19
CMR2	21
CMR3	26
CMR4	29
CMR5	31

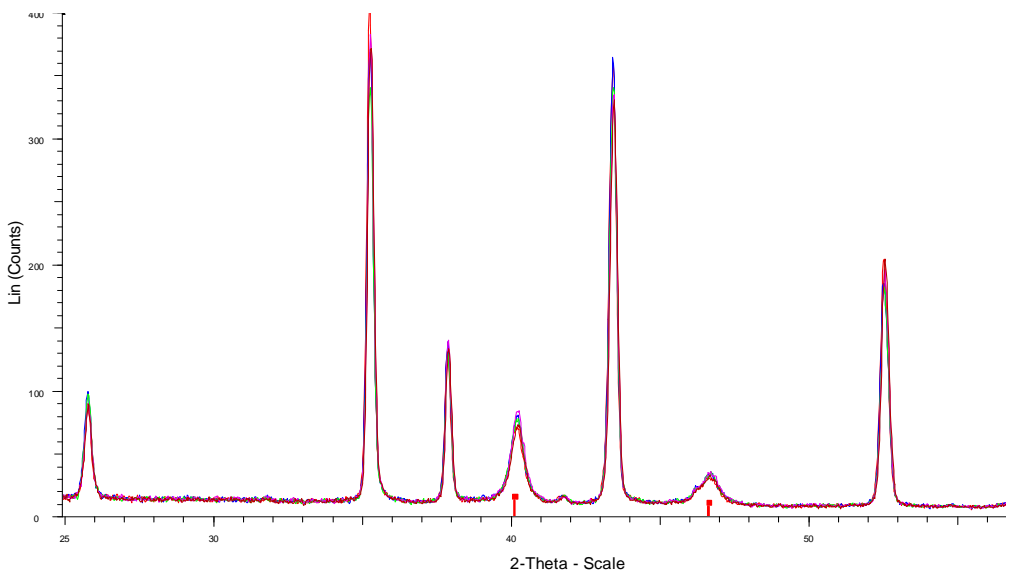
Figure 6-13 shows the diffractograms for the other membrane reactors of the series summarized in the Table 6-1.



Oscar Antonio Osegueda Chicas

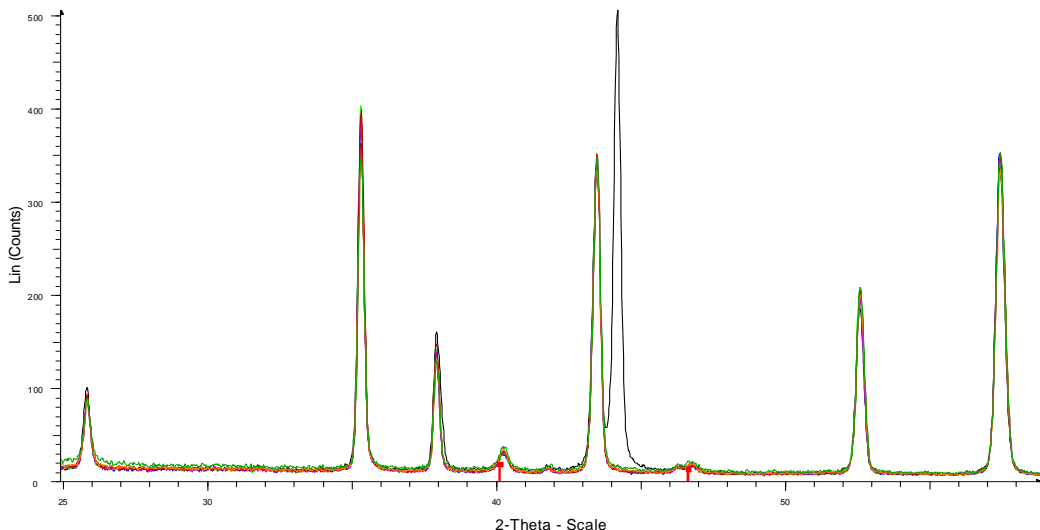
Depósito legal:

b)



■ 100nm-Pd-Ai2O3 (2) [002] - File: d8\_arj49007 [002].raw - Type: 2Th alone - Start: 24.900 ° - End: 58.900  
 Operations: Import [002]  
■ 100nm-Pd-Ai2O3 (2) [003] - File: d8\_arj49007 [003].raw - Type: 2Th alone - Start: 24.900 ° - End: 58.900  
 Operations: Import [003]  
■ 100nm-Pd-Ai2O3 (2) [004] - File: d8\_arj49007 [004].raw - Type: 2Th alone - Start: 24.900 ° - End: 58.900  
 Operations: Import [004]  
■ 100nm-Pd-Ai2O3 (2) [005] - File: d8\_arj49007 [005].raw - Type: 2Th alone - Start: 24.900 ° - End: 58.900  
 Operations: Import [005]  
■ 00-046-1043 (1) - Palladium, syn - Pd - Y: 3.14 % - d x by: 1. - WL: 1.54056 - Cubic - a 3.8901  
 Operations: Import [006]

c)



■ 500nm-Pd-Ai2O3 (2) [001] - File: d8\_arj49009 [001].raw - Type: 2Th  
 Operations: Import [001]  
■ 500nm-Pd-Ai2O3 (2) [002] - File: d8\_arj49009 [002].raw - Type: 2Th  
 Operations: Import [002]  
■ 500nm-Pd-Ai2O3 (2) [003] - File: d8\_arj49009 [003].raw - Type: 2Th  
 Operations: Import [003]  
■ 500nm-Pd-Ai2O3 (2) [004] - File: d8\_arj49009 [004].raw - Type: 2Th  
 Operations: Import [004]  
■ 500nm-Pd-Ai2O3 (2) [005] - File: d8\_arj49009 [005].raw - Type: 2Th  
 Operations: Import [005]  
■ 00-046-1043 (1) - Palladium, syn - Pd - Y: 2.62 % - d x by: 1. - WL:  
 Operations: Import [006]  
■ 500nm-Pd-Ai2O3 (2) [007] - File: d8\_arj49009 [007].raw - Type: 2Th  
 Operations: Import [007]  
■ 500nm-Pd-Ai2O3 (2) [008] - File: d8\_arj49009 [008].raw - Type: 2Th  
 Operations: Import [008]

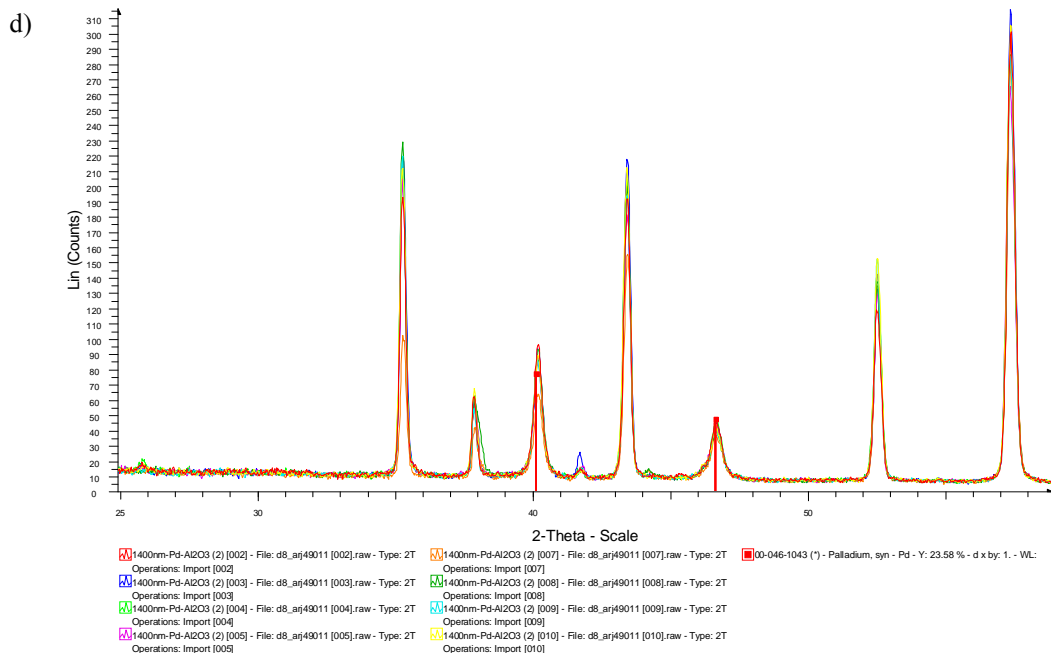


Figure 6-13  $\mu$ -XRD analysis carried out over the external surface of the a) CMR2, b) CMR3, c) CMR4 and d) CMR5

The membrane reactors obtained after Pd sputtering have also been studied by micro XRD technique. The diffractogram of sCMR13 is presented in Figure 6-14. The time of data collection at each step ( $0.004^\circ$ ) was maintained for 300 seconds. The signal of palladium phase was not detected. The analysis time was increased up to 900 second per frame without any incidence of Pd signal. We consider that the main reason for the absence of palladium signal is due to the extremely tiny Pd grain size. Despite the high concentration of the Pd on the outer surface of the

membrane reactor it is believed that the Pd particles are extremely small, below 5 nm.

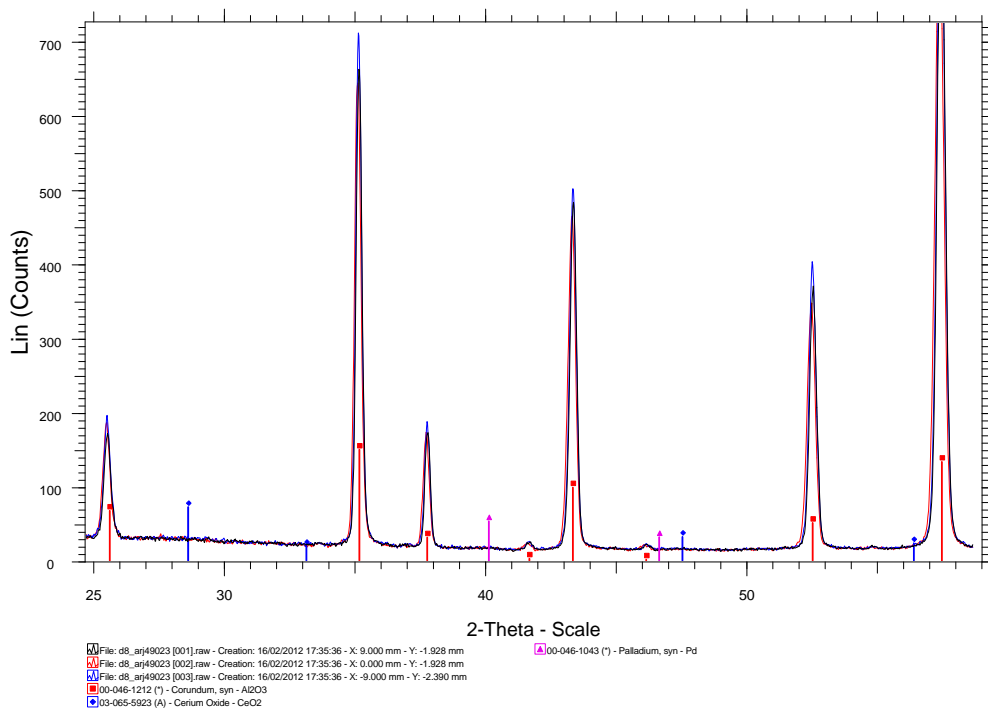


Figure 6-14  $\mu$ -XRD analysis carried out over the sCMR13

### 6.3 Palladium bimetallic membrane reactors

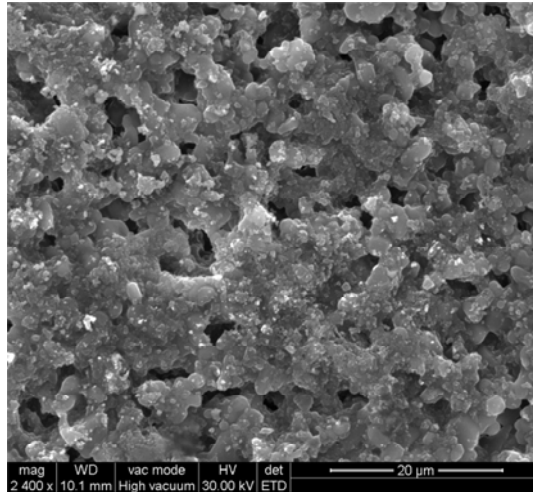
Palladium bimetallic membrane reactors were characterized with an ESEM microscope. As well as the monometallic CMRs, the ESEM images obtained from the bimetallic membrane reactors did not reveal any structural and morphological difference between the parent and the modified hollow fibers.

Figure 6-15 shows ESEM images from the external surface of sCMR15, and the surface seems as the original ceramic fiber.

Also, the Pd bimetallic membrane reactors were examined by  $\mu$ -XRD analysis to identify the different crystal phases loaded on the catalytic

membrane reactor. The Figure 6-16 shows the diffractogram of the CMR7. Two different phases were detected in the ceramic membrane. Black palladium crystals were detected as in the monometallic Pd CMRs. Also, cerium oxide was detected at  $2\theta$  angles of 28.62, 33.15, 47.58 and 56.45 with a correspondence to ICDD data file 03-065-5923. The diffractogram of sCMR15 with the same crystal phases as the CMR7 is shown in the Figure 6-17.

a)



b)

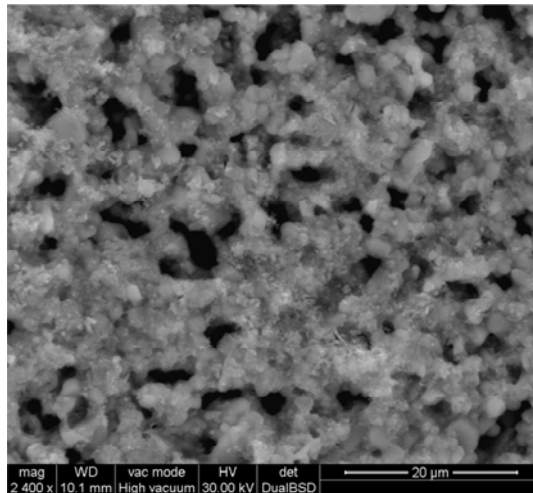


Figure 6-15 ESEM images of the sCMR15 a) electronic image and b) Backscattering mode image

The analysis was carried out during 900 second to observe Pd signal in the specific  $2\theta$  angles. Despite the large time of signal detection at specific  $2\theta$

angle the Pd phase is difficult to be confirmed which can be expected due to the small amount of Pd as well as the very small crystal size.

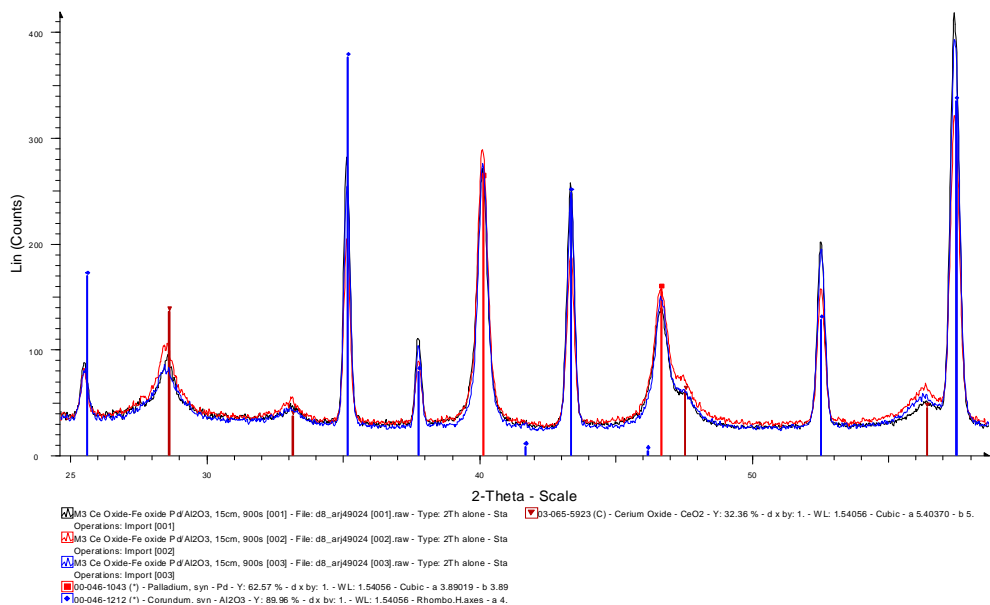


Figure 6-16  $\mu$ -XRD analysis carried out over bimetallic catalytic membrane reactor (CMR7)

The Figure 6-18 shows the micro XRD analysis carried out over the CMR9. Black Pd and  $\text{TiO}_2$  crystals phases are present in the membrane reactor.

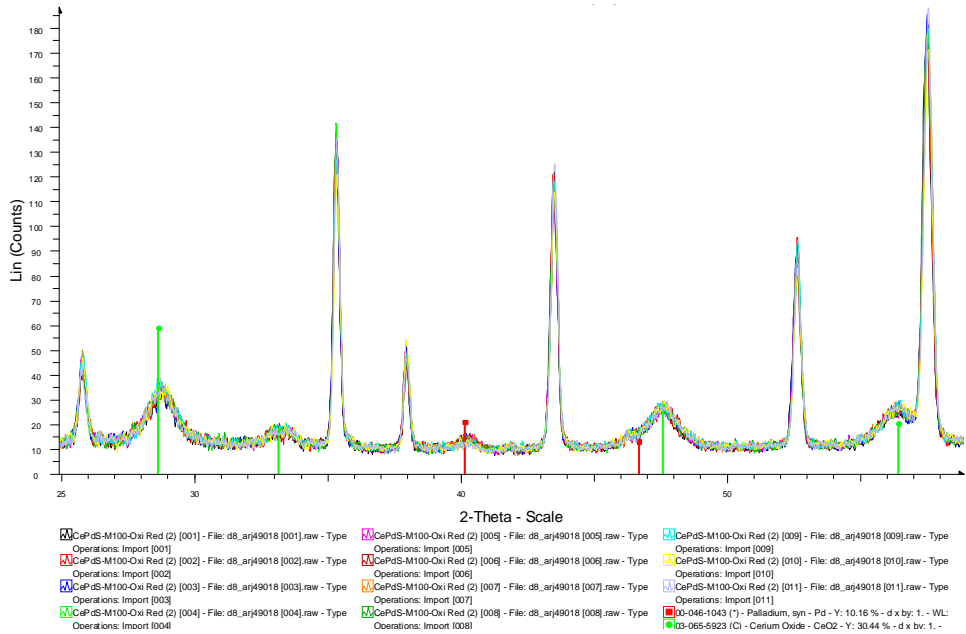


Figure 6-17 Diffractogram obtained from the bimetallic  $\text{CeO}_2$  – sputtered Pd, sCMR15

The rest of crystal phases loaded on the catalytic membrane reactor were confirmed with the  $\mu$ -XRD analysis.

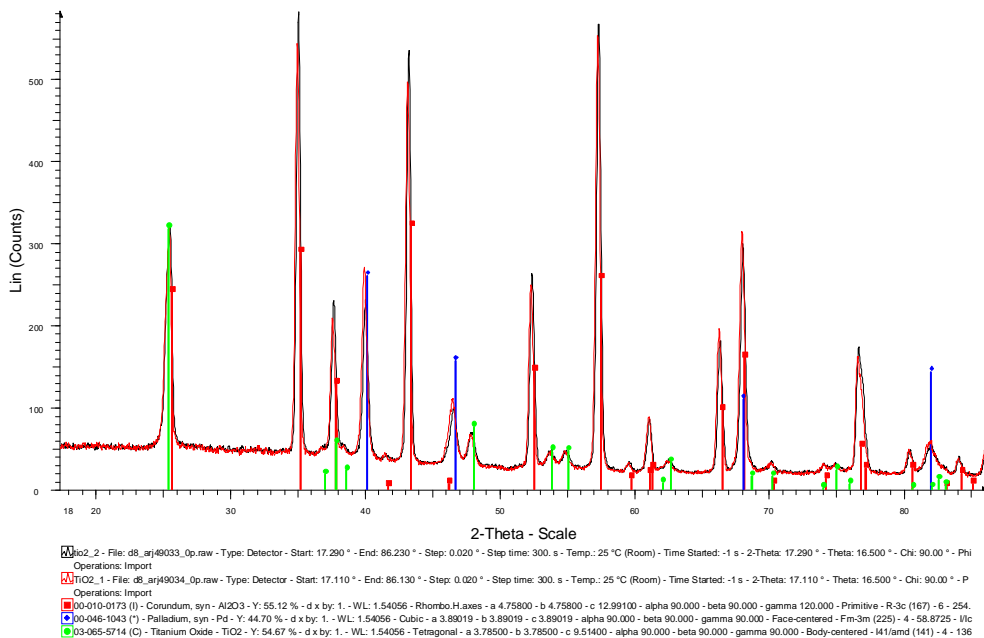


Figure 6-18 Diffractogram obtained from the CMR9

#### 6.4 Corundum powder with sputtered palladium

Due to the small amount of palladium deposited on the membrane by sputtering it was not possible to detect and characterize it by the techniques used. In order to increase the relative amount of Pd with respect to the support, a corundum powder was used. The pretreatment procedures were the same as for the membranes. A fine layer of powder was distributed onto a glass plate and introduced in the vacuum vessel of the sputtering apparatus. The Pd was sputtered in the same conditions as on the membranes. The post treatment of the powder was the same as for the membranes. Low magnification bright-field HRTEM images have been recorded in order to determine the mean particle size of the Pd particles (more than 200 particles have been measured). A representative example of such images is shown in Figure 6-19. In all cases Pd particles are very well

dispersed over the alumina support and no agglomerates have been detected, thus confirming that the sputtering method leads to a high Pd dispersion. The mean particle size of Pd particles is centered at 4.8 nm, being 95% of particles within the 2-7 nm range. Figure 6-19 presents a representative picture of the obtained images as well as the particle size distribution plot.

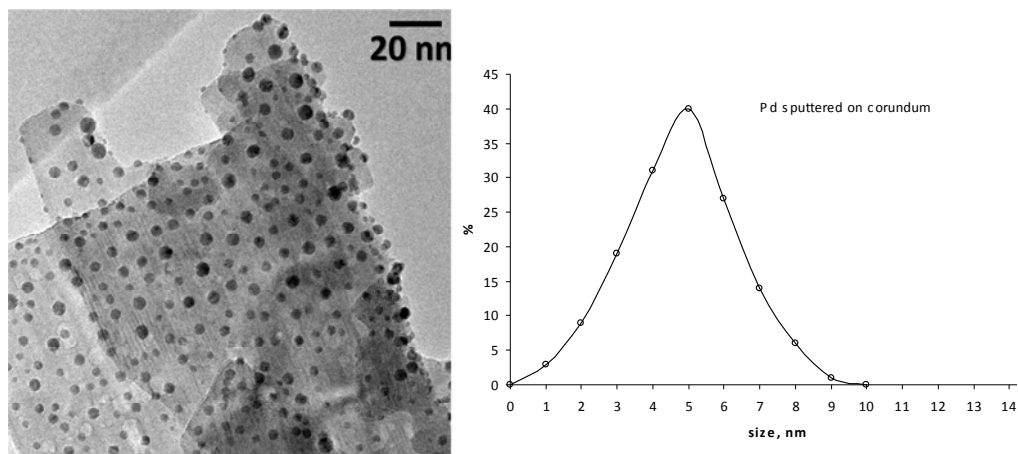


Figure 6-19 HRTEM image of Pd particles on corundum powder after sputtering and particle size distribution

As expected, the particles are very small and in the nanoscale range. These sizes are in agreement with the calculations made from the thickness of the Pd layer on the glass plate obtained by reflectometry.

## 6.5 Catalytic activity of CMRs in batch system

### 6.5.1 Hydrogen peroxide generation

After the preparation of the catalytic membrane reactors followed by the established activation procedure, they have been checked in hydrogen peroxide generation tests. This test also has been used as indicator for the deactivation/reactivation of the reactors.

Initially different configurations to supply synthetic air and hydrogen were checked in order to find the most appropriate experimental design. In the first configuration a mixture of synthetic air and hydrogen was fed through the membrane channel. The ratios of oxygen/hydrogen mixtures were kept below the explosion limit. Under this experimental setup null generation of  $H_2O_2$  was obtained. This result is attributed to the oxidation state of supported palladium on the catalytic membrane reactor [150]. At higher concentration of synthetic air there is a considerable increase of the ratio  $Pd^{2+}/Pd^0$ , therefore the deactivation of CMR is related with the oxidation of palladium surface where hydrogen cannot be activated, this effect was also observed in the synthesis of hydrogen peroxide with catalytic membrane reactors reported by Pashkova et al [40]. These findings were confirmed by experiments carried out in the opposite conditions, working above the explosion limit. In this case the hydrogen peroxide generation takes place. The excess of hydrogen maintained the Pd in the reduced state that is essential for the hydrogen activation. Therefore this configuration was discarded due to the low efficiency of the hydrogen.

It has been decided to introduce the  $H_2$  and the synthetic air separately. Hydrogen was supplied with a mass flow controller through the membrane channel. The  $H_2$  flew throughout the membrane wall to palladium particles in the reaction zone on the outer membrane surface. Meanwhile synthetic air was bubbled into the batch vessel. With this assembly different advantages are achieved: the Pd is protected from surface oxidation as well as the hydrogen dosage can be very precisely controlled in order to entirely use it in the reaction.

The hydrogen peroxide generation was performed in a semi batch operation setup as described in the experimental section. The kinetic results for

palladium CMRs under atmospheric pressure and 25 °C are presented in Table 6-2. The kinetic rates measured from the hydrogen peroxide generation curves are presented in Figure 6-20. The rates of generation were calculated from the initial curve slopes. It was assumed that in the beginning the hydrogen peroxide generation should prevail over hydrogen peroxide decomposition or other possible reverse reactions.

Table 6-2 Catalytic results in hydrogen peroxide generation in monometallic Pd  
 CMRs prepared by impregnation

CMR	Transmembrane pressure ( $\Delta P$ bar)	H <sub>2</sub> O <sub>2</sub> generation rate* (mol h <sup>-1</sup> m <sup>-2</sup> )	Max. H <sub>2</sub> O <sub>2</sub> generated (ppm)	Efficiency % (mol H <sub>2</sub> O <sub>2</sub> /mol H <sub>2</sub> )	mol H <sub>2</sub> O <sub>2</sub> /(mmol Pd·h)
CMR1	4.7	6.7	47	34	0.072
CMR2	3.3	3.2	27	15	0.034
CMR3	2.1	2.8	26	14	0.026
CMR4	1.9	2.8	19	14	0.030
CMR5	1.6	2.4	14	12	0.020
CMR18	4.2	0.0	0	0	0.000

\* The H<sub>2</sub>O<sub>2</sub> generation rates are apparent, i.e. hydrogen peroxide decomposition is not taken into account.

As can be expected, the highest H<sub>2</sub>O<sub>2</sub> generation rate was obtained for the 4 nm nominal pore size membrane reactor. In this case the Pd has the highest dispersion on the surface as well as smallest particle size. On the other hand, for this pore size the highest use of hydrogen is obtained. Under these conditions (6 Nml min<sup>-1</sup>) of hydrogen flow, the supplied hydrogen is chemically activated on the Pd surface, and subsequently involved in the

reaction with dissolved oxygen in the liquid phase. The results for the efficiency of the hydrogen peroxide generation are presented in the fourth column of Table 6-2. These values were calculated once hydrogen balance was done, and using the results for  $H_2O_2$  generation rates and the amount of introduced hydrogen. It should be mentioned that part of the hydrogen is oxidized to water and it is not discarded that some part may be simply lost as gaseous hydrogen that was not activated on the Pd active phase catalyst. The smallest nominal pore size minimizes the hydrogen loss as gas.

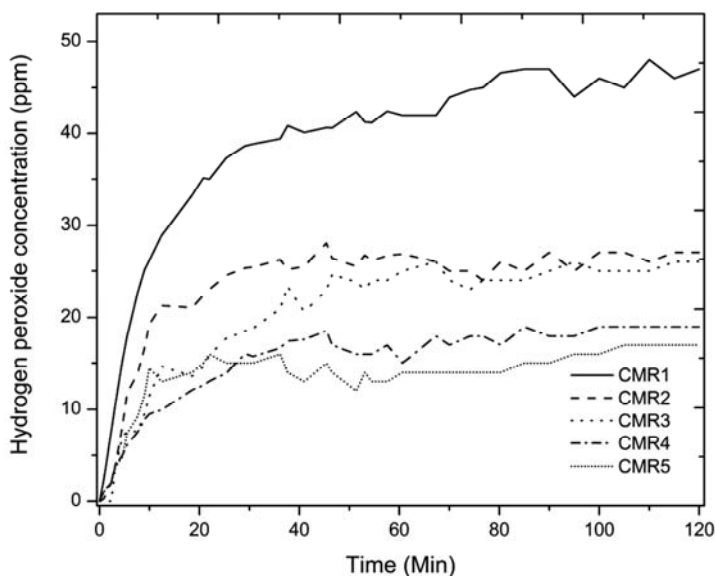


Figure 6-20 Hydrogen peroxide generation in different palladium active phase CMRs prepared by impregnation

The maximum reachable hydrogen peroxide concentrations were also determined. The highest value of 47 ppm was obtained for CMR1 (4 nm initial membrane pore size). This value is still far away from the  $H_2O_2$  concentration reported by S. Abate et al. using palladium membranes.

Concentration as high as 250 – 300 ppm were reported in an oxygen saturated acidic solution. They also used bromide promoters to avoid the hydrogen peroxide decomposition [37]. Pashkova et al. obtained a productivity of  $16.8 \text{ mol H}_2\text{O}_2 \text{ m}^{-2} \text{ h}^{-1}$  using a Pd membrane reactor in contactor mode, which is 2.5 fold higher than our system [40]. They operated their CMR in methanol as liquid phase to favor the  $\text{H}_2\text{O}_2$  stability and avoid its decomposition.

The common understanding of the upper limits of the concentration of the generated hydrogen peroxide attributes the phenomenon to two main causes. Firstly, the active phase catalyzes the reverse reaction, and the hydrogen peroxide either decomposes to water and oxygen or generates hydroxyl radicals [37-39, 64, 93]. Secondly, it is proposed that the hydrogen itself or the activated hydrogen can reduce the generated hydrogen peroxide [39,162]. To assess the effect of these suggested processes, we tried to determine the hydrogen peroxide decomposition rate following different procedures. The experiments were performed in MilliQ water. First, once an upper concentration of  $\text{H}_2\text{O}_2$  was reached the air flow was cutted off. No change was observed in the hydrogen peroxide concentration. Many different tests were performed in order to explain the observed apparent inactivity of the CMR once certain concentration of hydrogen peroxide was reached. Once the upper limit of hydrogen peroxide concentration was reached the air was cut thereafter it was altered supplying air stopping the hydrogen, etc. In all these cases no variation of the hydrogen peroxide concentration was detected. These results indicate that the active phase is completely deactivated. Further experiments consisted of a hydrogen peroxide addition (values between 60-100 ppm) to the experimental vessel once the plateau  $\text{H}_2\text{O}_2$  concentration was reached (see Figure 6-21, where

the excess  $\text{H}_2\text{O}_2$  was added at  $t \approx 80$  min). The experimental conditions were unchanged ( $6 \text{ Nml H}_2 \text{ min}^{-1}$  to the CMR and flowing air). As it can be seen from Figure 6-21, the  $\text{H}_2\text{O}_2$  concentration increases and remains unchanged for at least another 30 min. All these results suggest that the higher limit for the hydrogen peroxide generation is defined by the stability of the active phase. It is deactivated by the generated hydrogen peroxide. XPS experiments were carried out over the CMRs in order to determine the oxidation state of the Pd and its activity in the hydrogen peroxide generation. In those experiments, the sample was treated in different ways in order to keep similar conditions as in the  $\text{H}_2\text{O}_2$  generation reaction in our batch system.

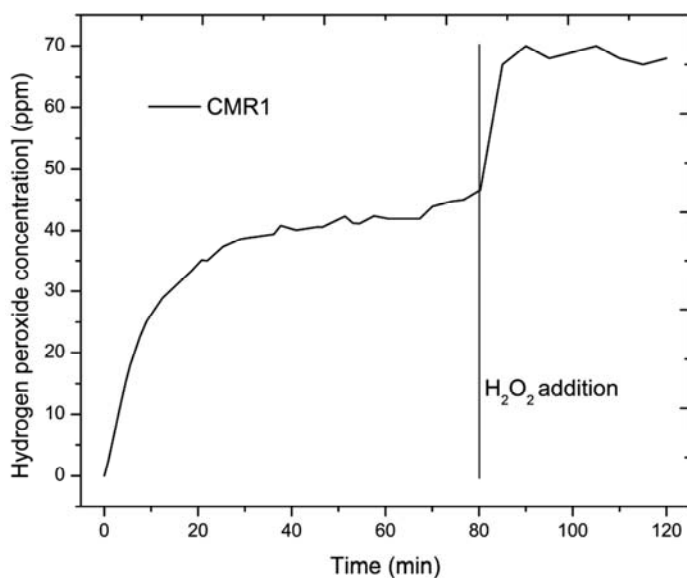


Figure 6-21 Effect of hydrogen on the *in situ* generated hydrogen peroxide concentration before and after hydrogen peroxide addition

As representative sample, the CMR1 was studied *in situ* by XPS in order to verify the oxidation state of palladium at the surface of the membrane following different treatments. The reaction conditions have been simulated inside the XPS chamber so it was possible to study the changes of the active phase during the reaction of hydrogen peroxide generation. Table 6-3 compiles the results obtained before and after exposure to H<sub>2</sub>O<sub>2</sub>. In both cases, both metallic Pd and oxidized Pd species are present at the surface of the membrane, as deduced from the binding energy values of the peaks recorded. In addition, the surface of the membrane shows similar contributions of Pd<sup>0</sup> and Pd<sup>2+</sup> after reduction at 140 °C (Pd<sup>2+</sup>/Pd<sup>0</sup>~1), whereas exposition to hydrogen peroxide at the same temperature results in a substantial enrichment of oxidized Pd at the surface of the membrane (Pd<sup>2+</sup>/Pd<sup>0</sup>~3). These results indicate that the generation of hydrogen peroxide causes the concomitant oxidation of Pd at the membrane surface.

Table 6-3 in-situ Pd 3d XPS data recorded over CMR1 after treatment under H<sub>2</sub> and H<sub>2</sub>O<sub>2</sub>

Treatment	Species	BE Pd 3d <sub>5/2</sub> / eV	BE Pd 3d <sub>3/2</sub> / eV	At. / %
H <sub>2</sub>	Pd <sup>0</sup>	334.8	340.0	49
	Pd <sup>2+</sup>	336.4	341.5	51
H <sub>2</sub> O <sub>2</sub>	Pd <sup>0</sup>	334.2	339.4	27
	Pd <sup>2+</sup>	335.4	340.6	73

Following this assumption we can conclude that the differences in the higher H<sub>2</sub>O<sub>2</sub> reached concentration (third column in Table 6-2) can be explained with the capacity of the introduced hydrogen to protect/

regenerate the palladium. As it can be expected for the lower pore size membrane the hydrogen is in closer contact to the Pd domains so it is better protected from the surface deactivation by the generated hydrogen peroxide. For the blank catalytic membrane (CMR18), in which no active phase was added, no activity for hydrogen peroxide generation has been observed.

The prepared bimetallic catalytic membrane reactors have also been tested in the generation of hydrogen peroxide. With the deposition of the second active phase the nominal pore size of the original membrane is altered but it has not been considered as a parameter to be evaluated. More extended study has not been performed but indications for the pore size reduction were indirectly obtained from the pressure needed for the permeation of the hydrogen through the membrane reactor. As it is described in the experimental section, the hydrogen pressure is continuously monitored in the outlet of the mass flow controller.

For the initial screening of the catalytic activity of these hybrid membrane reactors,  $\text{CeO}_2$ ,  $\text{TiO}_2$ ,  $\text{Fe}_2\text{O}_3$ ,  $\text{CuAl}_2\text{O}_4$ ,  $\text{Ag}_2\text{O}$  and  $\text{Au}_2\text{O}_3$  have been chosen as active phases. The preparation of catalytic membranes is described in the experimental section and the active phase compositions are presented in Table 4-2. Once the heterogeneous Fenton membrane reactors were prepared, palladium that catalyzes the hydrogen peroxide generation was incorporated in all of them.

The hydrogen peroxide generation performance has been studied for bimetallic Pd membranes reactors. The experimental curves of  $\text{H}_2\text{O}_2$  generation versus time are presented in the Figure 6-22 and Figure 6-23.

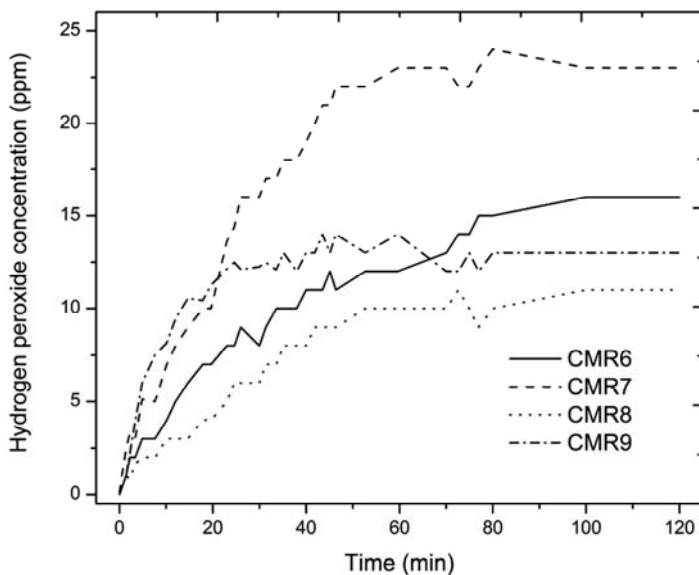


Figure 6-22 Hydrogen peroxide generation with bimetallic CMR6 to CMR9

The hydrogen peroxide generation rates, the maximum  $\text{H}_2\text{O}_2$  concentrations and the efficiencies of hydrogen utilization were calculated from these curves. The obtained results are presented in the Table 6-4.

It can be seen that all prepared membranes are active for hydrogen peroxide generation. As in the case of palladium membranes an upper limiting value of the peroxide concentration is reached. From the obtained data it can be seen that the membranes with ceria and titania as a second active phase have a higher rate of hydrogen peroxide generation as well as higher efficiency. In fact, the  $\text{Pd}/\text{TiO}_2$  membrane reactor has productivity rate similar to the reported in the literature around to  $6.11 \text{ mol H}_2\text{O}_2 \text{ m}^{-2} \text{ h}^{-1}$  under favorable condition to produce  $\text{H}_2\text{O}_2$  [40]. L. Shi et al. reported a  $\text{Pd}_{90.5}\text{Au}_{9.5}$  membrane reactor with a productivity rate of  $0.133 \text{ mol H}_2\text{O}_2 \text{ m}^{-2} \text{ h}^{-1}$  in an acidic mixture of water/methanol, which is 5 fold lower than the CMR11 listed in the Table 6-4. In order to get better understanding of the influence

of the second active phase on the hydrogen peroxide generation more extensive study should be undertaken.

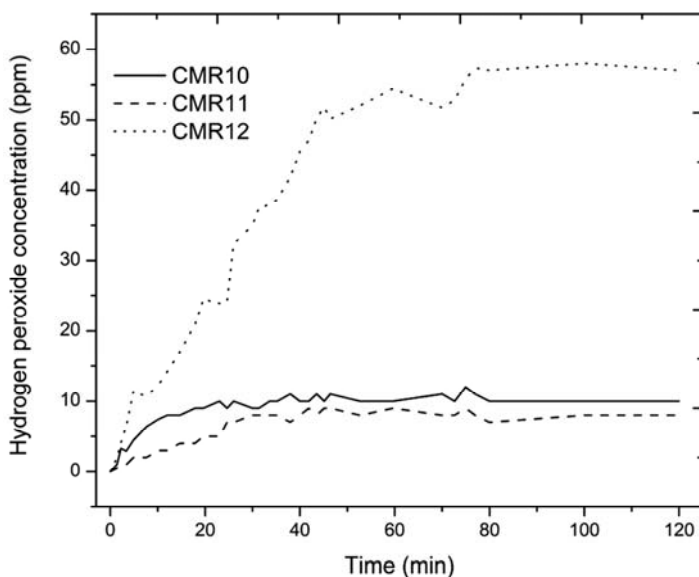


Figure 6-23 Hydrogen peroxide generation in different CMR impregnated with two active phase, from CMR10 to CMR12

In the case of bi-functional catalytic membrane reactors it is reached an upper limit of the concentration of  $H_2O_2$  as in the case of Pd CMR. This effect is attributed to the surface passivation of the metal palladium by the generated  $H_2O_2$  as in the former case. It is important to notice that the activity can be recovered quite simply only by taking out the membrane from the water leaving the hydrogen flowing through the membrane for a while at ambient temperature. Thereafter the membrane is submerged to the water and an increase in the hydrogen concentration is observed. If the water in the reaction vessel is changed the results are exactly the same as the

previous ones. It has been demonstrated that at this concentration the palladium is deactivated by surface oxidation [150].

Table 6-4 Catalytic results in hydrogen peroxide generation with bimetallic Pd  
 CMRs prepared by impregnation

CMR	Transmembrane pressure ( $\Delta p$ Bar)	H <sub>2</sub> O <sub>2</sub> generation rate* (mol h <sup>-1</sup> m <sup>-2</sup> )	Max. H <sub>2</sub> O <sub>2</sub> generated (ppm)	Efficiency % (mol H <sub>2</sub> O <sub>2</sub> /mol H <sub>2</sub> )	mol H <sub>2</sub> O <sub>2</sub> /(mmol Pd·h)
CMR6	1.8	2.1	16	8	0.020
CMR7	2.0	3.4	23	7	0.006
CMR8	1.7	1.4	11	8	0.018
CMR9	2.3	5.6	13	19	0.059
CMR10	1.5	3.2	10	6.7	0.014
CMR11	1.6	0.7	8	3	0.003
CMR12	2.3	9.7	57	34	0.085

\* The H<sub>2</sub>O<sub>2</sub> generation rates are apparent, i.e. hydrogen peroxide decomposition is not taken into account.

In the Table 6-5 are summarized the results for hydrogen peroxide generation obtained for the membranes with sputtered palladium. The amounts of palladium were calculated from the reference material as described in the experimental section. In all cases the amount of precious metal is more than 200 times less in respect to the impregnated membranes. In the case of sCMR13 which contained only Pd, the measured values were markedly higher than for all other membrane reactors. The rate of hydrogen peroxide generation is twice that for CMR1, the reactor with higher generation rate from the impregnated ones.

The rest of the palladium sputtered membrane reactors present quite similar results to those for the impregnated ones. This is an indication that the main part of the palladium in the impregnated membranes is not involved in the reaction. The main role of the noble metal in the studied reaction is the hydrogen activation that occurs on the metallic surface. A very high degree of metal dispersion is achieved in the sputtered membranes, that is translated into very high activity for hydrogen peroxide generation compared to the impregnated membranes. In the last column of Table 6-5 the activities for hydrogen peroxide generation are normalized with respect to the palladium content. A comparison between CMR2 and sCMR13 (both of them with the same 20 nm pore size supporting membrane) shows a very significant difference: the sputtered membrane has almost 1500 times higher activity. In all other cases there are large differences as well. The second active phases for sputtered membranes were the same as for the impregnated ones.  $\text{TiO}_2$  was not used due to its very low activity in the studied oxidation reaction as discussed in the next sections. The interference that these second phases could have on the results reported in Table 6-5 is unknown at this stage.

Table 6-5 Summarized results obtained for the different catalytic membrane reactors in the hydrogen peroxide generation

CMR	Transmembrane pressure ( $\Delta P$ Bar)	H <sub>2</sub> O <sub>2</sub> generation rate* (mol h <sup>-1</sup> m <sup>-2</sup> )	Max. H <sub>2</sub> O <sub>2</sub> generated (ppm)	Efficiency % (mol H <sub>2</sub> O <sub>2</sub> /mol H <sub>2</sub> )	mol H <sub>2</sub> O <sub>2</sub> /(mmol Pd·h)
sCMR13	4.5	13.7	70	64	50.184
sCMR14	2.3	3.0	14	13	4.640
sCMR15	1.2	1.9	16	8	1.465
sCMR16	2.3	0.6	3	2	7.326
sCMR17	2.6	2.2	19	9.4	5.373

\* The H<sub>2</sub>O<sub>2</sub> generation rates are apparent, i.e. hydrogen peroxide decomposition is not taken into account.

Once the maximum level of hydrogen peroxide in the solution was reached the Pd sputtered membrane reactors were deactivated as in the case of the impregnated ones. It is reasonable to suppose that the deactivation is due to the surface oxidation of Pd similarly to the impregnated membranes. This process is probably even faster due to the higher dispersion of palladium and minimum size of Pd particles. Following this considerations the reactors should be easily re-activated in contact with hydrogen as in the previous case. Surprisingly after applying this simple procedure of hydrogen flowing through the membranes they were not active in the studied reaction. The membranes were reduced by flowing hydrogen in a continuous reactor at different temperatures, up to 400 °C. The cooling step was performed by hydrogen or an inert gas. In both cases the membranes remained inactive after this procedure. In order to re-activate the membranes it was necessary to calcine in air at 400 °C, reduce by hydrogen at 400 °C and cool them in an

inert atmosphere. Thereafter the membranes presented exactly the same activities for hydrogen peroxide generation. All experiments were carried out in MilliQ water; no chemicals have been added to the experimental setup except the high purity hydrogen and air. Chemical contaminants that require oxidation were discarded as a possible cause for the deactivation. These results suggest that, in addition to the surface passivation of the palladium, there are additional changes in the noble metal. It may be assumed that hydrogen has an additional effect which is difficult to clarify by directly investigating the membrane reactors. We discuss this issue in the section where temperature programmed desorption results for palladium sputtered on corundum powder are presented.

### **6.5.2 Phenol oxidation with catalytic membrane reactors prepared by impregnation**

The catalytic membrane reactors with only palladium as active phase (CMR1 to CMR5) did not present any appreciable activity in the phenol oxidation reaction. Figure 6-24 presents the results for CMR1 at different reaction temperatures. Additionally, the results for a blank test, CMR18 (no active phase), are included. In this case the experimental conditions were maintained and the test was performed in order to verify if any stripping of the phenol occurs at the reaction temperature. It can be seen that the concentration of phenol decreases about 5% in 8 hours at both temperatures. This value is quite similar to the result of the blank test so the apparent activity can be attributed to the phenol stripping.

These results clearly indicate that in the studied case the palladium is not active in the reaction of generation of hydroxyl radicals. They also confirm that the most likely reaction pathway consists of hydrogen activation on Pd

surface followed by a reaction between oxygen and activated hydrogen to form hydrogen peroxide or water. In this case the palladium becomes deactivated when certain peroxide concentration is reached. A second active phase in the membrane reactors is needed in order to generate hydroxyl radicals active in the further oxidation of organic matter present in the water. This reaction should be faster than the peroxide generation itself in order to protect the palladium. The validity of the above statement was checked by a simple experiment. Previous to the insertion of the membrane reactor in the reaction vessel, a  $\text{Fe}^{2+}$  salt had been added to the phenol solution. The results for the CMR1 are presented in Figure 6-24. As can be seen the phenol concentration decreases by about 40% within 8 h of reaction. In the presented case the phenol elimination coincides with the TOC and COD decrease. It is important to note that the results of the phenol elimination depend linearly on time. This suggests a first-order reaction with respect to hydrogen peroxide generation, e.g. the phenol oxidation is the faster reaction.

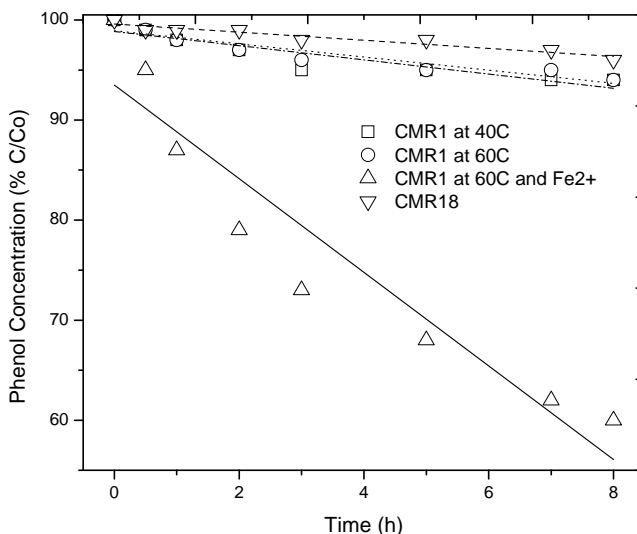
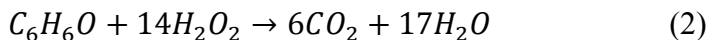


Figure 6-24 Phenol oxidation with CMR1

The calculated rate of phenol oxidation is  $0.05 \text{ mmol h}^{-1}$  assuming a linear dependence in the case of CMR1 in the presence of  $\text{Fe}^{2+}$ . The normalized value for hydrogen peroxide generation for the CMR1 presented in Table 6-2 is  $6.7 \text{ mol H}_2\text{O}_2 (\text{h m}^2)^{-1}$  which corresponds to  $5.5 \text{ mmol h}^{-1} \cdot \text{reactor}^{-1}$ . A comparison of these values suggests that about 10-15% of the generated peroxide is directly involved in the organic oxidation. The results therefore are not very far from the recommended conditions for the Fenton reaction where usually an oxidant excess of about 3-5 times with respect to the organic matter is considered [163]. The efficiency is calculated as:

$$E = \frac{H_2O_{2r}}{H_2O_{2p}} * 100 \quad (1)$$



where  $H_2O_{2r}$  is the required hydrogen peroxide to achieve complete mineralization of phenol and  $H_2O_{2p}$  is the theoretical amount of hydrogen peroxide generated with the catalytic membrane reactor using the kinetic rate calculated for every CMR.

As mentioned before, the experiments performed with CMR1 to CMR5 demonstrate that the presence of a second active phase in the reactors is required to ensure catalytic activity in the Fenton reaction.

Different heterogeneous active phases are reported in the literature to be active in the reaction of hydroxyl radical generation from hydrogen peroxide [96]. In the present study we chose  $Fe_2O_3$ ,  $CuAl_2O_4$ ,  $TiO_2$  and  $CeO_2$ .

Figure 6-25 presents the results for the phenol oxidation when the catalytic membrane reactors with second active phases  $CuAl_2O_4$  (CMR6),  $CeO_2$  (CMR7),  $Fe_2O_3$  (CMR8) and  $TiO_2$  (CMR9) were used. Despite the high activity of CMR9 for hydrogen peroxide generation, no detectable activity was observed for phenol oxidation. The results indicate that  $TiO_2$  in this case is not active in generating hydroxyl radicals that subsequently would oxidize the phenol. More detailed studies should be performed in order to elaborate a plausible explanation in this particulate case.

As seen in Figure 6-25, 15% of phenol elimination was reached with CMR6. The phenol mineralization monitored by TOC analysis was 5%. In this case no aromatic compounds were detected as intermediates in the HPLC chromatograms, and all signals detected corresponded to low

molecular organic acids. At this low concentration it was difficult to identify clearly the exact compounds.

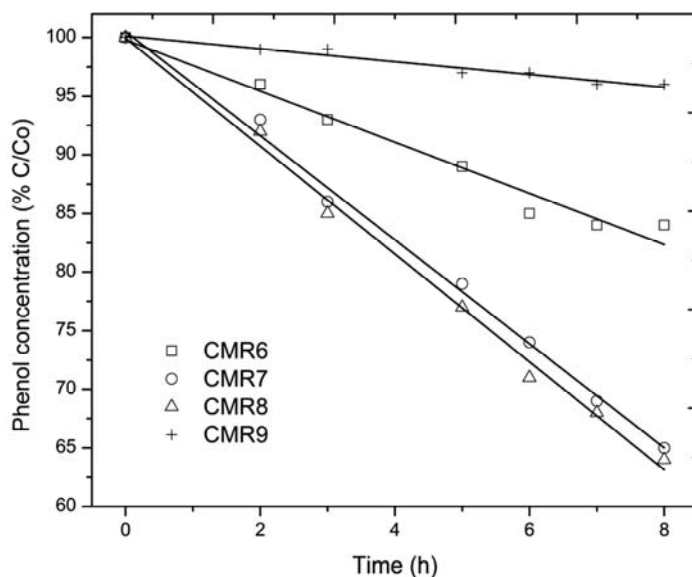
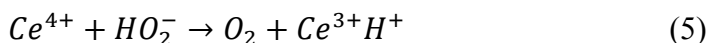
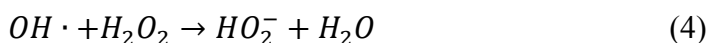
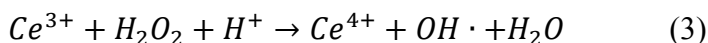


Figure 6-25 Phenol degradation with CMR6, CMR7, CMR8 and CMR9

CMR7 and CMR8 presented a higher activity in phenol abatement. Compared to the  $\text{CuAl}_2\text{O}_4\text{-Pd}$  membrane, these catalytic membranes reached 36% of phenol degradation. In the case of the CMR8, a small amount of catechol (less than 5 ppm) was detected in the reaction products along with traces of low molecular organic acids. A mineralization of 25% was reached after TOC measurements. Null oxidation was achieved with CMR10 and CMR11.

Figure 6-26 presents the results for the phenol oxidation obtained with CMR12. In this case previous to the palladium load iron and cerium oxides were introduced to the membrane.

The CMR catalytic redox properties are improved by the interaction between metallic palladium and cerium oxide, since the oxygen storage capacity of cerium oxide provides oxygen mobility in the membrane active phase [91]. In addition, E.G. Heckert et al have observed that cerium oxide redox capacity ( $Ce^{3+} - Ce^{4+}$ ) enhances the catalytic activity of cerium oxide to act like a hydroxyl radicals generator from hydrogen peroxide [164]. The analogous Fenton/ Haber Weiss reaction with cerium oxide are:



The reaction temperature was maintained at 60°C. This catalytic membrane reactor shows a high activity in phenol degradation, with a phenol abatement level of 93% after 7 hours of reaction. No intermediates were detected in the analyzed samples by HPLC. The phenol was oxidized to carbon dioxide and water. This complete mineralization was confirmed by the TOC analyses of the samples as well as COD measurements. As in the previous cases the phenol oxidation is a first order reaction with respect to peroxide generation. In this case the efficiency of the hydrogen peroxide for phenol oxidation is about 35%. This value was calculated as in the previous case and the ratio between phenol elimination ( $0.13 \text{ mmol h}^{-1}$ ) to the peroxide generation for CMR12 from Table 6-4 is  $5.5 \text{ mmol h}^{-1} \cdot \text{reactor}^{-1}$ .

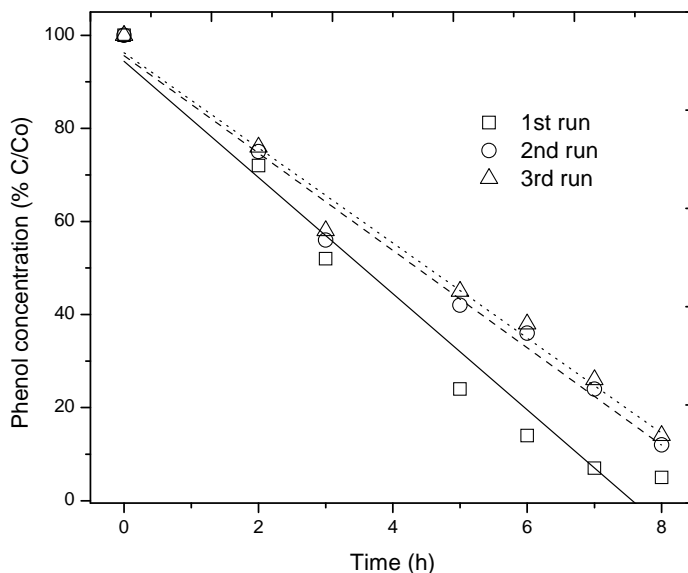


Figure 6-26 Catalytic phenol oxidation with a Pd-CeO<sub>2</sub>-Fe<sub>2</sub>O<sub>3</sub> membrane reactor

Once the reaction had finished, the phenol solution in the reaction vessel was renewed. As it can be seen from the experimental results presented in Figure 6-26, the results obtained in the second run are the same as those in the first one. Several consecutive tests have been performed without any appreciable loss of catalytic activity. This is a very important feature of the developed membrane reactors that indicates that they can be used in a continuous operation.

In the open scientific literature there are reports dealing in phenol hydrogenation using palladium as a catalyst [132, 165-167]. Under the experimental conditions of the present work we did not expect a similar reaction, but nevertheless a test was performed. CMR12 was used to determine possible phenol hydrogenation, and the experimental conditions were kept constant without air supply to the reaction vessel. No decrease in the phenol concentration was observed after 5 hours of reaction.

### **6.5.3 Phenol oxidation with catalytic membrane reactors prepared by sputtering method**

The sputtering preparation techniques were aimed at reducing the amount of precious metal. Very high dispersion is achieved at the same time which also led to higher overall activity. The proposed method also allows the deposition of the Pd exclusively into the reaction zone of the studied reaction.

sCMR13 that contains only Pd as an active phase showed a similar behavior in the studied reaction as the Pd impregnated membrane reactors. sCMR13 did not present any activity for the phenol oxidation under the studied conditions. Similarly to the case of the impregnated membrane,  $\text{Fe}^{2+}$  salt was added to the phenol solution previous to the reaction. The presence of ferrous ions in the homogeneous phase improves the phenol oxidation up to 12% conversion. This value is very low considering the high activity of this reactor in peroxide generation (Table 6-5). Initially it was deduced that due to the high rate of hydrogen peroxide generation the oxidant was not consumed sufficiently fast in the phenol oxidation which would lead to peroxide accumulation in the solution resulting in palladium deactivation. Additional experiments presented below revealed that other reactions are involved in the palladium deactivation.

The surface passivation of Pd due to the slow decomposition of hydrogen peroxide to reactive hydroxyl radicals may induce the oxidation of the palladium surface and subsequent deactivation, as it was observed in the  $\text{H}_2\text{O}_2$  generation by V.R. Choudhary et al [168].

The rest of sCMRs were also tested for phenol degradation. Figure 6-27 shows the phenol abatement using these catalytic membrane reactors. The phenol reduction with sCMR15 and sCMR16 reached 15% after 8 h of

reaction at 60 °C. In both cases the oxidized phenol was completely mineralized, TOC reduction of 15%. sCMR14 with copper aluminate spinel presented quite a low activity, about 10% of phenol abatement and 6% of TOC reduction. Small peaks were detected by HPLC at retention times that correspond to the low molecular organics acids. The phenol oxidation reactions as in the previously presented cases are first order with respect to peroxide generation. The efficiencies of the hydrogen peroxide involved directly in the phenol oxidation are lower than for the impregnated membrane reactors. In subsequent experiments these membrane reactors completely lost their activities in the studied reaction. As commented in section 6.5.3 above, in order to re-activate the reactors it was necessary to calcine, reduce and cool them down in an inert atmosphere.

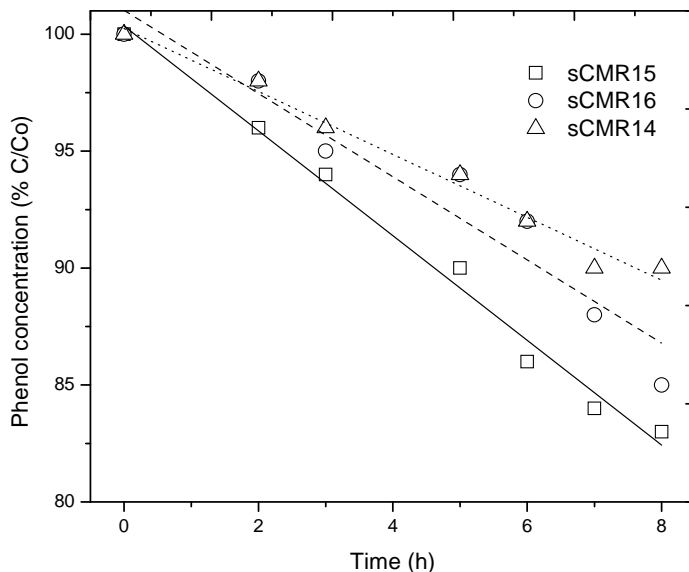


Figure 6-27 Phenol degradation with sCMR14, sCMR15 and sCMR16

The activity for phenol elimination obtained for sCMR17 is presented in Figure 6-28.

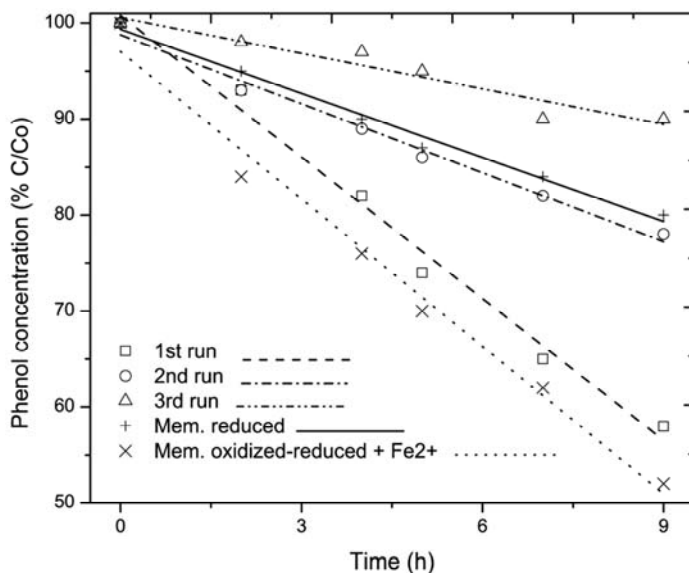


Figure 6-28 Phenol oxidation using sCMR17 at 60 °C and consecutive runs

In the first test sCMR17 presented 42% of phenol elimination and no intermediate products were detected (TOC reduction of 42% was observed). Consequently, a second test was performed after changing the phenol solution in the reaction vessel. In this case the activity of the membrane reactor dropped to 18% for phenol degradation and 10% for TOC elimination. In the third consecutive experiment negligible activity was obtained and for both measured parameters, phenol and TOC, about 10% of reduction was obtained. As commented before it was assumed that this decrease of activity is mainly due to the Pd deactivation. Taking into account the high dispersion of the Pd within the reaction zone it can be assumed that the hydrogen peroxide generation rate is significantly higher

than the consumption of the oxidant in the subsequent reaction of phenol oxidation thus leading to increased levels of peroxide which passivates the noble metal. If this assumption is true, then the Pd activity in the studied reaction should be recovered after reduction in a hydrogen flow. However, after the reduction step at 400 °C in flowing hydrogen followed by a cooling step under inert atmosphere, the activity for the phenol oxidation barely reached 20%. The membrane reactor has been calcined and reduced again at the same conditions. In the experiment performed afterwards Fe<sup>2+</sup> salt has been added to the reactor vessel. In this case the activity for phenol oxidation was similar to the first run, 40% of phenol elimination. However the TOC reduction was about 15% that indicates that with the addition of the homogeneous catalyst the reaction pathways are different. Small amounts of aromatic type compounds as well as low molecular acids have been detected as intermediates by HPLC analyses.

The membrane reactor has been calcined in air atmosphere at 400 °C and thereafter reduced in H<sub>2</sub> flow at 400 °C, the cooling step was done in inert gas flow. As it can be seen from Figure 6-28, the activity was recovered completely.

Some additional experiments with sCMR17 for phenol oxidation at temperature of 80 °C were carried out. Increasing the reaction temperature is expected to enhance the rate of hydrogen peroxide consumption in the oxidation reaction whilst decreasing the probability of palladium deactivation by the excess of reagent. The results are presented in Figure 6-29. Before this, the membrane reactor was calcined and reduced as described above.

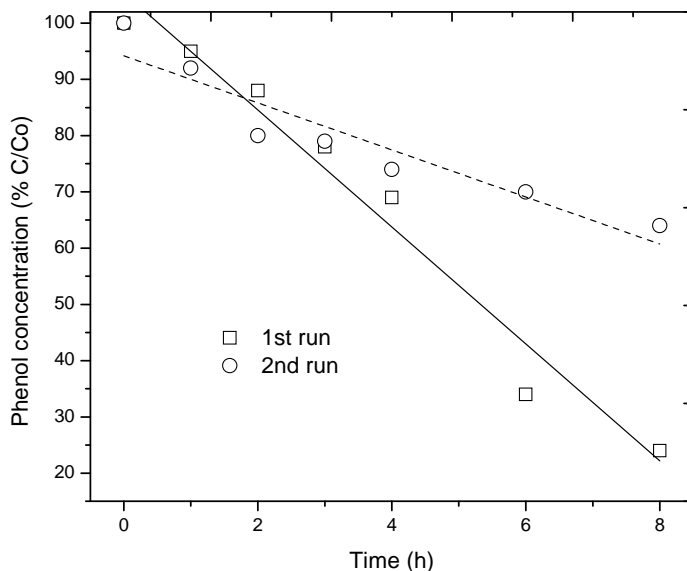


Figure 6-29 Phenol oxidation using sCMR17 at 80 °C

As seen in Figure 6-29, 74% of phenol oxidation was reached in the first run. No intermediate products were detected by HPLC which was also confirmed by the TOC measurements - 74% elimination. However in the second run the activities dropped more than twice, 36% of phenol oxidation. The final TOC of the solution was reduced with 25%, low molecular organic acids were detected by HPLC analyses.

Despite the high activities for hydrogen peroxide generation of the Pd sputtered membrane reactors compared to the impregnated ones there are some specific reactions which take place in the former case leading to the rapid deactivation of the reactors. The small size of the palladium particles obtained after sputtering increases their activity but at the same time makes them more vulnerable to undesired reaction, e.g. palladium hydride formation.

It is important to mention that when the second active phase is cerium oxide the membrane reactor appears to have a more stable activity compared to the other ones. A possible explanation for this difference could be the specific interaction between the small palladium crystals and the surrounding ceria which can favor the stabilization of the metal [169-173]. Possible implications of this strong metal support interaction (SMSI) in the studied reaction are being investigated in a more detail.

The formation of palladium hydride is an important concern in the dense Pd membrane when used in gas mixtures separation or in hydrogenation reactions [174-175]. Its formation provokes mechanical damage of the membranes, they become brittle. In order to overcome the problems associated with the hydride formation the working temperature is maintained above certain level, e.g. 300 °C [176-177].

In the Pd assisted catalytic reactions, especially in hydrogenation processes, the formation of palladium hydride is not considered as a major factor that can alter the catalyst activity; on the contrary, in some studies it is considered a beneficial source of hydrogen [178-179]. Other authors suggest that the palladium hydride, especially after it is transformed to  $\beta$ -Pd, is a main cause for the Pd deactivation, e.g. in hydrogenation reactions [180-181].

Generally the palladium deactivation is attributed to other undesired reactions such as coke formation, water condensation, sulphur and carbon monoxide presence [96, 182].

According to works in the open scientific literature the absorption of hydrogen leads after some time to Pd phase change, the  $\alpha$ -Pd to  $\beta$ -Pd. Some reports suggest that  $\beta$ -Pd (PdH<sub>x</sub> with  $x > 0.5$ ), once is formed is not active for hydrogen activation [180]. This consideration could explain the fast

deactivation of the membrane reactors with palladium loaded by sputtering. In the present case this process may be highly facilitated due to the high surface/bulk ratio. This process should be reversible according to the current scientific understanding.

#### 6.5.4 Effect of hydrogen on sputtered palladium nanoparticles

Some simple experiments were carried out in order to investigate the effects of hydrogen on the sputtered palladium nanoparticles. Corundum powder with sputtered palladium described in the previous sections was used. It was tested in TPD equipment coupled to a mass detector. A cycle program was developed that attempted to achieve the reaction conditions of the hydrogen peroxide generation tests as well as the activation procedure after deactivation. The different steps as well as their purpose are presented in Table 6-6.

Table 6-6 TPD program and the aim of each step

Step	T, gas flows, time	Aim of the step
1	60 °C, 20 sccm <sup>3</sup> min <sup>-1</sup> , 5% H <sub>2</sub> in Ar, 2 h	Reduction of the Pd, possible formation of $\beta$ -Pd
2	60 °C, 20 sccm <sup>3</sup> min <sup>-1</sup> , Ar, 30 min	Purging the lines
3	Heating ramp, 5 °C min <sup>-1</sup> up to 400 °C, 30 min at 400 °C; 20 sccm <sup>3</sup> min <sup>-1</sup> , Ar	Desorption of the H <sub>2</sub> from the $\beta$ -Pd
4	Cool down to 60 °C in 20 sccm <sup>3</sup> min <sup>-1</sup> , Ar	Restore the initial state of the studied sample

The program was repeated 3 times. Figure 6-30 presents the results from the mass detector for Pd sputtered on corundum. The different steps as well as the relevant temperatures are also shown. The y-axis is scaled in a range where the zone of interest is clearly visualised. It can be seen from the graph that hydrogen was desorbed at 320 °C in the first cycle. In the second cycle the peak that corresponds to hydrogen was almost undetectable. In the third cycles no hydrogen was detected. The sample was recovered and calcined at 400 °C and subsequently reduced in hydrogen flow and cooled in Ar atmosphere. This was the activation procedure found to be effective for the reactivation of Pd sputtered membrane reactors. Subsequently, the TPD sequence described above was repeated. The results are shown on Figure 6-31. As it can be seen, the mass detector response was exactly the same as in the first case.

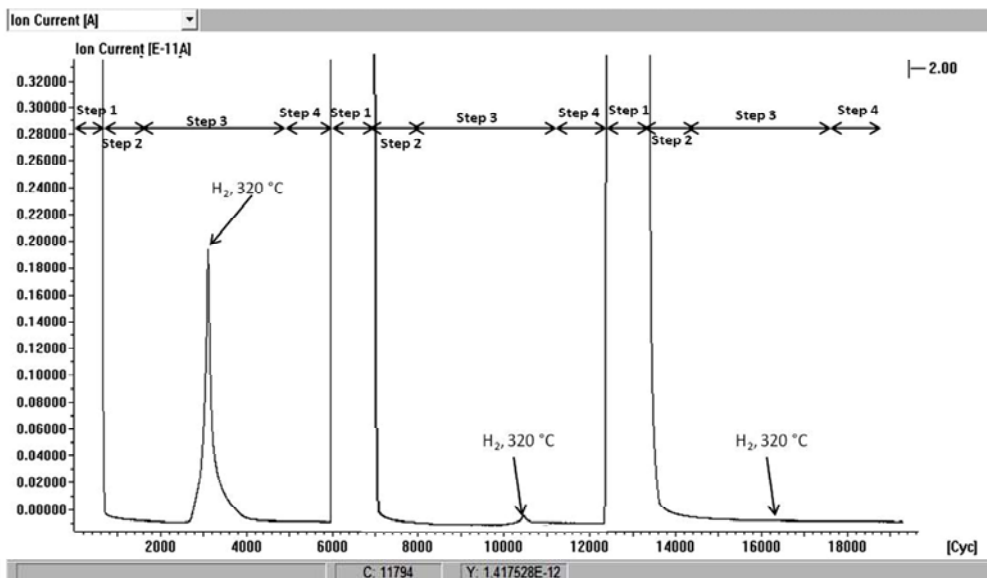


Figure 6-30 TPD-MS  $m/z = 2$  signal obtained from Pd sputtered on corundum

These experiments clearly demonstrate that hydrogen is absorbed by the palladium and probably  $\beta$ -Pd phase is formed. The absorbed hydrogen is strongly retained in the metal and is released at 320 °C. This temperature is similar to the one reported by other authors [182]. The results also demonstrate that some transformations of the palladium occur as can be concluded from its decreasing capacity for hydrogen storage. It is difficult to offer a plausible explanation of this observation at this stage.

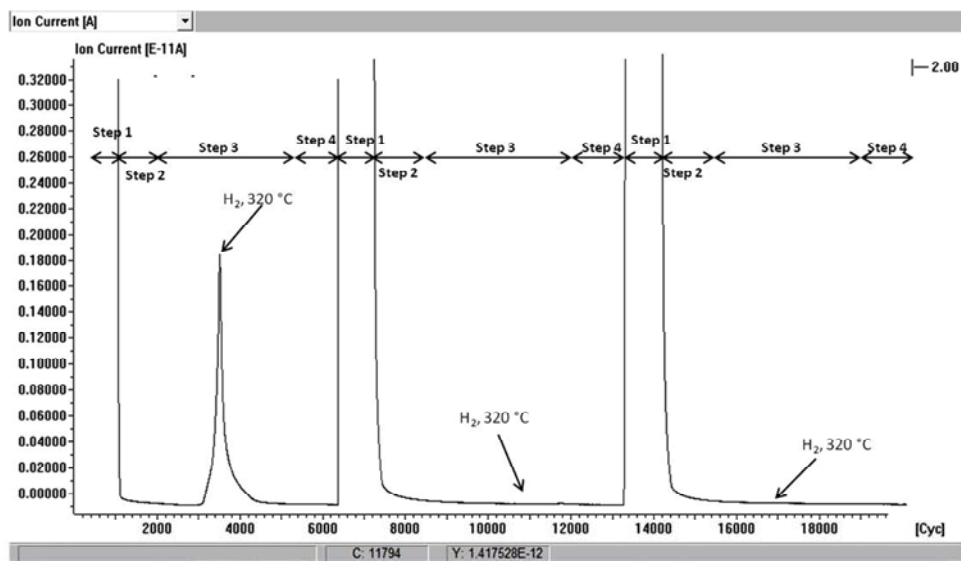


Figure 6-31 TPD-MS  $m/z = 2$  signal obtained from reactivated Pd-corundum

Palladium nanoparticles with defined sizes (4-6 nm) have been studied at different temperatures in various environments e.g. air, inert gas, hydrogen in [182]. The metal particles have been observed by HRTEM and selected area electron diffraction (SAED). These authors observed loss of crystallinity of the metal lattice especially when Pd was in a hydrogen

atmosphere. This finding was attributed to the metal support interactions occurring at high temperature.

We discard the possibility that the palladium deactivation observed with the catalytic membrane reactors is due to the interaction between the Pd and the support especially taking into account that it occurs at 60 °C.

In other study [183] similar experiments demonstrate that at 100 °C under hydrogen the Pd core/ Pt shell 4nm nanoparticles are completely reordered leading to formation of homogeneous Pd-Pt alloy (called solution by the authors).

A more extended study is underway in our laboratory in order to better understand the mechanisms involved in the palladium deactivation. In case we are able to confirm that the hydrogen plays a major role in the metal deactivation, especially for particles in the nanoscale range, additional steps will be considered for its stabilization without decreasing its activity for the hydrogen activation.

## **6.6 Catalytic activity of CMRs in continuous system**

Some experiments in continuous mode were conducted with our proposed module reactor. The designed system was evaluated in continuous operation in catalytic reduction of water contaminants. Pd-CeO<sub>2</sub> CuAl<sub>2</sub>O<sub>4</sub> and Pd-CeO<sub>2</sub>-Fe<sub>2</sub>O<sub>3</sub> membrane reactors were selected and used in the selective reduction of nitrates and hydrodechlorination of chlorinated organic compounds. The active phases were chosen according to the literature.

### **6.6.1 Selective reduction of nitrates**

The selected 30 cm length membrane reactor was placed in the metal housing. The nitrates solution (100ppm) was fed to the lumen side of the

membrane reactor. Whereas, H<sub>2</sub> was continuously dosed through the shell side. Also, one experiment was carried out introducing H<sub>2</sub> co-currently with the nitrate solution feed. The catalytic activity of the CMRs was evaluated in a single pass mode. The results are shown in the Table 6-7 after a mass balance in the outlet solution. The catalytic activity was stable up to 8 hour of operation.

The NO<sub>3</sub><sup>-</sup> conversion was calculated with the following equation:

$$X_{NO_3^-} = \frac{NO_3^-_t - NO_3^-_0}{NO_3^-_0} \times 100(\%)$$

The results show an appreciative catalytic activity using the Pd copper spinel membrane. As it can be observed from the Table 6-7, an important factor in the operation of the CMRs in continuous mode is the correcting dosing of the gas phase. In the experimental runs 1 and 2, once the H<sub>2</sub> flow was increased from 6 to 10 NmL min<sup>-1</sup> the nitrate conversion is 6.5 times lower. This fall in the conversion is attributed to a blowing effect of the gas phase. When the H<sub>2</sub> is dosed up to certain values the gas phase blows the liquid from the CMR surface. It is important to notice that when working above the bubble pressure point and introducing a large amount of gas it is mainly loss. At the same time the gas displaces the liquid from the reaction zone e.g. the active phase loaded onto the membrane. Similar effect is also commented by K. Duab et al. They attributed the low catalytic activity to the displacement of the liquid-gas boundary from the catalyst surface [184].

Table 6-7 Selective reduction of nitrates with CMRs under continuous operation regimen

Exp	H <sub>2</sub> (NmL min <sup>-1</sup> )	NO <sub>3</sub> <sup>-</sup> (ppm)	NH <sub>4</sub> <sup>+</sup> (ppm)	NO <sub>2</sub> <sup>-</sup> (ppm)	NO <sub>3</sub> <sup>-</sup>	Selectivity
					Conversion (%)	N <sub>2</sub> (%)
1 <sup>(1)</sup>	6	14	6	<0.03	86	76
2 <sup>(1)</sup>	10	87	1	<0.03	13	73.5
3 <sup>(2)</sup>	6	94	<0.03	<0.03	6	100
4 <sup>(3)</sup>	6	74	6.5	<0.03	16	13.9
5 <sup>(3)</sup>	10	98	<0.03	<0.003	2	100

<sup>(1)</sup>The experiments were carried out using the Pd-CeO<sub>2</sub> membrane reactor.

<sup>(2)</sup> H<sub>2</sub> was dosed through the membrane wall.

<sup>(3)</sup> H<sub>2</sub> was dosed co-currently with the nitrate solution feed.

<sup>(4-5)</sup> Experimental results obtained using the Pd-CeO<sub>2</sub>-Fe<sub>2</sub>O<sub>3</sub> membrane reactor

An important issue related with results is the selectivity to N<sub>2</sub> as final product. Despite the high nitrates conversion of 86% was achieved, an undesirable reaction took place in the CMR. Ammonia was detected in the outlet stream. The NH<sub>4</sub><sup>+</sup> concentration rises up to 6 ppm in the first experimental run, which has a higher toxic effect to human health. The nitrite concentration was below of the detection limit in all experimental runs.

A third experimental run was carried out using the same CMR. This time H<sub>2</sub> was co introduced to the lumen side of the membrane reactor. Under this operative condition, the nitrate conversion was 14 times lower compared with the first run. The low activity can be related with the low solubility of the H<sub>2</sub> at these working conditions. O.M. Illitch et al. and N. Wehbe et al. reported experimental results operating their CMR in a flow through mode

[185, 149]. In both cases the nitrates solution was pumped to the lumen of the membrane reactor. And the hydrogen was previously dosed to the solution in order to dissolve the maximum amount of the gas in the liquid. However, they reported diffusion limitations and an elevated generation of ammonia.

The Pd-CeO<sub>2</sub>-Fe<sub>2</sub>O<sub>3</sub> membrane reactor presents a low catalytic activity in the reduction of nitrates as well a low selectivity to N<sub>2</sub>. Almost null activity was observed operating this membrane reactor at 10 NmL min<sup>-1</sup>. N. Barrabés et al. have reported higher activities in NO<sub>3</sub><sup>-</sup> reduction using supported CeO<sub>2</sub> and Pt-CeO<sub>2</sub> [186]. A more detailed study has to be carried out in order to find the optimal conditions.

Consecutive tests have been performed with the Pd/ CeO<sub>2</sub> membrane reactor. The CMR was operated up to 4 times at the same conditions in the first experimental run (Table 6-7). Between each test, the CMR was previously dried with flowing H<sub>2</sub> at room temperature. The individual tests have been performed during 8 h as commented before. No changes in the activities were observed between the tests.

As we can observe, our experimental results are similar from the reported in the literature. As initially proposed, the obtained results validate the designed module reactor for continuous operation mode. In order to improve the results it must be optimised the catalytic active phases loaded onto the membrane. The catalyst screening could be done by using the batch system described in the experimental section.

### **6.6.2 Hydrodechlorination of chlorinated aromatic compounds**

Another experiment was carried out in the metal housing reactor. The Pd-CeO<sub>2</sub>-Fe<sub>2</sub>O<sub>3</sub> membrane reactor was used in the hydrodechlorination of 4-Cl-

phenol. A mixture of 4-Cl-phenol and formic acid was fed to the lumen side of the membrane reactor. The formic acid was used as hydrogen donor as it was previously reported by F.D. Kopinke et al. [144]. As they reported, supported Pd cluster are active in the catalytic decomposition of formic acid to  $H_2$  and  $CO_2$ . The hydrogen is chemisorbed and dissociated in the surface of the noble metal.

The module was operated as single pass mode in 24 hours test. The results are shown in the Figure 6-32.

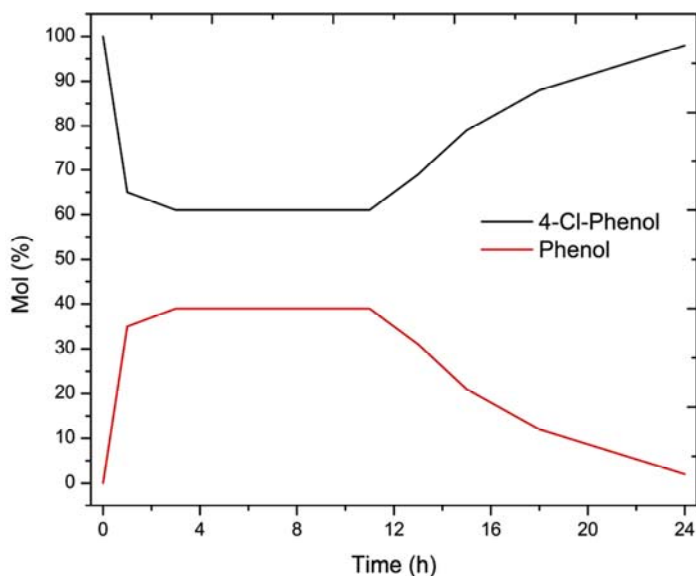


Figure 6-32 Hydrodechlorination of 4-Cl-phenol with CMR in continuous mode

The conversion of 4-Cl-phenol to phenol achieve up to 40% with the catalytic membrane reactor. The CMR presented steady state activity in the hydrodechlorination process during the first 11 h. However, after this time the activity started to decrease up to almost null conversion at the end of the test (24 h). The experiment demonstrates that the proposed mode of

operation of the CMR can be successfully used in this kind of processes. In order to improve the stability of the catalyst more investigation should be done. From the literature the deactivation of the catalyst is attributed to two main causes: i) oxidation of the Pd surface under acid condition. Although the formic acid is used as hydrogen donor, also it can induce the oxidation of the catalyst. Pd<sup>+2</sup> is not active in the catalytic decomposition of the formic acid. And ii) Cl<sup>-</sup> induce the poisoning of the Pd particles [144].

Another experiment was carried out in order to determine if the point i), palladium oxidation, is the cause of deactivation. In this experiment a formic acid solution was fed to the lumen of the CMR. The catalytic decomposition of the acid was monitored measuring TOC in the outlet stream. During the first 2 hours, the TOC decreased with 20% in the outlet feed. After this time, no formic acid decomposition was detected. Therefore, 4-Cl-phenol was injected to the feeding solution to observe if the hydrodechlorination reaction is reactivated. The outlet was constantly monitored but phenol was not detected. At this moment, more tests have been planned to determine the poisoning effect of the chloride to Pd particles.

Even though these results are not concluding, they open a path to operate our CMR with a wide variety of hydrogen sources. In the same way, the metal housing provides different configuration to be explored in the use of the membrane reactors.

UNIVERSITAT ROVIRA I VIRGILI  
DEVELOPMENT OF A NOVEL CATALYTIC MEMBRANE REACTOR: APPLICATION IN WASTEWATER  
TREATMENT  
Oscar Antonio Osegueda Chicas  
Depósito legal:

## **Chapter 7. Conclusions**

Different catalytic membrane reactors were successfully prepared to be used in a novel approach to treat water pollutants. In this work they were tested with model compound solutions in laboratory controlled conditions.

Commercial ultra and nanofiltration ceramic hollow fibers were chosen as support in the preparation of the CMRs. The fibers are made from  $\alpha$ -Al<sub>2</sub>O<sub>3</sub>, material highly resistant to severe conditions e.g. pH range from 1 to 14, broad temperature tolerance, large transmembrane pressure differences, chemical inertness. They resulted to be an exceptional support for the active phases loaded across the membrane wall or on the membrane surface.

The palladium has been chosen as the most appropriated active phase for the hydrogen peroxide generation due to its capability for hydrogen activating.

Two methods were successfully developed to incorporate palladium into the membranes: i) firstly the noble metal has been incorporated into the membranes by means of impregnation methods starting from precursor solutions, and ii) the second method is a novel procedure based on sputtering technique for selectively loading of the Pd on the CMRs. This method allowed us to locate the palladium on the external surface of the membrane reactor where the reactions take place. As well, the amount of the noble metal was reduced up to 260 times compared with the impregnation method.

Electronic microscopy techniques and XRD analysis confirmed a homogeneous distribution of the active phases through the membrane wall and external surface of the CMRs prepare by impregnation. Pd cluster with

sizes from 19 to 31 nm were identified along the entire membrane reactor. The cluster sizes are related with the voids in the membrane wall.

HRTEM was selected to observe the sputtered Pd particles. The mean particle size of Pd particles is centered at 4.8 nm, being 95% of particles within the 2-7 nm range. Also, a micro elemental analysis has shown a selective deposition of Pd particles on the surface on the CMR.

The developed preliminary studies demonstrated that the most efficient method for the hydrogen peroxide generation consist in a controlled dosing of the hydrogen to the inner part of the membrane reactor meanwhile the oxygen is supplied by bubbling air in the water solution. In order to screen the prepared catalytic membrane reactors simple semi batch equipment has been designed and assembled.

The prepared Pd based membrane reactors have been characterized by the following parameters: hydrogen peroxide generation rate per reactor area or metal load, maximum achievable hydrogen peroxide concentration and selectivity to the hydrogen peroxide with respect to the dosed hydrogen.

The monometallic and bimetallic catalytic membrane reactors were successfully tested in the generation of hydrogen peroxide in our experimental design in batch mode. The results have shown a high activity to generate hydrogen peroxide with the monometallic Pd membrane reactors. In the case of the sCMR13 (sputtered Pd) showed the higher activity  $13.7 \text{ mol H}_2\text{O}_2 \text{ h}^{-1} \text{ m}^{-2}$ . As we observed, the activity was intrinsically related with the size of the Pd phase. At lowest particle size higher was the activity in the generation of  $\text{H}_2\text{O}_2$ . The highest activity in the  $\text{H}_2\text{O}_2$  generation with the Pd impregnated membranes was obtained with CMR12:  $9.7 \text{ mol H}_2\text{O}_2 \text{ h}^{-1} \text{ m}^{-2}$ .

After normalization of the hydrogen peroxide generation to the amount of noble metal, the membrane reactors with sputtered Pd have almost 1500 times higher activity than the ones where the Pd was loaded by impregnation.

It has been shown that when a certain concentration of hydrogen peroxide is reached the Pd becomes inactive in the studied reaction. A plausible mechanism for the Pd deactivation was proposed that was further confirmed by the XPS analysis. It has been found that the excess of  $H_2O_2$  passivates the Pd surface. The initial activity of the membrane reactors is completely recovered by flowing hydrogen through the membrane wall at ambient temperature.

The experiments of phenol oxidation by the in-situ generated  $H_2O_2$  demonstrate the necessity of the second active phase that is responsible for the formation of  $\bullet OH$  radicals. The results demonstrated that once  $\bullet OH$  were formed the phenol oxidation is very fast thus preventing the Pd passivation by the excess of  $H_2O_2$ . The bimetallic CMRs with impregnated Pd demonstrate to be very stable in the oxidation process. No deactivation of the reactors was observed on stream. The membrane reactors have shown steady behavior in consecutive tests without decreasing the activity for phenol oxidation. Roughly, up to 30-40% of the generated hydrogen peroxide is directly involved in the phenol oxidation reaction. It has been observed that the transition metal oxide phase plays an important role in the phenol oxidation route e.g. when  $CeO_2$  or mixture  $CeO_2/Fe_2O_3$  have been used no intermediate products have been observed.

In both cases, Pd impregnated and Pd sputtered membrane reactors, the ICP analyses demonstrate no leaching of active phase to the reaction mixture.

Despite the very high activities for hydrogen peroxide generation of the membrane reactors with sputtered palladium they deactivate very fast in the phenol oxidation reaction. It has been proven that the hydrogen plays a major role in the loss of catalytic activity. The experimental results with the sCMRs as well as the TPD and HRTEM analyses of the sputtered Pd on corundum powder have shown that the tiny Pd particles absorb hydrogen until they are converted to PdH<sub>x</sub> with  $\beta$ -Pd structure. This process seems that is highly facilitated by the high surface/ bulk ratio of the sputtered Pd. The formed  $\beta$ -Pd hydride is not active in the hydrogen activation process. Once it is formed the generation of hydrogen peroxide is stopped. In order to recover the catalytic activity in the studied reaction it is necessary to calcine the sCMR followed by activation step. The transition metal oxide active phase can slow down the process as in the case of CeO<sub>2</sub>. Additional studies are strongly encouraged in order to get better understanding of the observed phenomenon.

The obtained results in the present thesis are very promising and validate the suitability of the proposed novel approach in terms of oxidation of target pollutants via *in situ* generated chemical oxidants.

The developed membrane reactors due to their modular nature are easily scalable up to process larger amount of effluent.

Concerning to the module reactor, two different reactions were efficiently carried out in order to determine the feasibility in the operation of the CMRs in continuous mode. The selective reduction of nitrates and hydrodechlorination of 4-Cl-phenol were selected as model reactions.

The preliminary results in the reduction of nitrates and hydrodechlorination of 4-Cl-phenol confirm the viability of the module reactor operated in continuous mode.



## REFERENCES

- [1] United Nation Environmental Programme (UNEP); Global environmental outlook GEO4 environmental for development, section B, chapter 4: Water, first edition (2007).
- [2] World Health Organization (WHO); Un-water global annual assessment of sanitation and drinking water (GLAAS) 2010: targeting resources for better results, first edition (2010).
- [3] M. Palaniappan, P.H. Gleick, L. Allen, M.J. Cohen, J.C. Smith, C. Smith; Clearing the waters, A focus on water quality solutions; United Nation Environmental Programme (UNEP) (2010), edited by N. Ross.
- [4] World Water Assessment Programme (WWAP); Water in changing world; United Nation Educational, Scientific and Cultural Organization (UNESCO), first edition (2009).
- [5] R. Dittmeyer, J. Caro; Catalytic membrane reactors from Handbook of Heterogeneous Catalysis, second edition (2008) Wiley-VCH International; edited by G. Ertl, H. Knözinger, F. Schüth, J. Weitkamp.
- [6] F. Gallucci, A. Basile, F. Ibney Hai; Introduction – A review of membrane reactors from Membrane for Membrane Reactors: Preparation, Optimization and Selection, first edition (2011) John Willey & Sons; edited by A. Basile, F. Gallucci.
- [7] K. Li; Ceramic membranes and membrane processes from Ceramic Membranes for Separation and Reaction, first edition (2007) John Willey & Sons; edited by K. Li.

- [8] A. Basile, F. Gallucci, S. Tosti; Synthesis, characterization, and applications of palladium membranes from Membrane Science and Technology, Vol. 13: Inorganic Membranes: Synthesis, Characterization and Application, first edition (2008) Elsevier; edited by R. Mallada and M. Menéndez.
- [9] G. Barbierie, F. Scura; Fundamental of chemical membrane reactors from Membrane Operation: Innovative Separations and Transformations, first edition (2009), Wiley-VCH International; edited by E. Drioli, L. Giorno.
- [10] E. Fontananova, E. Drioli; Catalytic membranes and membrane reactors from Comprehensive Membrane Science and Membrane Reactors, Vol. 3: Chemical and Biochemical Transformations in Membrane Systems, first edition (2010), Elsevier; edited by E. Drioli, L. Giorno.
- [11] E. Drioli, E. Curcio, G. Di Profio; State of art and recent progresses in membrane contactors; *Chemical engineering research and desing* 83 (2005) 223-233.
- [12] S. Pereira Nunes; Organic – inorganic membranes from Membrane Science and Technology, Vol. 13: Inorganic Membranes: Synthesis, Characterization and Applications, first edition (2008), Elsevier, edited by R. Mallada and M. Menéndez.
- [13] A. Buenkenhoudt, A. Kovalevsky, J. Luyten, F. Snijkers; Basic aspects in inorganic membrane preparation from Comprehensive Membrane Science and Engineering, Vol. 1: Basic Aspects of Membrane Science and Engineering, first edition (2010), Elsevier; edited by E. Drioli, L. Giorno.

- [14] A.F.Ismail, L.I.B. David; A review on the latest development of carbon membranes for gas separation; *Journal of membrane science* 193 (2001) 1-18.
- [15] B. Zhang, T. Wang, S. Liu, S. Zhang, J. Qiu, Z. Chen, H. Cheng; Structure and morphology of microporous carbon membrane materials derived from poly(phthalazinone ether sulfone ketene); *Microporous and mesoporous materials* 96 (2006) 79-83.
- [16] C. Telléz, M. Menéndez; Zeolite membrane reactors from Membrane for Membrane Reactors: Preparation, Optimization and Selection, first edition (2011) John Willey & Sons; edited by A. Basile, F. Gallucci.
- [17] E.E. McLeary, J.C. Jansen, F. Kapteijn; Zeolites based films, membranes and membrane reactors: Progress and perspective; *Microporous and mesoporous materials* 90 (2006) 198-220.
- [18] S. Wu, J.E. Gallot, M. Bousmina, C. Bouchard, S. Kaliaguine; Zeolite containing catalytic membranes as interphase contactors; *Catalysis today* 56 (2000) 113-129.
- [19] A.J. Burggraaf; Important characteristics of inorganic membranes from Membrane Science and Technology Series, Vol. 4: Fundamentals of Inorganic Membrane Science and Technology, first edition (1196) Elsevier; edited by A.J. Burggraaf, L. Cot.
- [20] S. Kumar, S. Shankar, P.R. Shan, S. Kumar; A comprehensive model for catalytic membrane reactor; *International journal of chemical reactor engineering* 4 (2006) A-5.
- [21] K. Li; Ceramic hollow fiber membranes and their applications from Comprehensive Membrane Science and Engineering, Vol. 1: Basic

- Aspects of Membrane Science and Engineering, first edition (2010), Elsevier; edited by E. Drioli, L. Giorno.
- [22] P. Luis, A. Garea, A. Irabien; Modelling of a hollow fiber ceramic contactor for SO<sub>2</sub> absorption; *Separation and purification technology* 72 (2010) 174-179.
- [23] J. Coronas, J. Santamaría; Catalytic reactors based on porous ceramic membranes; *Catalysis today* 51 (1999) 377-389.
- [24] M. Vospernik, A. Pintar, G. Berčič, J. Levec; Experimental verification of ceramic membrane potentials for supporting three-phase catalytic reactions; *Journal of membrane science* 223 (2003) 157-169.
- [25] S. Roy, T. Bauer, M. Al-Dahhan, P. Lehner, T. Turek; Monoliths as multiphase reactors: A review; *AIChE Journal* 50 (2004) 2918-2938.
- [26] N.A. Melosh, P. Davidson, B.F. Chmelka; Monolithic mesophase silica with large ordering domain; *Journal of american chemical society* 122 (2000) 823-829.
- [27] G.L. Drisko, A. Zelcer, V. Luca, R.A. Caruso, G.J. Soler Illia; One-pot synthesis of hierarchically structured ceramic monolith with adjustable porosity; *Chemistry of materials* 22 (2010) 4379-4385.
- [28] Y.S. Kim, X.F. Guo, G.J. Kim; Synthesis of carbon monolith with bimodal meso/macroscale pore structure and its applications in asymmetric catalysis; *Catalysis today* 150 (2010) 91-99.
- [29] G.Q. Lu, J.C. Diniz da Costa, M. Duke, S. Giessler, R. Socolow, R.H. Williams, T. Kreutz; Inorganic membranes for hydrogen production and purification: A critical review and perspective; *Journal of colloid and interface science* 314 (2007) 589-603.

- [30] D.M. Mattox; Handbook of Physical Vapor Deposition (PVD) Processing, second edition (2010), Elsevier.
- [31] H.O. Pierson; Handbook of Chemical Vapor Deposition (CVD). Principles, Technology and Applications, second edition (1999), William Andrew.
- [32] H. Hamilton; Palladium-based membranes for hydrogen separation; *Platinum metal review* 56 (2012) 117-123.
- [33] A. Basile, A. Iulianelli, T. Longo, S. Linguori, M. de Falco; Pd based selective membrane: State of the art from Membrane Reactors for Hydrogen Production, first edition (2011), Springer; edited by M. de Falco, L. Marrelli, G. Iaquaniello.
- [34] J. Shu, B.P.A. Grandjean, A. Van Neste, S. Kaliaguine; Catalytic palladium based membrane reactors: A review; *The Canadian journal of chemical engineering* 69 (1991) 1936-1960.
- [35] S. Miachon, J.A. Dalmon; Catalysis in membrane reactors: what about the catalysis; *Topics in catalysis* 29 (2004) 59-65.
- [36] A. Julbe, D. Farrusseng, C. Guizard; Porous ceramic membranes for catalytic reactors – overview and new ideas; *Journal of membrane science* 181 (2001) 3-20.
- [37] A. Abate, G. Centi, S. Melada, S. Perathoner, F. Pinna, G. Strukul; Preparation, performance and reaction mechanism for the synthesis of H<sub>2</sub>O<sub>2</sub> from H<sub>2</sub> and O<sub>2</sub> based on palladium membranes; *Catalysis today* 104 (2005) 323-328.
- [38] A. Pashkova, K. Svajda, R. Dittmeyer; Direct synthesis of hydrogen peroxide in a catalytic membrane reactor; *Chemical engineering journal* 139 (2008) 165-171.

- [39] L. Shi, A. Goldbach, G. Zeng, H. Zu; H<sub>2</sub>O<sub>2</sub> synthesis over PdAu membranes, *Catalysis today* 156 (2010) 118-123.
- [40] A. Pashkova, R. Dittmeyer, N. Kalterborn, H. Richter; Experimental study of porous catalytic membranes for direct synthesis of hydrogen peroxide; *Chemical engineering journal* 165 (2010) 924-933.
- [41] Z. Wu, M.D. Hatim, B.F.K. Kingsbury, E. Gbenedio, K. Li; A novel inorganic hollow fiber membrane reactor for catalytic dehydrogenation of propane; *AIChE journal* 55 (2009) 2389-2398.
- [42] S. Bhatia, C.Y. Thien, A.R. Mohamed; Oxidative coupling of methane (OCM) in a catalytic membrane reactor and comparison of its performance with other catalytic reactors; *Chemical engineering journal* 148 (2009) 525-532.
- [43] B.F.K. Kingsbury, Z. Wu, K. Li; A morphological study of ceramic hollow fiber membranes: A perspective on multifunctional catalytic membrane reactors; *Catalysis today* 156 (2010) 306-315.
- [44] D.M. Dotzauer, A. Abusaloua, S. Miachon, J.A. Dalmon, M.L. Bruening; Wet air oxidation with tubular ceramic membranes modified with polyelectrolyte/Pt nanoparticles film; *Applied catalysis B: Environmental* 91 (2009) 180-188.
- [45] M. Reif, R. Dittmeyer; Porous, catalytically active ceramic membranes for gas-liquid reactions: a comparison between catalytic diffuser and forced through flow concept; *Catalysis today* 82 (2003) 3-14.
- [46] J.M. Zheng, Z.W. Dai, F.S. Wong, Z.K. Xu; Shell side mass transfer in a transverse flow hollow fiber membrane; *Journal of membrane science* 261 (2005) 114-120.

- [47] T. Westermann, T. Melin; Flow through catalytic membrane reactors: Principles and applications; *Chemical engineering and processing: Process intensification* 48 (2009) 17-28.
- [48] M. Pera-Titus, S. Miachon, J.A. Dalmon; Increased gas solubility in nanoliquids: Improved performance in interfacial membrane contactors; *AIChE Journal* 55 (2009) 434-441.
- [49] T. Westermann, N. Kopriwa, A. Schröder, T. Melin; Effective dispersion model for flow through catalytic membrane reactors combining axial dispersion and pore size distribution; *Chemical engineering science* 65 (2010) 1609-1615.
- [50] M.M. Yousef Motamedhashemi, F. Egofoopoulos, T. Tsotsis; Application of a flow through catalytic membrane reactor (FTCMR) for the destruction of a chemical warfare simulant; *Journal of membrane science* 376 (2011) 119-131.
- [51] A. Basile, E. Drioli, F. Santella, V. Violante, G. Capannelli, G. Vitulli; A study on catalytic membrane reactors for water shift reaction; *Gas separation & purification* 10 (1996) 53-61.
- [52] K. Sato, T. Hanaoka, S. Niwa, C. Stefan, T. Namba, F. Mizukami; Direct hydroxylation of aromatic compounds by a palladium membrane reactor; *Catalysis today* 104 (2005) 260-266.
- [53] Z. Wu, B. Wang, K. Li; A novel dual-layer ceramic hollow fiber membrane reactor for methane conversion; *Journal of membrane science* 352 (2012) 63-70.
- [54] G. Li, M. Kanezashi, T. Yoshioka, T. Tsuru; Ammonia decomposition in catalytic membrane reactors: Simulation and experimental studies; *AIChE Journals* 59 (2013) 168-179.

- [55] H.S. Wu, Y.S. Fu; Reactivity of phenol allylation using a phase transfer catalysis in ion exchange membrane reactor; *International journal of chemical engineering* (2012) DOI:10.1155/2012/196083.
- [56] G. Langhendries, G.V. Baron, I.F.J. Vankelecom, R.F. Parton, P.A. Jacobs; Selective hydrocarbon oxidation using a liquid phase catalytic membrane reactor; *Catalysis today* 56 (2000) 131-135.
- [57] A. Löfberg, H. Bodet, C. Pirovano, M.C. Steil, R.N. Vannier, E. Bordes-Richard; Selective oxidation of hydrocarbons in a catalytic dense membrane reactor: Catalytic properties of BIMEVOX (Me = Ta); *Catalysis today* 118 (2006) 223-227.
- [58] R. Di Felice, G. Capannelli, A. Comite; Multiphase membrane reactors from from Comprehensive Membrane Science and Membrane Reactors, Vol. 3: Chemical and Biochemical Transformations in Membrane Systems, first edition (2010), Elsevier; edited by E. Drioli, L. Giorno.
- [59] R. Dittmeyer, K. Svajda, M. Reif; A review of catalytic membrane layers for gas liquid reactions; *Topics in catalysis* 29 (2004) 3-27.
- [60] R. Burch, P.R. Ellis; An investigation of alternative catalytic approach for the direct synthesis of hydrogen peroxide from hydrogen and oxygen; *Applied catalysis B: Environmental* 42 (2003) 203-211.
- [61] J.M. Campos-Martin, G. Blanco-Brieva, J.L.G. Fierro; Hydrogen peroxide synthesis: An Outlook beyond the anthraquinone process; *Angewanted chemical international edition* 45 (2006) 6962-6984.
- [62] J.K. Edwards, B. Solsona, E. Ntainjua, A.F. Carley, A.A. Herzing, C.J. Kiely, G.J. Hutchings; Switching off hydrogen peroxide

- hydrogenation in the direct synthesis process; *Science* 323 (2009) 1037-1041.
- [63] R.J. Lempert, P. Norling, C. Pernin, S. Resetar, S.J. Mahnovski; Report: Next generation environmental technologies. Benefits and barriers; prepared by Office of science and technology policy from RAND organization (2003).
- [64] S. Chinta, J.H. Lunsford; A mechanistic study of H<sub>2</sub>O<sub>2</sub> and H<sub>2</sub>O formation from H<sub>2</sub> and O<sub>2</sub> catalyzed by palladium in an aqueous medium; *Journal of catalysis* 225 (2004) 249-255.
- [65] M. Yildiz, A.N. Akin; Direct formation of H<sub>2</sub>O<sub>2</sub> from H<sub>2</sub> and O<sub>2</sub>; *Turkish journal of chemistry* 31 (2007) 479-486.
- [66] Y. Voloshin, A. Lawal; Overall kinetics of hydrogen peroxide formation by direct combination of H<sub>2</sub> and O<sub>2</sub> in a microreactor; *Chemical engineering science* 65 (2010) 1028-1036.
- [67] P. Biasi, S. Zancadella, F. Pinna, P. Canu, T.O. Salmi; Hydrogen peroxide direct synthesis: from catalyst preparation to continuous reactors; *Chemical engineering transactions* 24 (2011) 49-54.
- [68] P. Biasi, N. Gemo, J.R. Hernández Carucci, K. Eränen, P. Canu, T.O. Salmi, Kinetics and mechanism of H<sub>2</sub>O<sub>2</sub> direct synthesis over a Pd/C catalyst in a batch reactor; *Industrial & Engineering chemistry research (ACS)* 51 (2012) 8903-8912.
- [69] U. Rossi, S. Zancadella, L. Artiglia, G. Granozzi, P. Canu; Direct synthesis of H<sub>2</sub>O<sub>2</sub> on model Pd surfaces; *Chemical engineering journal* 207-208 (2012) 845-850.

- [70] T. Inoue, K. Ohtaki, S. Murakami, S. Matsumoto; Direct synthesis of hydrogen peroxide base on microreactor technology; *Fuel processing technology* (2012) DOI:10.1016/j.fuproc.2012.04.009
- [71] N. Gemo, P. Biasi, P. Canu, T.O.Salmi; Mass transfer and kinetics of H<sub>2</sub>O<sub>2</sub> synthesis in a batch slurry reactor; *Chemical engineering journal* (2012) DOI: <http://dx.doi.org/10.1016/j.cej.2012.07.015>
- [72] B.E. Solsona, J.K. Edwards, P. Landon, A.F. Carley, A. Herzing, C.J. Kiely, G.J. Hutchings; Direct synthesis of hydrogen peroxide from H<sub>2</sub> and O<sub>2</sub> using Al<sub>2</sub>O<sub>3</sub> supported Au-Pd catalyst; *Chemistry of materials* 18 (2006) 2689-2695.
- [73] V.R. Choundhary, C. Samanta, T.V. Choundhary; Direct oxidation H<sub>2</sub> to H<sub>2</sub>O<sub>2</sub> over Pd-based catalyst: Influence of oxidation state, support and metal additives; *Applied catalysis A: General* 308 (2006) 128-133.
- [74] G. Li, J. Edwards, A.F. Carley, G.J. Hutchings; Direct synthesis of hydrogen peroxide from H<sub>2</sub> and O<sub>2</sub> using zeolite-supported Au-Pd catalysts; *Catalysis today* 122 (2007) 361-364.
- [75] S. Ma, G. Li, X. Wang; Direct synthesis of hydrogen peroxide from H<sub>2</sub>/O<sub>2</sub> and oxidation of thiophene over supported gold catalysts; *Chemical engineering journal* 156 (2010) 532-539.
- [76] P. Biasi, F. Menegazzo, F. Pinna, K. Eräne, T.O. Salmi, P. Canu; Continuous H<sub>2</sub>O<sub>2</sub> direct synthesis over PdAu catalysts; *Chemical engineering journal* 176-177 (2011) 172-177.
- [77] E.N. Ntaijua, M. Piccinini, J.C. Pritchard, J.K. Edwards, A.F. Carley, C.J. Kiely, G.J. Hutchings; Direct synthesis of hydrogen

- peroxide using ceria-supported gold and palladium catalysts; *Catalysis today* 178 (2011) 47-50.
- [78] P. Biasi, P. Canu, F. Menegazzo, F. Pinna, T.O. Salmi; Direct synthesis of hydrogen peroxide in a trickle bed reactor: Comparison of Pd based catalysts; *Industrial & Engineering chemistry research (ACS)* 51 (2012) 8883-8890.
- [79] Y.F. Han, J.H. Lunsford; Direct formation of H<sub>2</sub>O<sub>2</sub> from H<sub>2</sub> and O<sub>2</sub> over Pd/SiO<sub>2</sub> catalysts: The role of the acid and the liquid phase; *Journal of catalysis* 230 (2005) 313-316.
- [80] V.R. Choundhary, Y.V. Ingole, C. Samanta, P. Jana; Direct oxidation of hydrogen to hydrogen peroxide over Pd (or PdO)/Al<sub>2</sub>O<sub>3</sub> in aqueous reaction medium: Influence of different acids and halides anions in reaction medium on formation and destruction of H<sub>2</sub>O<sub>2</sub>; *Industrial & Engineering chemistry research (ACS)* 46 (2007) 8566-8573.
- [81] V.R. Choundhary, P. Jana; Direct H<sub>2</sub>-to-H<sub>2</sub>O<sub>2</sub> over highly active/selective Br-F-Pd/Al<sub>2</sub>O<sub>3</sub> catalyst in aqueous acidic medium: Influence of process conditions on the H<sub>2</sub>O<sub>2</sub> formation; *Applied catalysis A: General* 352 (2009) 35-42.
- [82] V.R. Choundhary, P. Jana; In situ generation of hydrogen peroxide from reaction of O<sub>2</sub> and hydroxylamine from hydroxylammonium salt in neutral aqueous or non aqueous medium using reusable Pd/Al<sub>2</sub>O<sub>3</sub> catalyst; *Catalyst communication* 8 (2007) 1578- 1582.
- [83] Q. Liu, J.C. Bauer, R.E. Schaak, J.H. Lunsford; Supported palladium nanoparticles: An efficient catalyst for the direct formation of H<sub>2</sub>O<sub>2</sub>

- from H<sub>2</sub> and O<sub>2</sub>; *Angewandte chemie international edition* 47 (2008) 6221-6224.
- [84] J.K. Edwards, E. Ntainjua, A.F. Carley, A.A. Herzing, C.J. Kiely, G.J. Hutchings; Direct synthesis of H<sub>2</sub>O<sub>2</sub> from H<sub>2</sub> and O<sub>2</sub> over gold, palladium, and gold-palladium catalyst supported on acid pretreated TiO<sub>2</sub>; *Angewandte chemie international edition* 48 (2009) 8512-8515.
- [85] T. Moreno Rueda, J. García Serna, M.J. Cocero Alonso; Direct production of H<sub>2</sub>O<sub>2</sub> from H<sub>2</sub> and O<sub>2</sub> in a biphasic H<sub>2</sub>O/scCO<sub>2</sub> system over a Pd/C catalyst: Optimization of reaction conditions; *The journal of supercritical fluids* 62 (2012) 119-125.
- [86] H. Lee, S. Kim, D.W. Lee, K.W. Lee; Direct synthesis of hydrogen peroxide from hydrogen and oxygen over Pd core silica shell catalyst; *Catalysis communication* 12 (2011) 968-971.
- [87] G. Centi, R. Dittmeyer, S. Perathoner, M. Reif; Tubular inorganic membrane reactors: advantages and performance of multiphase hydrogenation reactions; *Catalysis today* 79-80 (2003) 139-149.
- [88] A. Abate, G. Centi, S. Melada, S. Perathoner, F. Pinna, g. Strukul; Preparation, performances and reaction mechanism for the synthesis of H<sub>2</sub>O<sub>2</sub> from H<sub>2</sub> and O<sub>2</sub> based on palladium membranes; *Catalysis today* 104 (2005) 323-328.
- [89] S. Melada, F. Pinna, G. Strukul, S. Perathoner, G. Centi; Palladium modified catalytic membranes for the direct synthesis of H<sub>2</sub>O<sub>2</sub>: preparation and performance in aqueous solution; *Journal of catalysis* 235 (2005) 241-248.

- [90] S. Melada, F. Pinna, G. Strukul, S. Perathoner, G. Centi; Direct synthesis of  $H_2O_2$  on monometallic a bimetallic catalytic membranes using methanol as reaction medium; *Journal of catalysis* 237 (2006) 213-219.
- [91] L. Shi, A. Goldbach, G. Zeng, H. Xu;  $H_2O_2$  synthesis over PdAu membranes; *Catalysis today* 156 (2010) 118-123.
- [92] L. Shi, A. Goldbach, G. Zeng, H. Xu; Direct  $H_2O_2$  synthesis over Pd membranes at elevated temperatures; *Journal of membrane science* 348 (2010) 160-166.
- [93] T. Inoue, Y. Tanaka, D.A. Pacheco Tanaka, T.M. Suzuki, K. Sato, M. Nishioka, S. Hamkawa, F. Mizukami; Direct production of hydrogen peroxide from oxygen and hydrogen applying membrane permeation mechanism; *Chemical engineering science* 65 (2010) 436-440.
- [94] S. Abate, P. Lanzafame, S. Perathoner, G. Centi; SBA-15 as a support for palladium in the direct synthesis of  $H_2O_2$  from  $H_2$  and  $O_2$ ; *Catalysis today* 169 (2011) 167-174.
- [95] R. Alnaizy, A. Akgerman; Advanced oxidation of phenolic compounds; *Advances in environmental research* 4 (2000) 233-244.
- [96] O.P. Pestunova, O.L. Ogorodnikova, V.N. Parmon; Studies of phenol wet peroxide oxidation in presence of solid catalyst; *Chemistry for sustainable development* 11 (2003) 227-232.
- [97] J.M. Britto, S. Botelho de Oliveira, D. Rabelo, M.C. Rangel; Catalytic wet peroxide oxidation of phenol from industrial wastewater on activated carbon; *Catalysis today* 133-135 (2008) 582-587.

- [98] Water, air, and climate change brand of Ministry of water, land and air protection of British Columbia; Summary report (2002): Ambient working, water quality guidelines for phenol.
- [99] R. Andrezzi, V. Caprio, A. Insola, R. Marotta; Advanced oxidation processes (AOP) for water purification and recovery; *Catalysis today* 53 (1999) 51-59.
- [100] W. Glaze, J.w. Kang, D.H. Chapin; The chemistry of water treatment processes involving ozone, hydrogen peroxide and ultraviolet radiation; *Ozone science & Engineering* 9 (1997) 335-352.
- [101] N.K. Shamas, J.Y. Yang, P.C. Yuan, Y.T. Huang; Chemical oxidation from Handbook of Environmental Engineering, Vol. 3: Physicochemical treatment processes, first edition (2005) Humana Press; edited by L.K. Wang, Y.T. Hung, N.K. Shamas.
- [102] B.G. Petri, R.J. Watts, A.L. Teel, S.G. Huling, R.A. Brown; Fundamental of ISCO using hydrogen peroxide from In Situ Chemical Oxidation of Groundwater Remediation, first edition (2011) Springer Science +Business Media; edited by R.L. Siegrist, M. Crimi, T.J. Simpkin.
- [103] A. Santos, P. Yustos, B. Durban, F. García-Ochoa; Catalytic wet oxidation of phenol: kinetics of mineralization rate; *Industrial & Engineering chemistry research (ACS)* 40 (2001) 2773-2781.
- [104] M. Vospornik, A. Pintar, J. Levec; Application of a catalytic membrane reactor to catalytic wet air oxidation of formic acid; *Chemical engineering and processing* 45 (2006) 404-414.

- [105] G. Langhendries, G.V. Baron, I.F.J. Vankelecon, R.F. Parton, P.A. Jacobs; Selective hydrocarbon oxidation using a liquid phase catalytic membrane reactor; *Catalysis today* 56 (2000) 131-135.
- [106] S. Perathoner, G. Centi; Wet hydrogen peroxide catalytic oxidation (WHPCO) of organic waste in agro-food and industrial streams; *Topics in catalysis* 33 (2005) 207-224.
- [107] R.H.S. Jansen, J.W. de Rijk, A. Zwijnenburg, M.H.V. Mulder, M. Wessling; Hollow fiber membrane contactor – A means to study the reaction kinetics of humic substances ozonation; *Journal of membrane science* 257 (2005) 48-59.
- [108] S.K. Bhargava, J. Tardio, j. Prasad, K. Föger, D.B. Akolekar, S.C. Grocott; Wet oxidation and catalytic wet oxidation; *Industrial & Engineering chemistry research (ACS)* 45 (2006) 1221-1258.
- [109] J.A. Melero, F. Martínez, J.A. Botas, R. Molina, M.I. Pariente; Heterogeneous catalytic wet peroxide oxidation systems for the treatment of an industrial pharmaceutical wastewater; *Water research* 43 (2009) 4010-4018.
- [110] M. Alame, A. Abusaloua, M. Pera-Titus, N. Guilhaume, K. Fiaty, A. Giroir-Fendler; High performance catalytic wet air oxidation (CWAO) of organic acids and phenol in interfacial catalytic membrane contactors under optimized wetting conditions; *Catalysis today* 157 (2010) 327-333.
- [111] M. Gutiérrez, P. Pina, M. Torres, M.A. Cauqui, J. Herguido; Catalytic wet oxidation of phenol using membrane reactors: A comparative study with slurry type reactors; *Catalysis today* 149 (2010) 326-333.

- [112] A. Georgi, R. Gonzalez-Olmos, R. Köhler, F.D. kopinke; Fe-Zeolites as catalysts for wet hydrogen peroxide oxidation of organic groundwater contaminants: Mechanistic studies and applicability tests; *Separation science and technology* 45 (2010) 1579-1586.
- [113] R.C. Martins, R.M. Quinta-Ferreira; Remediation of phenolic wastewaters by advanced oxidation processes (AOPs) at ambient conditions: Comparative studies; *Chemical engineering science* 66 (2011) 3243-3250.
- [114] Y.Y. Zhang, C.He, V.K. Sharma, X.Z. Li, S.H. Tian, Y. Xiong; A new reactor coupling heterogeneous Fento-like catalytic oxidation with membrane separation for degradation of organic pollutants; *Journal of chemical technology and biotechnology* 86 (2011) 1488-1494.
- [115] R. Molinari C. Lavorato, T. Poerio; Performance of vanadium based catalyst in a membrane contactor for the benzene hydroxylation of phenol; *Applied catalysis A: General* 417-418 (2012) 87-92.
- [116] A. Itoh, Y. Kuroda, T. Kitano, G. Zhi-Hu, A. Kunai, K. Sasaki; Catalytic oxidation of benzoic acid in acetic acid: aromatic hydroxylation with in situ-generated hydrogen peroxide; *Journal of molecular catalysis* 69 (1991) 215-222.
- [117] F. Frusteri, E.N. Savinov, A. Parmaliana, E.R. Savinova, V.N. Parmon, N. Giordano; Partial oxidation of ethane by in situ generated H<sub>2</sub>O<sub>2</sub>; *Catalysis letters* 27 (1994) 355-360.
- [118] M.G. Clerici, P. Ingallina; Oxidation reactions with in situ generated oxidants; *Catalysis today* 41 (1998) 351-364.

- [119] S. Yuan, Y. Fan, Y. Zhang, M. Tong, P. Liao; Pd-catalytic in situ generation of H<sub>2</sub>O<sub>2</sub> from H<sub>2</sub> and O<sub>2</sub> produced by water electrolysis for the efficient electron Fenton degradation of rhodamine B; *Environmental science & Technology* 45 (2011) 8514-8520.
- [120] S.I. Niwa, M. Eswaramoorthy, J. Nair, A. Raj, N. Itoh, H. Shoji, T. Namba, F. Mizukami; A one step conversion of benzene to phenol with a palladium membrane; *Science* 295 (2002) 105-107.
- [121] G.D. Vulpescu, M. Ruitenbeek, L.L. van Lieshout, L.A. Correia, D. Meyer, P.P.A.C. Pex; One step selective oxidation over a Pd-based catalytic membrane; evaluation of the oxidation of benzene to phenol as a model reaction; *Catalysis communications* 5 (2004) 347-351.
- [122] L. Bortolotto, R. Dittmeyer; Direct hydroxylation of benzene to phenol in a novel microstructured membrane reactor with distributed dosing hydrogen and oxygen; *Separation and purification technology* 73 (2010) 51-58.
- [123] R. Dittmeyer, L. Bortolotto; Modification of the catalytic properties of a Pd membrane catalyst for direct hydroxylation of benzene to phenol in a double-membrane reactor by sputtering of different catalyst systems; *Applied catalysis A: General* 391 (2011) 311-318.
- [124] V.R. Choundhary, A.G. Gaikwad, S.D. Sansare; Nonhazardous direct oxidation of hydrogen to hydrogen peroxide using a novel membrane catalyst; *Angewandte chemie international edition* 40 (2001) 1776-1779.

- [125] S.G. Huling, B.E. Pivetz; Summary report (2006): In situ chemical oxidation; Office of research and development of Environmental Protection Agency.
- [126] I. Kumakiri, J. Hoktad, T.A. Peters, A.G. Melbye, H. Raeder; Oxidation of aromatic compounds in water and seawater by catalytic membrane process; *Journal of petroleum science and engineering* 79 (2011) 37-44.
- [127] H. Jiang, L. Meng, R. Chen, W. Jin, W. Xing, N. Xu; A novel dual membrane reactor for continuous heterogeneous oxidation catalysis; *Industrial & Engineering Chemistry Research (ACS)* 50 (2011) 10458-10464.
- [128] B.P. Chaplin, M. Reinhard, W.F. Schneider, C. Schüth, J.R. Shapley, T.J. Strathmann, C.J. Werth; Critical review of Pd-based catalytic treatment priority contaminants in water; *Environmental Science & Technology* 46 (2012) 3655-3670.
- [129] Y. Liu, F. Yang, P.L. Yue, G. Chen; Catalytic hydrodechlorination of chlorophenols in water by Palladium/Iron, *Water Research* 35 (2001) 1887-1890.
- [130] F.D. Kopinke, K. Makenzie, R. Köhler; Catalytic hydrodechlorination of groundwater contaminants in water and gas phase using Pd/Al<sub>2</sub>O<sub>3</sub>; *Applied Catalysis B: Environmental* 44 (2003) 15-24.
- [131] G. Yuan, M.A. Keane; Catalyst deactivation during liquid phase hydrodechlorination of 2,4-dichlorophenol over supported Pd: influence of the support; *Catalysis Today* 88 (2003) 27-36.

- [132] E.Díaz, J.A. Casas, A.F. Mohedano, L. Calvo, M.A. Gilarranz, J.J. Rodríguez; Kinetics of 4-chlorophenol hydrodechlorination with alumina and activated carbon supported Pd and Rh catalysts; *Industrial & Engineering chemistry research (ACS)* 48 (2009) 3351-3358.
- [133] E.V. Gobulina, E.S. Lokteva, S.A. Kachevsky, A.O. Turakulova, V.V. Lunin; Development and design of Pd containing supported catalysts for hydrodechlorination; 10<sup>th</sup> International symposium “Scientific bases for the preparation of heterogeneous catalysis” (2010) Elsevier; edited by E.M. Gaigneaux, M. Devillers, S. Hermans, P. Jacobs, J. Martens, P. Ruiz.
- [134] G. Neri, M.G. Musolino, C. Milone, D. Pietropaolo, S. Galvagno; Particle size effect in the catalytic hydrogenation of 2,4-dinitrotoluene over Pd/C catalysts; *Applied catalysis A: General* 208 (2001) 307-316.
- [135] M.A. Keane; A review of catalytic approaches to waste minimization: case study-liquid-phase catalytic treatment of chlorophenols; *Journal of chemical technology and biotechnology* 80 (2005) 1211-1222.
- [136] V.I. Simagina, E.S. Tayban, E.D. Grayfer, A.G. Gentsler, O.V. Komova, O.V. Netskina; Liquid phase hydrodechlorination of chlorobenzene by molecular hydrogen: The influence of reaction medium on process efficiency; *Pure and applied chemistry* 81 (2009) 2107-2114.
- [137] S. Suresh; Reductive remediation of pollutants using metals; *The open waste management journal* 2 (2009) 6-16.

- [138] C.S. Srikanth, V.P. Kumar, B. Viswanadham, K.V.R. Chary; Hydrodechlorination of 1,2,4-trichlorobenzene over supported ruthenium catalysts on various supports; *Catalysis communications* 13 (2011) 69-72.
- [139] Y. Shao, Z. Xu, H. Wan, Y. Wan, H. Chen, S. Zheng, D. Zhu; Enhance liquid phase catalytic hydrodechlorination of 2,4-dichlorophenol over mesoporous carbon supported Pd catalysts; *Catalysis communication* 12 (2011) 1405-1409.
- [140] F. Cárdenas-Lizana, D. Lamey, N. Perret, S. Gómez-Quero, L. Kiwi-Minsker, M.A. Keane; Au/Mo<sub>2</sub>N as a new catalyst formulation for the hydrogenation of p-chlorinitrobenzene in both liquid and gas phases; *Catalysis communications* 21 (2012) 46-51.
- [141] R. Navon, S. Eldad, K. Mackenzie, F.D. Kopinke; Protection of palladium catalysts for hydrodechlorination of chlorinated organic compounds in wastewaters; *Applied catalysis B: Environmental* 119-120 (2012) 241-247.
- [142] L. Teevs, K.D. Vorlop, U. Prüße; Model study on the aqueous phase hydrodechlorination of clopyralid on noble metal catalysts; *Catalysis communication* 14 (2011) 96-100.
- [143] J. Andersin, P. Parkkinen, K. Honkala; Pd-catalyzed hydrodehalogenation of chlorinated olefins: Theoretical insights to the reaction mechanism; *Journal of catalysis* 290 (2012) 118-125.
- [144] F.D. Kopinke, K. Mackenzie, R. Koehler, A. Georgi; Alternative sources for hydrogen for hydrodechlorination of chlorinated organic compounds in water by Pd catalysts; *Applied catalysis A: General* 271 (2004) 119-128.

- [145] M. Cobo, C.A. González, E.G. Sánchez, C. Montes; Catalytic hydrodechlorination of trichloroethylene with 2-propanol over Pd/Al<sub>2</sub>O<sub>3</sub>; *Catalysis today* 172 (2011) 78-83.
- [146] O.M. Ilinich, E.N. Gribov, P.A. Simonov; Water denitrification over catalytic membranes: hydrogen spillover and catalytic activity of macroporous membrane loaded with Pd and Cu; *Catalysis today* 82 (2003) 49-56.
- [147] N. Barrabés, J. Just, A. Dafinov, F. Medina, J.E. Sueiras, Y. Cesteros, P. Salagre; Catalytic reduction of nitrates on Pt-Cu and Pd-Cu/AC using a continuous reactor. Effect of copper nanoparticles; *Applied catalysis B: Environmental* 62 (2005) 77-85.
- [148] N. Barrabés, K. Föttinger, A. Dafinov, F. Medina, J.E. Sueiras, G. Rupprechter; Selective hydrodechlorination of trichloroethylene on noble metal-promoted Cu hydrotalcite-derived catalyst; *Journal of catalysis* 263 (2009) 239-246.
- [149] N. Wehbe, N. Guilhaume, K. Fiaty, S. Miachon, J.A. Dalmon; Hydrogenation of nitrates in water using mesoporous membranes operated in a flow through catalytic contactor; *Catalysis today* 156 (2010) 208-215.
- [150] O. Osegueda, A. Dafinov, J. Llorca, F. Medina, J. Sueiras; In situ generation of hydrogen peroxide in catalytic membrane reactor; *Catalysis today* 193 (2012) 128-136.
- [151] O. Osegueda, A. Dafinov, J. Llorca, F. Medina, J. Sueiras; Novel catalytic membrane reactor for heterogeneous catalytic oxidation of phenol by in situ generated hydrogen peroxide: An environmental sound approach; submitted.

- [152] A. Alejandre, F. Medina, P. Salagre, A. Fabregat, J. Sueiras; Characterization and activity of copper and nickel catalyst for the oxidation of phenol aqueous solutions; *Applied catalysis B: Environmental* 18 (1998) 307-315.
- [153] R. Chechetto, R.S. Brusa, A. Motiello, A. Basile; PVD techniques for metallic membranes reactors from Membranes for Membranes Reactors: Preparation, Optimization and Selection, first edition (2011) John Wiley & sons, edited by A. Basile, F. Galluci.
- [154] A. Basile, E. Drioli, F. Santella, V. Violante, G. Capannelli, G. Vitulli; A study on catalytic membrane reactors for water shift reaction; *Gas separation purification* Vol. 10 No. 1 (1996) 53-61.
- [155] R.J. Farrauto, M.C. Hobson; Catalyst characterization from Encyclopedia of Physical Science and Technology, third edition (2001) Academic Press, edited by R.A. Meyers.
- [156] C. Causserand, P. Aimar; Characterization of filtration membranes from Comprehensive Membrane Science and Membrane Reactors, Vol. 1: Basics aspects of membrane science and engineering, first edition (2010), Elsevier; edited by E. Drioli, L. Giorno.
- [157] K.C. Khulbe, C.Y. Feng, T. Matsuura; Membrane characterization from Desalination and Water Resource (DESWARE), (2010) Encyclopedia of Life Support Systems – UNESCO, edited by D.A. Gobaisi.
- [158] B.F.K. Kingsbury, K. Li; A morphological study of ceramic hollow fiber membranes; *Journal of membrane science* 328 (2009) 134-140.

- [159] M.D. Irfan Hatim, X. Tan, Z. Wu, K. Li; Pd/Al<sub>2</sub>O<sub>3</sub> composite hollow fiber membranes: Effect of substrate resistances on H<sub>2</sub> permeation properties; *Chemical engineering science* 66 (2011) 1150-1158.
- [160] A.E. Childress, P. Le-Clech, J.L. Daugherty, C. Chen, G.L. Leslie; Mechanical analysis of hollow fiber membrane integrity in water reuses applications; *Desalination* 180 (2005) 5-14.
- [161] V. Perez, S. Miachon, J.A. Dalmon, R. Bredesen, G. Pettersen, H. Raeder, C. Simon; Preparation and characterization of a Pt/ceramic catalytic membrane; *Separation and purification technology* 25 (2001) 33-38.
- [162] G. Scatchard, G. M. Kavanagh, L. B. Ticknor; Vapor-liquid equilibrium. VIII. Hydrogen peroxide – water mixtures; *Journal of American chemical society (JACS)* 74 (1952) 3715-3966.
- [163] A.M. De Luis, J.I. Lombraña, A. Menéndez, J. Sanz; “Analysis of the toxicity of phenol solutions treated with H<sub>2</sub>O<sub>2</sub>/UV and H<sub>2</sub>O<sub>2</sub>/Fe oxidative systems”; *Industrial & Engineering chemistry research (ACS)* 50 (2011) 1928-1937.
- [164] E.G. Heckert, S. Seal, W.T. Self, “Fenton-like reaction catalyzed by the rare earth inner transition metal cerium”, *Environmental science and technology* 48 (2008) 5014-5019.
- [165] Y. Xue, Q. Luan, D. Yang, X. Yao, K. Zhou, “Direct evidence of hydroxyl radical scavenging activity of cerium oxide nanoparticles”, *Journal of physical chemistry* 115 (2011) 4433-4438.
- [166] A.K. Talukdar, K.G. Bhattacharyya; “Hydrogenation of phenol over supported platinum and palladium catalyst”, *Applied catalysis A: General* 96 (1993) 229-239.

- [167] H. Liu, T. Jiang, B. Han, s. Liang, Y. Zhou; “Selective phenol hydrogenation to cyclohexanone over dual supported Pd-Lewis acid catalyst”; *Science* 326 (2009) 1250-1252.
- [168] V.R. Choudhary, Y.V. Ingole, C. Samanta, P. Jana; “Direct oxidation of hydrogen to hydrogen peroxide over Pd (or PdO)/Al<sub>2</sub>O<sub>3</sub> in aqueous reaction medium: Influence of different acids and halides anions in reaction medium on formation and destruction of H<sub>2</sub>O<sub>2</sub>”; *Industrial & Engineering chemistry research (ACS)* 46 (2007) 8566-8573.
- [169] K. Mori, K. Furubayashi, S. Okada, H. Yamashita; “Unexpected Pd-catalyzed hydrogenation of phenol to 2-cyclohexene-1-one: enhance activity and selectivity assisted by molecular oxygen”, *Chemical Communication* 48 (2012) 8886-8888.
- [170] P.A. Weyrich, H. Treviño, W.F. Hölderich, W.M.H. Sachtler; “Characterization of Ce promoted, zeolite supported Pd catalysts”; *Applied catalysis A: General* 163 (1997) 31-44.
- [171] M.F. Luo, Z.Y. Hou, X.X. Yuan, X.M. Zheng; “Characterization study of CeO<sub>2</sub> supported Pd catalyst for low-temperature carbon monoxide oxidation”; *Catalysis letters* 50 (1998) 205-209.
- [172] C.E. Gigola, M.S. Moreno, I. Costilla, M.D. Sánchez; “Characterization of Pd-CeO<sub>x</sub> interaction on  $\alpha$ -Al<sub>2</sub>O<sub>3</sub> support”; *Applied surface science* 254 (2007) 325-329.
- [173] H. Idriss; “Ethanol reactions over the surfaces of noble metal/cerium oxide catalyst”; *Platinum metals review* 48 (2004) 105-115.

- [174] M.P. Kapoor, Y. Ichihashi, K. Yuichi, W.J. Shen, Y. Matsumura; “Catalytic methanol decomposition over palladium deposited on mesoporous cerium oxide”; *Catalysis letters* 88 (2003) 83-87.
- [175] A. Adrover, M. Giona, L. Capobianco, V. Violante; “Effect of self-stress on hydrogen diffusion in Pd membranes in the coexistent of  $\alpha$  and  $\beta$  phases”; *Journal of alloys and compounds* 368 (2004) 287-297.
- [176] F.A. Lewis; “The hydrides of palladium and palladium alloys”; *Platinum metals review* 4 (1960) 132-137.
- [177] M. Johansson, E. Skúlason, G. Nielsen, S. Murphy, R. M. Nielsen, I. Chorkendorff; “Hydrogen absorption on palladium and palladium hydride at 1 bar”; *Surface science* 604 (2010) 718-729.
- [178] D. Wang, J. Tong, H. Xu, Y. Matsumura; “Preparation of palladium membranes over porous stainless steel tube modified with zirconium oxide”; *Catalysis today* 93-95 (2004) 689-693.
- [179] R.J. Rennard, R.J. Kokes; “Hydrogenation of ethylene and propylene over palladium hydride”; *The journal of physical chemistry* 70 (1966) 2543-2549.
- [180] A. Benedetti, G. Fagherazzi, F. Pinna, G. Rampazzo, M. Selva, G. Strukul; “The influence of a second phase metal component (Cu, Sn, Fe) on Pd/SiO<sub>2</sub> activity in the hydrogenation of 2,4-dinitrotoluene”; *Catalysis Letters* 10 (1991) 215-224.
- [181] Á. Mastalir, Z. Király, F. Berger; “Comparative study of size-quantized Pd-montmorillonite catalysts in liquid-phase semihydrogenations of alkynes”; *Applied catalysis A: General* 269 (2004) 161-168.

- [182] B. Jenewein, S. Penner, H. Gabash, B. Klötzer, D. Wang, A. Knop-Gericke, R. Schlögl, K. Hayek; “Hydride formation and stability on a Pd-SiO<sub>2</sub> thin-film model catalyst studied by TEM and SAED”; *Journal of catalysis* 241 (2006) 155-161.
- [183] H. Kobayashi, M. Yamauchi, H. Kitagawa, Y. Kubota, K. Kato, M. Takata; “Atomic level Pd-Pt alloying and largely enhanced hydrogen-storage capacity in bimetallic nanoparticles reconstructed from core/shell structure by a process of hydrogen adsorption/desorption”; *Journal of American chemical society (JACS)* 132 (2010) 5576-5577.
- [184] K. Daub, V.K. Wunder, R. Dittmeyer; “CVD preparation of catalytic membrane reactors of nitrates in water”; *Catalysis today* 67 (2001) 257-272.
- [185] O.M. Ilinitich, F.P. Cuperus, L.V. Nosova, E.N, Gribov; “Catalytic membrane in reduction of aqueous nitrates: operational principles and operation”; *Catalysis today* 56 (2000) 137-145.
- [186] N. Barrabés Rabanal; “Selective hydrogenation catalysts for environmental processes: nitrates and chlorinated compounds”; Dissertation thesis (2009) Universitat Rovira I Virgili.